

ALISA KRASNOVA

Greenhouse gas fluxes  
in hemiboreal forest ecosystems





**ALISA KRASNOVA**

Greenhouse gas fluxes  
in hemiboreal forest ecosystems



UNIVERSITY OF TARTU  
Press

Department of Geography, Institute of Ecology and Earth Sciences, Faculty of Science and Technology, University of Tartu, Estonia

Dissertation was accepted for the commencement of the degree of *Doctor philosophiae* in geography (landscape ecology and environment protection) at the University of Tartu on April 11, 2022 by the Scientific Council of the Institute of Ecology and Earth Sciences University of Tartu.

Supervisors: Assoc. Prof. Kaido Soosaar  
Institute of Ecology and Earth Sciences  
Department of Geography  
University of Tartu, Estonia

Prof. Ülo Mander  
Institute of Ecology and Earth Sciences  
Department of Geography  
University of Tartu, Estonia

Prof. Steffen M. Noe  
Institute of Forestry and Engineering  
Estonian University of Life Sciences, Estonia

Opponent: Prof. Asko Noormets, Texas A&M University, USA

Commencement: University of Tartu Oecologicum, J. Liivi 2–127, Tartu, on June 22<sup>th</sup>, 2022, at 10.15

Publication of this dissertation is granted by the Institute of Ecology and Earth Sciences, University of Tartu.

ISSN 1406-1295

ISBN 978-9949-03-880-0 (print)

ISBN 978-9949-03-881-7 (pdf)

Copyright: Alisa Krasnova, 2022

University of Tartu Press

[www.tyk.ee](http://www.tyk.ee)

# CONTENTS

ORIGINAL PUBLICATIONS.....	6
ABBREVIATIONS AND ACRONYMS .....	8
ABSTRACT .....	9
1. INTRODUCTION.....	11
2. MATERIAL AND METHODS .....	14
2.1. Description of study sites.....	14
2.2. Equipment .....	16
2.3. Eddy-covariance flux calculation.....	20
2.4. Chamber flux calculation .....	23
2.5. Data analysis .....	23
3. RESULTS AND DISCUSSION .....	26
3.1. The carbon dioxide fluxes in different forests within a hemiboreal zone (Articles I–III).....	26
3.1.1. Environmental parameters.....	26
3.1.2. Ecosystem CO <sub>2</sub> flux .....	27
3.1.3. Soil CO <sub>2</sub> flux .....	32
3.1.4. Environmental drivers of CO <sub>2</sub> fluxes .....	33
3.1.5. The heatwave influence on CO <sub>2</sub> fluxes .....	35
3.2. Methane fluxes in a hemiboreal riparian forest (Article IV).....	39
3.3. Nitrous oxide fluxes in a hemiboreal riparian forest (Article V).....	42
3.4. Synthesis of the climate-forcing role of CO <sub>2</sub> , CH <sub>4</sub> , and N <sub>2</sub> O in hemiboreal forests.....	46
4. CONCLUSIONS .....	48
REFERENCES.....	50
SUMMARY IN ESTONIAN .....	68
ACKNOWLEDGEMENTS .....	71
PUBLICATIONS .....	73
CURRICULUM VITAE .....	178
ELULOOKIRJELDUS.....	180

## ORIGINAL PUBLICATIONS

This thesis is based on the following publications which are referred to in the text by Roman numerals. Published papers are reproduced in print with the permission of the publisher.

- I. **Krasnova, A.**, Kukumägi, M., Mander, Ü., Torga, R., Krasnov, D., Noe, S.M., Ostonen, I., Püttsepp, Ü., Killian, H., Uri, V., Lõhmus, K., Sõber, J., Soosaar, K., 2019. Carbon exchange in a hemiboreal mixed forest in relation to tree species composition. *Agricultural and Forest Meteorology* 275, 11–23. <https://doi.org/10.1016/j.agrformet.2019.05.007>
- II. Uri, V., Kukumägi, M., Aosaar, J., Varik, M., Becker, H., Aun, K., **Krasnova, A.**, Morozov, G., Ostonen, I., Mander, Ü., Lõhmus, K., Rosenvald, K., Kriiska, K., Soosaar, K. 2019. The carbon balance of a six-year-old Scots pine (*Pinus sylvestris* L.) ecosystem estimated by different methods. *Forest Ecology and Management*, 433, 248–262. <https://doi.org/10.1016/j.foreco.2018.11.012>
- III. **Krasnova, A.**, Mander, Ü., Noe, S.M., Uri, V., Krasnov, D., Soosaar, K., 2022. Hemiboreal forests' CO<sub>2</sub> fluxes response to the European 2018 heat-wave. *Agricultural and Forest Meteorology*. Under revision.
- IV. Mander, Ü., **Krasnova, A.**, Schindler, T., Megonigal, P., Escuer-Gatius, J., Espenberg, M., Machacova, K., Maddison, M., Pärn, J., Ranniku, R., Pihlatie, M., Kasak, K., Niinemets, Ü., Soosaar, K. 2022. Long-term dynamics of soil, tree stem and ecosystem methane fluxes in a riparian forest. *Science of the Total Environment*. 809, 151723. <https://doi.org/10.1016/j.scitotenv.2021.151723>
- V. Mander, Ü., **Krasnova, A.**, Escuer-Gatius, J., Espenberg, M., Schindler, T., Machacova, K., Pärn, J., Maddison, M., Megonigal, P., Pihlatie, M., Kasak, K., Niinemets, Ü., Junninen, H., Soosaar, K. 2021. Forest canopy mitigates soil N<sub>2</sub>O emission during hot moments. *npj Climate and Atmospheric Science* 4, 39. <https://doi.org/10.1038/s41612-021-00194-7>

Author's contribution to the articles denotes: '\*' a minor contribution, '\*\*' a moderate contribution, '\*\*\*' a major contribution.

Categories	Author's contribution				
	I	II	III	IV	V
Original idea	***	*	***	*	**
Study design	***	*	***	**	**
Data processing and analysis	***	***	***	***	***
Interpretation of the results	***	**	***	**	***
Writing the manuscript	***	**	***	**	**

## ABBREVIATIONS AND ACRONYMS

CC1	–	clear-cut area, “Kõnnu“ site
CC2	–	clear-cut area, “Tenso” site
CH <sub>4</sub>	–	methane
CO <sub>2</sub>	–	carbon dioxide
CON	–	coniferous forest, “Soontaga” site
DEC	–	deciduous (alder) forest, “Agali” site
EC	–	eddy-covariance
GHG	–	greenhouse gas
GPP	–	gross primary production
GWP	–	global warming potential
MDS	–	marginal distribution sampling method of gap-filling
MIX1	–	mixed broadleaf-conifer forest, “Liispõllu” site
MIX2	–	mixed broadleaf-conifer forest, “SMEAR Estonia” site, main tower
N <sub>2</sub> O	–	nitrous oxide
NEE	–	net ecosystem exchange of C-CO <sub>2</sub>
NLR	–	non-linear regressions method of gap-filling
Reco	–	ecosystem respiration
Rh	–	heterotrophic respiration
RH	–	relative humidity
Rs	–	total ecosystem respiration
SWC	–	soil water content
Ta	–	air temperature
TA	–	temperature anomaly
Ts	–	soil temperature
U*	–	friction velocity
VPD	–	vapour pressure deficit

## ABSTRACT

The climate on our planet has been changing at an unprecedented rate over the last century. The rise in global temperature is attributed to the increase in the concentration of greenhouse gases (GHG). Forests are essential components of global GHG cycles and can damp or enhance the anthropogenic impact. Forest ecosystems are usually CO<sub>2</sub> sinks, but their carbon uptake ability depends on various factors including age, soil type, environmental conditions, and management practices. A hemiboreal forest zone is located between boreal and temperate forest biomes and is represented by mixed forest stands with varying tree species ratios and management practices. The role of hemiboreal forests in GHG cycling remains understudied due to the high variability of forest stands. Riparian forests are located in an interface between terrestrial and water ecosystems. The supply of carbon and nitrogen from the ground and surface waters and the variability in aerobic and anaerobic conditions makes riparian forests hotspots for N<sub>2</sub>O and CH<sub>4</sub>. Grey alder is a fast-growing pioneer tree frequently found in riparian zones. Due to the symbiosis with atmospheric nitrogen fixating *Frankia* bacteria, alders play an essential role in the forest nitrogen cycle. In the late spring-summer 2018, Europe experienced a heatwave accompanied by rainfall reduction, creating “hotter drought” conditions. As the intensity, duration, and frequency of heatwaves will increase in the future, it is essential to understand the effect of elevated temperatures on the GHG fluxes in various forest ecosystems.

This thesis aimed to analyse the GHG fluxes and the main environmental factors controlling them in hemiboreal forest ecosystems. It answers the following research questions: (1) what is the carbon balance of different forest ecosystems in a hemiboreal zone? (2) what are the main environmental drivers of the carbon balance? (3) how does the heatwave affect carbon fluxes of different forest ecosystems? (4) what is the climate forcing role of CH<sub>4</sub> and N<sub>2</sub>O in a riparian forest?

Eddy-covariance method was used to study CO<sub>2</sub> fluxes on an ecosystem scale in six forest ecosystems located in the geographical vicinity of Southern Estonia: coniferous (CON, pine/spruce, Soontaga), deciduous (DEC, riparian alder, Agali), two mixed (MIX1, spruce/birch, Liispõllu, and MIX2, pine/spruce/birch, SMEAR Estonia) forest stands and two clear-cut areas (CC1, Kõnnu, and CC2, Tenso). The heatwave impact on carbon fluxes was studied in the four sites (CON, DEC, CC2, MIX2). Chamber measurements of soil fluxes were performed in the MIX1 and CC1 sites (soil respiration) and DEC site (soil CH<sub>4</sub> and N<sub>2</sub>O fluxes). Ecosystem CH<sub>4</sub> and N<sub>2</sub>O fluxes were calculated with the eddy-covariance technique and stem fluxes were measured with stem chambers in the DEC site.

Half of the six studied sites were net sinks of CO<sub>2</sub> (MIX1, DEC and CON). Both clear-cuts and one mixed forest (MIX2) were net carbon sources on an annual basis. The presence of clear-cut areas in the MIX2 tower footprint could contribute to high respiration values and the consequent positive net carbon exchange (annual carbon release). The net ecosystem exchange seasonal cycle shape, being closer to a clear-cut than a forest stand, provides further confirmation.

Air temperature is the major environmental driver of respiration. The temperature response curve parameters varied for different forest ecosystems, years, seasons, and soil moisture conditions. While solar radiation is the major driving factor of photosynthesis, its effect is modified by the air temperature. High temperature values (above the temperature optima of the photosynthesis) resulted in GPP reduction when accompanied by low SWC and high VPD. Light response curves parameters also differed between ecosystems and exhibited a clear seasonality.

European heatwave 2018 impact varied for different forest ecosystems of a hemiboreal zone. The only common trait was the reduction of photosynthesis (GPP) and respiration during the temperature anomaly, but the magnitude of the change differed. A mixed conifer-broadleaved forest stand (MIX2) was more vulnerable to the combination of heat and drought than previously assumed, especially with clear-cut areas in the forest stand. Riparian alder forest (DEC) sink strength was higher as a result of favourable conditions in spring before the temperature anomaly. The upland coniferous forest (CON) was the least affected of the four studied sites. Its net carbon uptake was slightly decreased due to the stimulation of respiration, while GPP remained similar to the previous year. The clear-cut (CC2) experienced the most severe drought and did not benefit from the warmer spring conditions. A high reduction in GPP leads to the lack of carbohydrate reserves for the upcoming season and a possible increase in the number of years needed to reach the carbon compensation point. The rise of harvesting activities in the form of clear-cutting may alter the balancing of the hemiboreal zone carbon footprint.

A riparian alder forest (the DEC site) was studied for the methane and nitrous oxide fluxes from soil and stems and ecosystem scale. It was an annual methane sink and a minor source of nitrous oxide. The climate forcing potential of both gases was much smaller (0.1% for CH<sub>4</sub> and 1–6% for N<sub>2</sub>O) compared with the total CO<sub>2</sub> uptake.

A global increase in the frequency of extreme weather events and disturbances causing alterations in the GHG balance of forest ecosystems is very likely to happen in the following decades. The variability of forest types and their responses creates a potential for the hemiboreal zone to be sustainable in the changing climate. However, careful forest management practices are required, as the increase in clear-cutting may negatively impact the resistance of a forest to climate extremes and decrease its carbon sequestration.

# 1. INTRODUCTION

Over the course of the last century, the climate on our planet has been changing at an unprecedented rate. The rise in global temperature is attributed to the increase in the concentration of gases that have positive radiative forcing and are responsible for the “greenhouse” effect (IPCC, 2021). The primary greenhouse gases (GHG) in the Earth’s atmosphere are water vapour (H<sub>2</sub>O), carbon dioxide (CO<sub>2</sub>), methane (CH<sub>4</sub>), nitrous oxide (N<sub>2</sub>O), ozone (O<sub>3</sub>), as well as halocarbons and other chlorine- and bromine-containing substances.

Carbon dioxide is the GHG with the most considerable contribution from human activities. Anthropogenic emissions (fossil fuel combustion, cement production, flaring, land-use change) are responsible for increasing global concentrations (Pachauri et al., 2015). Out of the total emissions, 81% were caused by fossil CO<sub>2</sub> emissions, and 19% by land-use change (for the period 1959–2019, Friedlingstein et al., 2020). Terrestrial and marine carbon sinks are formed by organisms with the ability for photosynthetic carbon uptake (Chapin et al., 2011).

Methane is the second most crucial human-influenced GHG, with 28 times higher radiative forcing than CO<sub>2</sub> on a 100 years horizon and 80 times higher over the 20 years (IPCC, 2021). Atmospheric methane has been responsible for ~20% of global warming since the preindustrial era (Kirschke et al., 2013). Global anthropogenic sources of CH<sub>4</sub> include fossil fuels exploitation, transportation, and usage; agriculture and waste management, biomass and biofuel burning, and constitute ~60% of the total CH<sub>4</sub> emissions (Saunio et al., 2020). The natural sources of CH<sub>4</sub> are represented mainly by wetlands, while upland soils commonly act as methane sinks.

Nitrous oxide is the third most important contributor to the current radiative forcing, with a global warming potential 273 times higher than CO<sub>2</sub> (IPCC, 2021). Moreover, N<sub>2</sub>O is the primary ozone-depleting agent in the stratosphere (Saikawa et al., 2014). The rapid growth of N<sub>2</sub>O concentration in the atmosphere since pre-industrial times is primarily associated with nitrogen application to soils (Murphy et al., 2022).

Forest ecosystems are an essential component of the biosphere. Being sources and sinks of GHGs and energy, they affect the atmosphere’s chemical composition and can damp or enhance the anthropogenic impact. Net ecosystem exchange (NEE) of the forest is a sum of two opposite processes: carbon uptake by plants (gross primary production, GPP) and the total ecosystem respiration (Reco), the latter consisting of soil and above-ground plant respiration. When the Reco of an ecosystem exceeds the GPP over a certain period of time (typically a year), the NEE is positive, and the ecosystem is a net carbon source. In the opposite case, when carbon sequestration (GPP) is higher than Reco, NEE is negative, and the ecosystem is a net carbon sink over the studied period. Forest ecosystems commonly act as sinks of CO<sub>2</sub>, but their sink strength varies and depends on the set of factors, including stand age and tree species composition, soil type, climatic conditions, and management practices. Young forests typically sequester less CO<sub>2</sub>

than releasing (Amiro et al., 2010; Coursolle et al., 2012; Peichl et al., 2010). While the mature forest ecosystems are carbon sinks, their net carbon uptake commonly decreases as stands become older (> 120 years) (Gundersen et al., 2021; Hadden and Grelle, 2017; Luysaert et al., 2008; Soloway et al., 2017). Over the lifetime, a forest ecosystem might switch back and forth from being a sink or source (Baldocchi et al., 2018; Hadden and Grelle, 2016). Furthermore, forest management practices such as thinning and clear-cutting can decrease the forest sink strength or even turn an ecosystem into a source of CO<sub>2</sub> (Bergeron et al., 2008; Grant et al., 2007; Lindroth et al., 2018; Mkhabela et al., 2009; Vestin et al., 2020).

Methane flux in the forest depends primarily on the water balance (Dutaur and Verchot, 2007; Hiltbrunner et al., 2012; Ni and Groffman, 2018). Forest soils are sinks of methane (Dlugokencky et al., 2011), with decreasing sink strength as the soil moisture increases (Jungkunst et al., 2008; Shoemaker et al., 2014). The methane uptake by forest soils has been decreasing over the last decades, especially in the areas with increasing precipitation (Ni and Groffman, 2018). Trees were found to be sources of CH<sub>4</sub> (Barba et al., 2019; Covey and Megonigal, 2019; Schindler et al., 2020), with the source strength increasing from upland to wetland forest (Pitz et al., 2018).

Microbial production of N<sub>2</sub>O makes soils the dominant source of forest nitrous oxide (Butterbach-Bahl et al., 2013; Davidson et al., 2000; Mander et al., 2008). The main pathways from the soil to the atmosphere are direct diffusion, ebullition in water-logged conditions, and plant-mediated transport (Clough et al., 2005; Machacova et al., 2016; Pihlatie et al., 2005; Wen et al., 2017). The change in soil moisture and temperature is the main factor modifying the N<sub>2</sub>O emissions in the forest ecosystems (Butterbach-Bahl et al., 2013).

A hemiboreal (boreo-nemoral) transitional zone is located between boreal and temperate forest biomes (Ahti et al., 1968; Shorohova et al., 2009), approximately between latitudes 56 °N and 60 °N (Löhmus and Kraut, 2010) and could potentially expand in a northerly direction in the future (Hickler et al., 2012; Saetersdal et al., 1998). Forests of the hemiboreal zone are represented by the mixed forest stands with varying tree species ratios and management practices. The role of hemiboreal forests in GHG cycling remains understudied due to the high variability of forest stands. Riparian forests are located in an interface between terrestrial and aquatic ecosystems (Gregory et al., 1991; Naiman and Décamps, 1997). The variability in aerobic and anaerobic conditions and a supply of carbon and nitrogen from the ground and surface waters makes riparian forests hotspots for N<sub>2</sub>O and CH<sub>4</sub> (Mander et al., 2008; Martin et al., 1999; Sommer, 2006). Grey alder (*Alnus incana* (L.) Moench) is a pioneer tree species, frequently occupying riparian zones. Alders play an essential role in the nitrogen cycle due to the symbiosis with nitrogen fixing Frankia bacteria (Roy et al., 2007; Vogel et al., 1997; Weber et al., 1988).

In the late spring-summer 2018, Europe experienced a heatwave in line with previously observed “mega-heatwaves” in 2003 and 2010 (Bastos et al., 2020; Peters et al., 2020). It was characterised not only by the elevated air temperatures but rainfall reduction, creating “hotter drought” conditions (Allen et al., 2015;

Buras et al., 2020). During the next century, the heatwaves intensity, duration, and frequency are projected to increase (Barriopedro et al., 2011; Perkins and Alexander, 2013; Perkins-Kirkpatrick and Gibson, 2017; Schär et al., 2004); thus, it is essential to understand the effect of elevated temperatures on the GHG fluxes in various forest ecosystems.

**The aim of this thesis** was to analyse the GHG fluxes and the main environmental factors controlling them in hemiboreal forest ecosystems.

The thesis answers the following research questions:

1. What is the carbon balance of different forest ecosystems in a hemiboreal zone? (Articles I–III)
2. What are the main environmental drivers of the carbon balance? (Articles I–III)
3. How does the heatwave affect carbon fluxes of different forest ecosystems? (Article III)
4. What is the climate forcing role of CH<sub>4</sub> and N<sub>2</sub>O in a riparian forest? (Articles IV–V)

## 2. MATERIAL AND METHODS

### 2.1 Description of study sites

The studies were conducted in Southern Estonia, in the hemiboreal forest zone. Due to its species heterogeneity, we chose the sites that are the most representative for the area but vary greatly in dominating tree species composition. The ensemble included an upland coniferous forest (the CON site, Soontaga station, **Article III**), two mixed conifer-broadleaved forests (the MIX1 site, Liispõllu, **Article I** and the MIX2 site, Apna, **Article III**), a riparian alder forest stand (the DEC site, Agali, **Articles III–V**) and two clear-cut areas (the CC1 site, Kõnnu, **Article II** and the CC2 site, Tenso, **Article III**) (Table 1, Fig. 1).



**Figure 1.** The location of the study sites in Estonia. Map data © OpenStreetMap

**Table 1.** Study sites description

	MIX1	CC1	CON	DEC	MIX2	CC2
Publications	I	II	III	III, IV, V	III	III
Site type	Mixed forest	Clear-cut	Upland coniferous forest	Riparian alder forest	Mixed forest with clear-cuts	Clear-cut
Station name and coordinates	SMEAR Estonia, Liispõllu 58°16'N 27°16'E	Kõnnu 58°17'N 27°09'E	Soontaga 58°01'N 26°04'E	Agali 58°17'N 27°17'E	SMEAR Estonia, Apna 58°16'N 27°18E	Tenso 58°15'N 26°54'E
Dominating tree species	Norway spruce ( <i>Picea abies</i> L.). Karst), Birch sp. ( <i>Betula pendula</i> Roth., <i>Betula pubescens</i> Ehrh.).	Scots pine ( <i>Pinus sylvestris</i> L.)	Scots pine ( <i>Pinus sylvestris</i> L.) Norway spruce ( <i>Picea abies</i> L. Karst)	Grey alder ( <i>Alnus incana</i> L.).	Scots pine ( <i>Pinus sylvestris</i> L.) Norway spruce ( <i>Picea abies</i> L. Karst), Birch sp. ( <i>Betula pendula</i> Roth., <i>Betula pubescens</i> Ehrh.).	Silver birch seedlings ( <i>Betula pendula</i> Roth.), grasses ( <i>Graminae</i> )
Stand age at the time of the measurements	36 years old	6–8 years old	200 years old (60 to 268)	38–40 years old	70 years old (48 to 170)	2–3 years old
Soil	Gleyed and gleyic pseudopodzol	Gleyic folic podzol	Sandy podzol	Gleyic luvisol with a 10cm humus layer	Gleyed and gleyic pseudopodzolic soils, often with a raw humus horizon in wetter places.	Glossic podzoluvisol
Flux measurement years used in the studies	2014–2015	2016–2017	2017–2018	2017–2019	2017–2018	2017–2018

The two sites of SMEAR Estonia (Station for Measurements of Ecosystem-Atmosphere Relationships, Noe et al., 2015) were chosen to study carbon fluxes of a mixed conifer-broadleaved forest. The MIX1 site (**Article I**) footprint area included two circular study plots (30 m in diameter), where soil flux studies were conducted. The “mixed” plot had a nearly equal share of Norway spruce (*Picea abies* (L.) H. Karst.) and Birch species (*Betula pendula* Roth., *Betula pubescens* Ehrh.), while the “coniferous” plot was spruce-dominated. The MIX2 site (**Article III**) tower footprint area is a mosaic of Scots pine (*Pinus sylvestris* L.), spruce, and birch compartments with prominent clear-cut areas. The CON site represented an upland coniferous forest (**Article III**) and is an old (up to 230 y.o) pine-dominated forest stand with Norway spruce trees in the second layer. The two clear-cuts chosen for the study differed in age and species composition. The CC1 site at the time of the study was a 6–8 years old clear-cut area with young Scots pine trees (**Article II**). The second clear-cut, the CC2 site, was a 2–3 years old clear-cut area with Silver birch seedlings. We chose a riparian grey alder (*Alnus incana* L.) forest stand (the DEC site) to investigate CH<sub>4</sub> and N<sub>2</sub>O fluxes (**Articles IV and V**) in addition to CO<sub>2</sub> flux (**Article III**).

## 2.2. Equipment

All study sites were equipped with EC systems mounted on measurement towers of varying heights (Table 2). The measurement height was chosen based on the canopy height and limited by the area of interest size. The same model of an enclosed infra-red gas analyser (LI-7200, LI-COR Inc., Lincoln, NE, USA) was installed at every site for high frequency CO<sub>2</sub> concentration measurements (**Articles I–III**). For the CH<sub>4</sub> and N<sub>2</sub>O concentration measurements (**Articles IV–V**), the DEC site tower was equipped with a 30 m Teflon tube that sampled air continuously at the speed of 15 L min<sup>-1</sup> with a high-capacity free scroll vacuum pump (Agilent, Santa Clara, CA, USA). A filter was installed to protect against pollen and dust particles. An Aerodyne quantum cascade laser absorption spectrometer (QCLAS) (Aerodyne Research Inc., Billerica, MA, USA) was installed in the heated and ventilated cottage near the tower to continuously analyse CH<sub>4</sub> and N<sub>2</sub>O concentrations from the inlet tube. To obtain the three wind components, fast 3D sonic anemometers (HS-50, Gill Instruments, Lymington, UK or Metek uSonic Class A, Metek GmbH, Elmshorn, Germany) were mounted on all the towers near the gas analysers’ inlets. All EC measurements were performed at 10 Hz, and all gas analysers reported water-corrected gas concentrations (mixing ratio).

**Table 2.** Measured parameters and equipment

	<b>MIX1 (I)</b>	<b>CC1 (II)</b>	<b>CON (III)</b>	<b>DEC (III-V)</b>	<b>MIX2 (III)</b>	<b>CC2 (III)</b>
EC: Measurement height, m	24	4.35	39	21.2	30	4.25
EC: Anemometer(s)	Gill HS-50, Metek uSonic Class A	Gill HS-50	Metek uSonic Class A	Gill HS-50, Metek uSonic Class A	Metek uSonic Class A	Gill HS-50
EC: gas analyser for CO <sub>2</sub>	LI-7200 (LI-COR Inc., Lincoln, NE, USA)					
EC: gas analyser for CH <sub>4</sub> and N <sub>2</sub> O	-	-	-	Aerodyne QCLAS	-	-
Soil chambers	Portable closed dynamic chamber system (PP Systems SRC-1 chamber with a CIRAS-2 gas analyzer (Differential CO <sub>2</sub> /H <sub>2</sub> O Infrared Gas Analyzers)		-	Automatic dynamic chamber system + Picarro G2508 (Picarro Inc., USA)	-	-
Stem chambers	-	-	-	Static closed tree stem chamber systems for stem flux measurements (Machacova et al., 2017) + gas chromatograph (GC-2014; Shimadzu, Kyoto, Japan)	-	-

	<b>MIX1 (I)</b>	<b>CC1 (II)</b>	<b>CON (III)</b>	<b>DEC (III-V)</b>	<b>MIX2 (III)</b>	<b>CC2 (III)</b>
Meteorological parameters: air temperature and relative humidity	HMP45A humidity and temperature probe, Vaisala, Vantaa, Finland from Rõka station	HC2A-S3 – Standard Meteo Probe / RS24T (Rotronic AG, Bassersdorf, Switzerland) and Campbell CR100 data logger (Campbell Scientific Inc., Logan, UT, USA).			PT-100 elements (METEK GmbH, Elmshorn, Germany)	HC2A-S3 – Standard Meteo Probe / RS24T (Rotronic AG, Bassersdorf, Switzerland) and Campbell CR100 data logger (Campbell Scientific Inc., Logan, UT, USA).
Meteorological parameters: solar radiation	CMP3 pyranometer, Kipp & Zonen, Delft, Netherlands from Rõka station	LI-190SL (LI-COR Biosciences, Lincoln, USA)		Delta-T-SPN-1 sunshine pyranometer (Delta-T Devices Ltd., Cambridge, UK)		LI-190SL (LI-COR Biosciences, Lincoln, USA)
Soil temperature	STP-1, PP Systems International, Inc., USA at 5 cm dep	Discreet measurements by STP-1 (PP Systems International, Inc., USA); Continuous measurements by soil external temperature sensor, WatchDog Technologies, Inc, USA)	SC 107 (Campbell Scientific Inc.)	SC 107 (Campbell Scientific	ML3 ThetaProbe (Delta-T Devices Ltd, Cambridge, United Kingdom)	SC 107 (Campbell Scientific Inc.)

	<b>MIX1 (I)</b>	<b>CC1 (II)</b>	<b>CON (III)</b>	<b>DEC (III-V)</b>	<b>MIX2 (III)</b>	<b>CC2 (III)</b>
Soil moisture	HH2 ver. 2, Delta-T Devices Ltd, Cambridge, UK).	Discreet measurements by HH2 Moisture Meter Version 2 (Delta-T Devices Ltd, UK); Continuous measurements by Water Scout sensor model SM 100, Technologies, Inc, USA	ML3 ThetaProbe (Delta-T Devices Ltd, Cambridge, United Kingdom)			
Ancillary measurements		The carbon leaching: 6 plate lysimeters (stainless steel; collecting area 627 cm <sup>2</sup> )		Dissolved O <sub>2</sub> : YSI Professional Plus Multiparameter Water Quality Instrument with a Quatro field cable (YSI Incorporated, Yellow Springs, OH, USA).		

Soil fluxes were measured at the MIX1, CC1, and DEC sites (Table 2). Total soil respiration ( $R_s$ ) and heterotrophic respiration ( $R_h$ ) were measured monthly at the MIX1, and CC1 sites (**Articles I–II**) with a portable closed dynamic chamber system (Table 2) from PVC collars (10 cm in diameter, 5 cm height) pre-installed on site. Heterotrophic respiration ( $R_h$ ) was measured from trenching cylinders pushed to the depth of 45 cm (Kukumägi et al., 2017). The CC1 site was also equipped with an automatic  $\text{CO}_2$  exchange system ACE (ADC BioScientific Ltd., Hoddesdon, UK). Soil  $\text{CH}_4$  and  $\text{N}_2\text{O}$  fluxes at the DEC site (**Articles IV–V**) were measured continuously with 12 automatic dynamic chambers (volume of  $0.032 \text{ m}^3$  and covered a  $0.16 \text{ m}^2$  soil surface). During the measurement, each chamber was automatically closed for 9 minutes (after the removal of flushing and stabilization time, 5 minutes were used for flux calculation). The air was sampled through the multiplexer tube system and analysed by a Picarro G2508 gas analyser (Picarro Inc., Santa Clara, CA, USA) installed in a heated and ventilated cottage at the site. Soil temperature and moisture were manually measured simultaneously with manual chamber measurements in the MIX1 and CC1 sites (**Articles I–II**). Continuous soil temperature and moisture measurements with automatic systems were performed at all other sites (**Articles II–V**, Table 2).

Stem fluxes of  $\text{CH}_4$  and  $\text{N}_2\text{O}$  were measured manually with static closed tree stem chamber systems (Machacova et al., 2017; Schindler et al., 2020). The chambers were installed on the stems of twelve trees, three per tree on different heights. The air samples were taken weekly from September 2017 until December 2018 and analysed in the laboratory at the University of Tartu within a week using a gas chromatograph (GC-2014; Shimadzu, Kyoto, Japan). Auxillary measurements performed on sites can be found in Table 2.

### 2.3. Eddy-covariance flux calculation

The EC fluxes were calculated as a covariance of gas mixing ratio ( $\text{CO}_2$  in **Articles I–III**,  $\text{CH}_4$  in **IV** and  $\text{N}_2\text{O}$  in **V**) and vertical wind speed and averaged over the 30-minute periods using the EddyPro software (LI-COR, Lincoln, NE, USA). Statistical screening, despiking (Mauder et al., 2013; Vickers and Mahrt, 1997), and linear detrending (block averaging in **Article II**) was applied to the raw data. The anemometer tilt was corrected with the double axis rotation. Time-lag compensation was performed using the covariance maximisation method. A time lag window of  $5 \pm 2$  seconds was chosen for  $\text{CH}_4$  and  $\text{N}_2\text{O}$  flux calculation based on the flow rate and the tube's length and cross-section. Low and high frequency corrections were applied for all the gas fluxes (Moncrieff et al., 1997, 2004).

The EC flux data filtering procedure included the removal of technical maintenance periods for all the sites' data. The quality control (QC) flag system (quality classes 1–9, Foken et al., 2004) based on the developed turbulence and steady-state tests' results were used to assess the quality of  $\text{CO}_2$  fluxes in **Article I**,  $\text{N}_2\text{O}$  and  $\text{CH}_4$  fluxes in **Articles IV–V**. The  $\text{N}_2\text{O}$  or  $\text{CH}_4$  flux value was removed from the analysis if one of the following criteria was true for the half-hour averaging

period: out of range averaged concentration (300–350 ppb for N<sub>2</sub>O and 1.8–2.5 ppm for CH<sub>4</sub>), more than 1000 spikes, QC flag exceeding 7. The flux footprint area of each tower was calculated according to the Kljun et al. (2015) model. Fluxes that originated outside the area of interest were removed from the analysis. That included non-forested areas in the DEC site, the lake area in the CON site, the forest area in the CC1 site, and guy-wire tunnels in the MIX2 site located within 90% of the cumulative footprint.

Storage correction was applied. As none of the study sites was equipped with a profile system under the EC measurement point, storage flux was estimated using the one-point approach (Greco and Baldocchi, 1996; Hollinger et al., 1994). The method uses gas concentrations measured by the EC system and assumes a uniform change in the air column under it (Eq.1, **Article V**). The calculated storage flux was then added to the EC flux to obtain net ecosystem exchange (NEE = CO<sub>2</sub> EC flux + CO<sub>2</sub> storage flux) and storage corrected CH<sub>4</sub> and N<sub>2</sub>O values. In all included publications and throughout the thesis text, NEE refers to the exchange of CO<sub>2</sub>, and storage-corrected EC fluxes of CH<sub>4</sub> and N<sub>2</sub>O are referred to as ecosystem flux of respective gas. All EC fluxes follow the atmospheric sign convention, where the negative value denotes the direction of the flux from the atmosphere to the ecosystem, while the positive flux is the opposite.

Friction velocity (U\*) filtering was performed for all the nighttime CO<sub>2</sub> and CH<sub>4</sub> fluxes. The U\* threshold was estimated with the moving point test (Papale et al., 2006) implemented in the ReddyProcWeb online tool (Wutzler et al., 2018). In the case of the MIX2 site, the test provided a high threshold (0.43 m s<sup>-1</sup>) that would result in a significant loss of nighttime data; thus, a fixed 0.3 m s<sup>-1</sup> threshold was chosen (Lindroth et al., 2020, 2018). The U\* threshold calculated for CO<sub>2</sub> flux (0.29 m s<sup>-1</sup>) was applied to CH<sub>4</sub> fluxes at the DEC site (**Article IV**). As we found no influence of the friction velocity on N<sub>2</sub>O fluxes, the U\* filtering was not performed in **Article V**. The final filtering included the elimination of single outstanding CO<sub>2</sub> flux values and CH<sub>4</sub> or N<sub>2</sub>O flux values higher than eight times the standard deviation (Wang et al., 2013).

In order to acquire cumulative fluxes on different time scales (hourly to compare with soil flux and yearly to obtain the annual budget estimates), filtered NEE, CH<sub>4</sub>, and N<sub>2</sub>O ecosystem fluxes were gap-filled using the marginal distribution sampling method (MDS, Reichstein et al., 2005; Wutzler et al., 2018) implemented in REddyProcWeb online tool. The MDS method combines lookup Tables and the mean diurnal course approach. The method assumes that the flux is similar under similar meteorological conditions within a certain time window. For the time intervals with insufficient meteorological data coverage, the missing flux values are filled with the average quality-controlled flux from the same time of the day within the time window.

The second gap-filling method was utilised to fill the gaps in NEE in **Articles I and III** to cross-check the annual sums. The nonlinear regressions method (NLR) uses Lloyd and Taylor (1994) respiration model (eq.1) to obtain missing nighttime values (assuming that in the absence of sunlight, all NEE values are equal to Reco).

$$R_{eco} = R_{ref} \times e^{E_0 \times \left( \frac{1}{T_{ref} - T_0} \right) - \left( \frac{1}{T - T_0} \right)} \quad (1)$$

where  $E_0$  is the activation energy,  $T_{ref}$  is a reference temperature set to 15 °C in the ReddyProcWeb tool,  $R_{ref}$ , is respiration at the reference temperature.  $T_0$  is kept constant at -46.02 °C.

Daytime NEE gaps were filled with values modelled using a rectangular hyperbolic light–response curve based on Michaelis-Menten equation (Eq. 2) (Lasslop et al., 2010).

$$NEE = \frac{\alpha \times R_g \times GPP_{max}}{\alpha \times R_g + GPP_{max}} + R_{day} \quad (2)$$

where  $\alpha$  is the light use efficiency,  $R_g$  is solar radiation,  $GPP_{max}$  is the ecosystem photosynthetic capacity (gross primary production at saturating light),  $R_{day}$  is daytime Reco expressed as in Eq. 1.

In order to estimate GPP and Reco, the partitioning of NEE (**Articles I–III**) was also conducted using ReddyProcWeb online tool. The “nighttime” method (Reichstein et al., 2005) was used in all three CO<sub>2</sub> studies, while the “daytime” method (Lasslop et al., 2010) was additionally applied in **Articles I and III**. As follows from the names, the “nighttime” method uses nighttime NEE (periods when solar radiation is less than 15 W m<sup>-2</sup>) to obtain the parameters of the Lloyd and Taylor model equation (Eq.1) over defined time windows. The model parameters are then used to calculate daytime Reco using air temperature measurements for each time window. Daytime GPP is computed as  $GPP = NEE - Reco$ , while nighttime GPP is assumed to be zero.

While being widely used, the “nighttime” method entirely relies on the presence of a sufficient amount of quality-controlled nighttime measurements. During the summer months, Northern territories in Europe lack the full extent of low solar radiation hours, thus limiting the amount of nighttime measurements. The application of quality control filtering further reduces this amount as periods with low mixing (below the friction velocity threshold) are usually observed at night and early morning. Finally, the range of temperatures may not be sufficient to fit the Lloyd and Taylor curve within a short time span. Considering all the reasons mentioned above, we chose to add the “daytime” method for the annual budgets estimates in **Articles I and III**. The “daytime” method is based on quality-controlled daytime NEE measurements that are usually more abundant. A sum of Lloyd and Taylor respiration model representing Reco and hyperbolic light response curve representing GPP is fitted to the daytime NEE to obtain the models’ parameters used to calculate GPP and Reco (Eq. 2).

The  $GPP_{max}$  (ecosystem photosynthetic capacity) in the hyperbolic light response curve model is modified to account for the decrease in GPP under a high vapour pressure deficit (VPD). The “daytime” partitioning results are modelled values and thus do not sum up to the measured NEE (Lasslop et al., 2010). Both

“nighttime” and “daytime” partitioning procedures were performed within the same data processing sessions of the ReddyProcWeb tool and are described in more detail by Wutzler et al. (2018).

## 2.4 Chamber flux calculation

The CIRAS-2 gas analyser built-in software provided soil CO<sub>2</sub> flux values in **Articles I and II**. CH<sub>4</sub> and N<sub>2</sub>O fluxes from soil and stems (**Articles IV–V**) were calculated as a linear change of gas concentration in the chamber headspace over time (Livingston and Hutchinson, 1995). Stem CH<sub>4</sub> and N<sub>2</sub>O fluxes were filtered out if the R<sup>2</sup> of linear fit for the CO<sub>2</sub> concentration change, measured from the same sample, was lower than 0.9. To make stem flux values comparable to soil and ecosystem fluxes, they were recalculated to m<sup>2</sup> of ground area.

## 2.5 Data analysis

To compare the carbon balance of different forest ecosystems, we calculated annually accumulated NEE, GPP and Reco for each study site. While the measurements were performed in different years, we assume that the interannual variability within the three-year period (2015–2017) is not too high in the absence of extreme events. The year 2018 featured a heatwave with high air temperatures in May and drought and temperature anomaly in July. Thus, for the thesis, the annual balances of the CC2 and DEC sites were computed not by calendar year, taking into account the data availability (April 2017–March 2018 for the CC2 site and May 2017–April 2018 for the DEC site). The MIX2 and CON sites had full calendar years of measurements; thus, 2017 and 2018 are presented separately. Monthly sums of the GPP, Reco and NEE were calculated for all the measurements span of all six study sites.

The detailed description of soil and stem flux data analysis can be found in corresponding articles (**Articles I and II** for the soil respiration data at the MIX1 and CC1 sites, **Article IV** for the soil and stem CH<sub>4</sub> fluxes, **Article V** for the soil and stem N<sub>2</sub>O fluxes). As there was no forest heterotrophic respiration (Rh) measured simultaneously with the CC1 site, we used the Bond-Lamberty model (Bond-Lamberty et al., 2004) prediction to assess if the clear-cut area Rh was elevated.

The influence of air temperature on respiration can be described by an exponential function and various models, including the most widely used Lloyd and Taylor (Eq. 1, Lloyd and Taylor, 1994) and Q10 (Eq. 3, van't Hoff, 1898). We studied the relationship between air temperature and Reco in the MIX1 site utilizing the Q10 model at 3-months intervals from July 2014 to December 2015 (**Article I**).

$$R_{eco} = R_{ref} \times Q_{10}^{\frac{T-T_{ref}}{10}} \quad (3)$$

where  $T$  is the air temperature in °C,  $T_{ref}$  is a reference temperature set to 10 °C, and the fitted parameters are  $R_{ref}$ , respiration at the reference temperature and  $Q_{10}$ , temperature sensitivity.

Lloyd and Taylor equation (Eq.1) was chosen for growing seasons of 2017–2018 in the MIX2, CC2, CON and DEC sites in **Article III**. Reference temperature was set to 10 °C as in the original publication by Lloyd and Taylor (1994) to obtain the ER10 value (ecosystem respiration at 10 °C). This parameter allows for comparing respiration at different time intervals and ecosystems with the fixed value of the primary driver (air temperature). An exponential function was utilised to describe the relationship between soil temperature and  $R_s$  (or  $R_h$ ) for the MIX1 (**Article I**) and the CC1 (**Article II**) sites, as well as for the gap-filling of the discrete  $R_s$  and  $R_h$  measurements data to obtain the accumulated values.

Solar radiation ( $R_g$ ) is the primary environmental driver of GPP, but the EC method does not allow for direct measuring of photosynthesis, as NEE also includes the opposite flux. Nevertheless, the influence of  $R_g$  on NEE follows the photosynthetic light response curve (LRC). It can be represented as a rectangular hyperbolic model based on the Michaelis-Menten equation with the addition of the daytime ecosystem respiration ( $R_{day}$ ). The fitted parameters – light use efficiency ( $\alpha$ ), photosynthetic capacity ( $GPP_{max}$ ) and  $R_{day}$  describe the shape of the curve (Eq. 2).

We analysed LRC parameters monthly for the MIX1 site (**Article I**). Weekly fits of LRC were performed for the CC2, MIX2, CON, and DEC sites (**Article III**) to acquire the  $GPP_{max}$  and study the factors influencing it. In **Article II**, the presence of some forested areas inside the footprint could affect the conclusions about the clear-cut area carbon balance. To test it, we separated the forest-dominated wind sectors and used light response curves (Eq. 2) for different temperature classes to assess the difference.

The influence of air temperature on  $CO_2$  flux for different ecosystems was studied in **Article III**. Nighttime measured NEE (representing nighttime Reco) was used in Lloyd and Taylor’s respiration model (Eq. 1) to analyse the impact of air temperature for each vegetation period and site separately. Due to the high variability of Reco, bin-averaged data was used. We examined the effect of air temperature on GPP and obtained the temperature optimum of photosynthesis ( $T_{opt}$ ), using GPP calculated with the “daytime” method. The GPP computed with the “nighttime” approach is not suitable for this analysis because the air temperature is used as the primary environmental driver.  $T_{opt}$  was calculated for each year and site as the air temperature value corresponding to the maximum bin-averaged GPP after the application of loess smoothing (Bennett et al., 2021). The temperature anomaly (TA) in **Article III** was defined as a period lasting five or more consecutive days when average air temperature exceeded 90% quantile of long-term measurements.

To assess the climate-forcing role of all three GHG fluxes, the annual sums were recalculated in CO<sub>2</sub>-equivalent units. The global warming potential for the 100 years was based on the IPCC 2021 report: GWP100=1 for CO<sub>2</sub>, GWP100=27.9 for CH<sub>4</sub>, and GWP100=273 for N<sub>2</sub>O (IPCC, 2021). The sums of N<sub>2</sub>O and CH<sub>4</sub> were calculated based on soil only and ecosystem (EC) fluxes separately.

All the EC data handling and analysis were performed in MATLAB (R2017a-R2020b, The MathWorks, Inc, 236 USA). Statistica 7.1 and 13.0 software (StatSoft Inc.) and R version 4.0.2 (R Development Core Team, 2020) were used for soil and stem flux data analysis.

### 3. RESULTS AND DISCUSSION

#### 3.1. The carbon dioxide fluxes in different forests within a hemiboreal zone (Articles I-III)

##### 3.1.1. Environmental parameters

The studies of CO<sub>2</sub> fluxes were conducted from the year 2014 till the end of 2018. All the stations were located in geographical vicinity, and the forests were growing in the same climatic conditions. Regional weather parameters for the study period as well as the preceding years are presented in Fig. 2a.

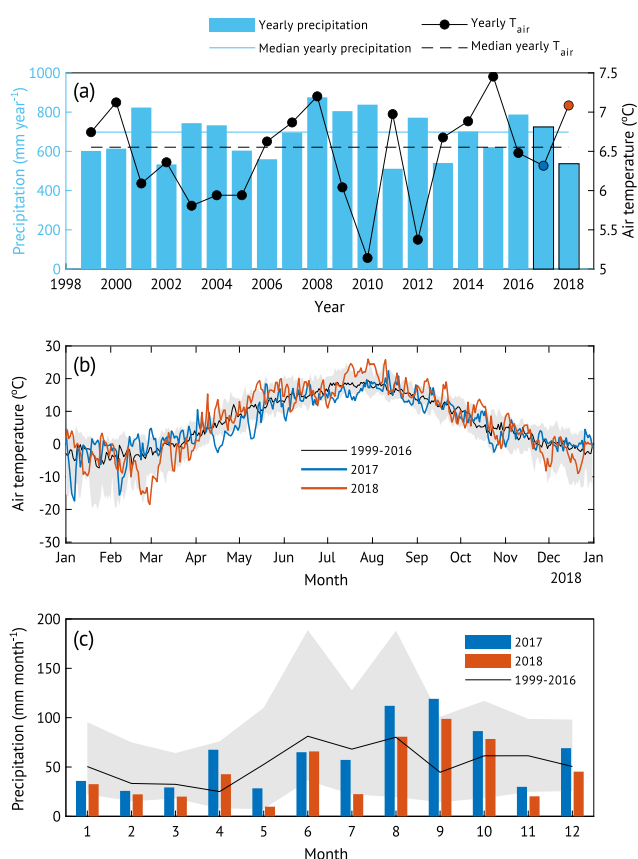


**Figure 2.** Regional environmental conditions: (a) yearly average air temperature and precipitation sums. The lines are the medians of 1999–2016. The highlighted bars and markers correspond to study years (2017 & 2018); (b) daily average air temperature in the two study years (2017 and 2018), median of 1999–2016; (c) monthly precipitation for 2017 and 2018 (bars) and median of 1999–2016. The shaded area at (b) and (c) represents 10% and 90% quantiles. All data is measured at Tõravere meteo station, 40km on average away from the study sites. Source: Article III, Figure 1.

The highest average yearly air temperature was recorded in 2015, while the precipitation in this year was just slightly below the long-term median. The coldest year was 2017, with precipitation close to the median. Out of the five study years, the lowest total amount of precipitation was recorded in 2018.

In the spring-summer 2018, Europe experienced a heatwave (Bastos et al., 2020; Peters et al., 2020). In the area of our studies, the air temperature was unusually high for several days in May, followed by close to long-term median values until the middle of July, when the daily average air temperature was constantly higher than 90% quantile for 19 consecutive days (Fig. 2b). The latter period is further termed the temperature anomaly (TA). Furthermore, May, July, and November 2018 received limited precipitation compared to the long-term median (Fig. 2c).

Weather conditions of separate studies can be found in Fig. 3 (I), Fig. 3 & 10 (II), Fig. 2 (III). As our study sites are located in geographical vicinity, the temperature and solar radiation conditions were similar with only interannual differences. However, soil moisture conditions varied between the sites, even within the same year of measurements (Fig. 2c in III).

### 3.1.2. Ecosystem CO<sub>2</sub> flux

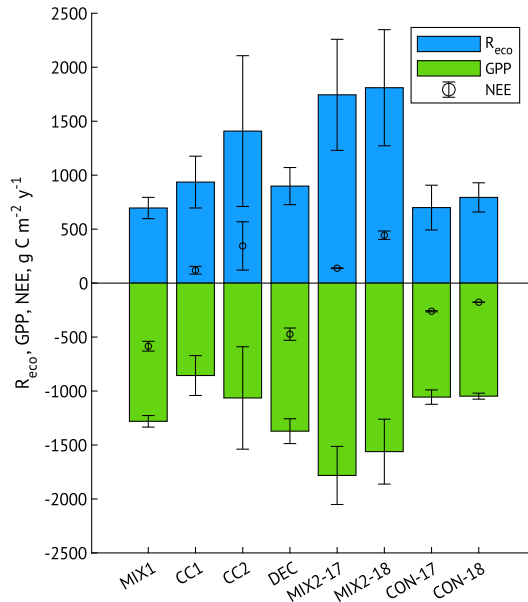


**Figure 3.** The annual sums of net ecosystem exchange (NEE, circles), ecosystem respiration (Reco, blue bars) and gross primary production (GPP, green bars) in the eight study site-years: MIX1 2015; CC1 April 2016–March 2017; CC2 April 2017–March 2018; DEC May 2017–April 2018; MIX2 2017 and 2018; CON 2017 and 2018

Among all eight studied site-years, half was a net carbon sink (negative annual NEE): the MIX1 and DEC sites and the CON site over the two study years. Both clear-cut areas, the CC1 and the CC2, and the MIX2 site over the two years were net carbon sources (positive annual NEE) (Fig. 3). The MIX1 site in 2015 was the most substantial net carbon sink out of all the studied site-years with the annual NEE of  $-586 \pm 45 \text{ g C m}^{-2} \text{ y}^{-1}$ . The value is in the same range previously reported for a spruce/fir forest in Denmark (Jensen et al., 2017) and a spruce forest in Germany (Grünwald & Bernhofer, 2007). While the DEC site showed higher monthly uptake than the MIX1 site during the summer months, it was a stronger carbon source during the rest of the season, especially in autumn months (Fig. 4), resulting in a slightly weaker annual net sink ( $-473 \pm 57 \text{ g C m}^{-2} \text{ y}^{-1}$ ). Uri et al. (2017) have previously estimated the DEC site net ecosystem production (NEP) of  $386 \pm 40 \text{ g C m}^{-2} \text{ y}^{-1}$  (average  $\pm$  sd of 2013–2014). Given that NEE can be viewed as an approximation of NEP with an atmospheric sign convention (Chapin et al., 2011), our annual estimate is in line. The CON site was a net carbon sink in both study years with values similar to other boreal pine forests (Kolari et al., 2004) (Table 3)

The MIX2 site was the strongest net carbon source, especially in 2018, followed closely by the two clear-cuts (the CC1 and CC2 sites). Both the MIX2 and the CC2 sites demonstrated exceptionally high positive NEE fluxes in the second part of the growing season and autumn months (Fig. 4b). The CC1 site was also a net carbon source in August–December but gained smaller values than the CC2 and MIX2 sites. After the harvesting in the form of clear-cutting, a forest site becomes a net carbon source (Aguilos et al., 2014; Humphreys et al., 2005; Ney et al., 2019; Noormets et al., 2015; Vestin et al., 2020). The direct removal of trees results in the elimination of canopy photosynthesis. At the same time, heterotrophic respiration is stimulated with the increased rates of decomposition and extra heating (Grant et al., 2010; Ney et al., 2019; Vestin et al., 2020).

While forests typically act as net carbon sinks (Harris et al., 2021; Luyssaert et al., 2010), there are reported cases of forests, similar to the MIX2 site, being annual net carbon sources. For example, spruce/pine/birch mixed forest in Sweden (Norunda station) was previously reported to be a consistent annual net carbon source since the start of the measurements in 1994, with the range of 270 to  $688 \text{ g C m}^{-2} \text{ year}^{-1}$  in 2007–2016 (Janssens et al., 2001; Lindroth et al., 2018). A mixed temperate-boreal forest in Canada was a net carbon source in two out of seventeen years of carbon flux study (Froelich et al., 2015). Based on long-term research, Hadden & Grelle (2016) showed a Swedish spruce forest turning from net carbon sink to a source due to enhanced Reco in spring and autumn. A forest can be a source of carbon due to its age and/or species composition and in response to disturbance or environmental factors (Baldocchi, 2008; Froelich et al., 2015; Luyssaert et al., 2008).

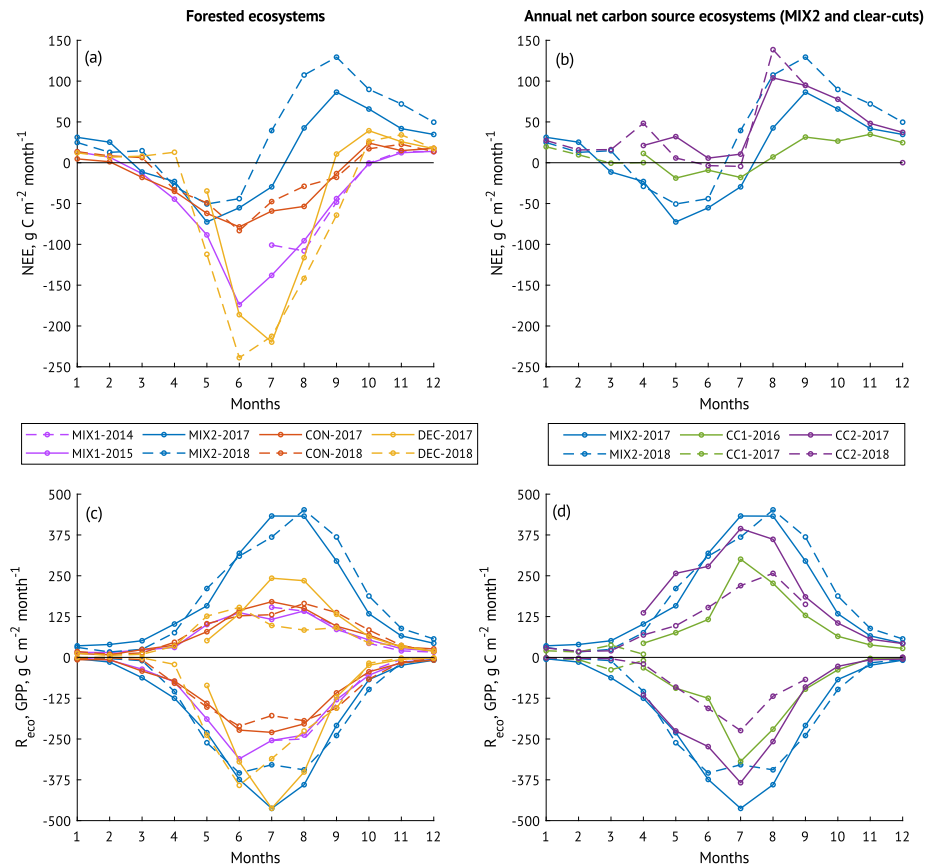


**Figure 4.** Seasonal cycles of forested ecosystems (left panels) and net annual source ecosystems (right panels) NEE (a,b), Reco (c & d, positive values), GPP (c & d, negative values)

Most of the studied site-years' NEE seasonal cycle followed the expected pattern for the site type and climatic zone (Baldocchi, 2008; Xiao et al., 2008), with the pronounced period of net carbon uptake of varying magnitude in summer months and net carbon release during the dormancy period (Fig. 4a,b). The beginning and the end of vegetation season depends on the air temperature and solar radiation, and thus their direct comparison obtained from different years is meaningless.

The CON site NEE seasonal cycle represents a typical coniferous forest with a gradual beginning and end of a vegetation period and mild net carbon uptake (Kolari et al., 2004; Xiao et al., 2008). The NEE seasonal cycle of the DEC site is typical for a deciduous forest (Chapin et al., 2011; Liu et al., 2022), with a more steep change from positive to negative NEE values in spring (the leaves expansion) and the opposite in the end of the vegetation season (senescence) (Fig. 4a, solid line). The vegetation season of 2018 (Fig. 4a, dashed lines) was affected by the heatwave and is discussed in the corresponding chapter. The MIX1 site is a mixed conifer-broadleaved forest, and this can be traced in the shape of its NEE cycle: the spring transition is more gradual compared to a deciduous forest, as

coniferous species start photosynthesis earlier and slowly increase the carbon uptake. At the same time, in the summer months, NEE reaches more negative values than the CON site. The MIX2 site features a seasonal cycle of NEE that resembles a coniferous forest in the first half of the year (similar to the CON site in this study). The second half is characterised by high positive NEE values and has a shape reminiscent of a clear-cut area (Fig. 4b). Indeed, the footprint of the MIX2 site tower includes several clear-cuts of varying age and size. The seasonal NEE cycle of both clear-cut areas (CC1 and CC2) in our study included two periods of high positive NEE (the lower one in spring and much higher one in late summer/early autumn) and separate short periods of carbon consumption (negative daily NEE). The CC1 site has less intensive respiratory parts in the cycle, while the pattern remains similar to the CC2 site, and clear-cuts in other studies (Grant et al., 2010; Mamkin et al., 2019; Ney et al., 2019).

NEE is a net value calculated as a difference between GPP and Reco, and thus its dynamics is consequential to the variability in its composing fluxes. The shift of NEE towards a more negative value may be a result of a GPP increase but also a Reco decrease. The same holds true for the opposite case. Annual GPP and Reco estimates in our sites as well as in similar sites from the literature can be found in Table 3. The seasonal cycle of GPP followed a similar pattern across all sites, with the maximum uptake in July and close to zero values during the dormancy period (Fig. 4c,d, negative values).

The MIX2 site was the most productive (the highest annual GPP), followed closely by DEC and the MIX1 sites. Similarly high GPP was previously reported for more southern forests in Poland and Germany (Grünwald and Bernhofer, 2007; Ziemblińska et al., 2016), while a boreal pine forest in Finland had lower values (Ilvesniemi et al., 2009); net carbon source forest in Sweden had GPP in the same range as the MIX2 site in our study (Table 3). As expected, the lowest annual GPP was observed for the clear-cuts (the CC1 and CC2 sites), with the CC2 site, having slightly higher GPP but also the highest uncertainty. Both clear-cuts' annual GPP exceeded previously reported values for clear-cuts of various ages in Sweden and Canada (Coursolle et al., 2012; Vestin et al., 2020) but was close to a GPP of a 3–4 year old clear-cut in Germany (Ney et al., 2019). The CON site exhibited similar annual GPP values as observed in both clear-cuts in our study and a pine forest in Finland (Ilvesniemi et al., 2009). In contrast, a pine forest in Poland had 1.5–2 times higher values (Ziemblińska et al., 2016). As annual GPP depends on the daylight and growing season length, southern forests, in general, sequester more carbon per year than more northern ones (Baldocchi, 2008). Air temperature and water availability also influence the annual sum.

The total annual Reco of the DEC site was higher than other sites in this thesis with the exception of the MIX2 site, and featured noticeable peaks in the summer months. The MIX1 site Reco was of similar magnitude as that of the CON site. Both ecosystems' Reco seasonal cycle was similar, although the CON site had higher Reco in July and slightly higher in autumn months (Fig. 4c, positive values). The values were similar to the pine forest in Finland and smaller than all other forest sites (Table 3).

**Table 3.** The range of carbon exchange components in various ecosystems,  $\text{g C m}^{-2} \text{ year}^{-1}$ . NEE is represented as the average and standard deviation of two gap-filling methods. GPP and Reco is the average and standard deviation of two flux partitioning methods. Literature data are represented as the range of values reported for the corresponding years.

Site	NEE	GPP	Reco	Years	Reference
Mixed spruce/birch forest in this study (MIX1)	$-586 \pm 45$	$-1281 \pm 53$	$696 \pm 99$	2015	I: (Krasnova et al., 2019)
6-y.o. clear-cut in this study (CC1)	$119 \pm 36$	$-856 \pm 185$	$936 \pm 240$	April 2016– March 2017	II: (Uri et al., 2019)
3-y.o. clear-cut in this study (CC2)	$344 \pm 224$	$-1064 \pm 475$	$1409 \pm 699$	April 2017– March 2018	III: (Krasnova et al., 2022)
Alder forest in this study (DEC)	$-473 \pm 57$	$-1372 \pm 115$	$899 \pm 172$	May 2017– April 2018	
Mixed pine/spruce/birch forest in this study (MIX2)	$138 \pm 3$	$-1782 \pm 269$	$1745 \pm 515$	2017	
	$444 \pm 39$	$-1562 \pm 301$	$1810 \pm 538$	2018	
Pine/spruce forest in this study (CON)	$-261 \pm 6$	$-1056 \pm 67$	$700 \pm 207$	2017	
	$-177 \pm 1$	$-1048 \pm 28$	$794 \pm 135$	2018	
Pine forest in Finland	$-137 \dots -247$	$-952 \dots -1104$	$761 \dots 898$	1997–2007	(Ilvesniemi et al., 2009)
Spruce/fir forest in Denmark	$-553 \dots -937$	$-1644 \dots -2000$	$981 \dots 1118$	2009–2014	(Jensen et al., 2017)
Mixed pine/spruce/birch forest in Sweden	$270 \dots 688$	$-1059 \dots -1646$	$1519 \dots 2106$	2007–2016	(Lindroth et al., 2018)
Pine forest in Poland	$-494 \dots -765$	$-1863 \dots -2367$	$1388 \dots 1613$	2008–2013	(Ziemblińska et al., 2016)
Spruce forest in Germany	$-395 \dots -698$	$-1590 \dots -2095$	$1135 \dots 1397$	1996–2005	(Grünwald and Bernhofer, 2007)
3-y.o. clear-cuts in Sweden	$303 \dots 443$	$-254 \dots -403$	$697 \dots 706$	2012–2013	(Vestin et al., 2020)
3–4 y.o. clear-cut in Germany	$236 \dots 242$	$-1036 \dots -1062$	$1272–1303$	2016–2018	(Ney et al., 2019)

The MIX2 site Reco was consistently higher than all other study sites with the peak in July/August and the biggest annual Reco, in the same range as previously reported for a mixed forest in Sweden (Fig. 4c,d, positive values; Table 3). The second-highest annual Reco was estimated for the CC2 clear-cut, although the uncertainty was the highest out of all sites. The CC2 site Reco reached the highest values in the beginning of July, while the CC1 site Reco peaked slightly later.

High Reco values of the MIX2 site could also be a result of clear-cut areas within the atmospheric tower footprint. This is further confirmed by the seasonal cycle more typical for a clear-cut than a forest (Fig. 4b). Moreover, the footprint area includes roads and guywire tunnels that can accumulate CO<sub>2</sub> from the clear-cuts during the calm periods, while developed turbulence can bring it upwards in the later hours. The nighttime flux partitioning method would then overestimate the daytime Reco and, as a consequence, the GPP values. This could be a reason for the higher difference between the methods, with “daytime” partitioned fluxes being smaller.

### 3.1.3. Soil CO<sub>2</sub> flux

Total soil respiration (Rs) and heterotrophic respiration (Rh) were measured at the MIX1 (**Article I**) and the CC1 (**Article II**) sites. In the MIX1 site, Rs was measured at two sample plots differing in species composition: “coniferous” and “mixed”. The sum of Rs over the growing season (May-October 2015) was slightly higher for both sample plots than the accumulated Reco over the same period:  $615 \pm 30$  and  $576 \pm 83$  g C m<sup>-2</sup> period<sup>-1</sup> for the average Rs and Reco respectively (Table 5 in **I**). The discrete chamber measurements of Rs followed a similar seasonal pattern as Reco (Fig 4 in **I**) except for July and September 2015, when Reco was much smaller than Rs. Coniferous plot Rs demonstrated a decrease in July 2015 that was reflected in Reco, while the Mixed plot exhibited the seasonal peak at the same time (Fig 2A in **I**). The opposite was observed for September 2015, when Mixed plot Rs decreased, while the Coniferous plot demonstrated a slight increase in Rs. The difference between the Rs of the two sample plots was significant. As there was no difference in Rh, the variability was rather caused by the autotrophic component of Rs. The Rh/Rs ratio of the two sample plots was 0.65. Wind sectors analysis revealed no difference between the Reco calculated for the sectors corresponding to sample plots’ locations.

The average cumulative Rs was within the range of values previously reported for temperate and boreal forests (Bond-Lamberty and Thomson, 2010; Gaumont-Guay et al., 2014; Kukumägi et al., 2017; Subke et al., 2006; Wei et al., 2010), while total Reco was closer to boreal forests than temperate ones (Table 3 and Table 7 in **I**). Among the six sites in this study, the MIX1 site annual Reco was one of the smallest, similar to the Reco of upland pine forest (the CON site in this thesis).

As Reco is the sum of Rs and above ground plant respiration, the accumulated Reco cannot logically be smaller than the total Rs over the same period. The

upscaling of  $R_s$  to a site level in a mixed forest is challenging due to the intrinsic heterogeneity in the carbon sources distribution (Knohl et al., 2008; Leon et al., 2014; Yuste et al., 2005). While our measurements represent two different plots, they do not cover all the footprint area variety. Moreover, the chambers were located within 30% of the cumulative footprint area and not in the main wind direction (Fig. 1 in I). The uncertainty introduced by the flux partitioning method was 14% of the annual Reco, and the nighttime method estimate was higher than  $R_s$ , while the daytime one was lower. The nighttime method relies on nighttime measurements when the footprint is bigger compared to the daytime and may include more carbon sources. In general, Reco is a spatially integrated signal originating from various sources in the heterogeneous footprint, while the chamber method allows for comparing  $R_s$  of different parts of a heterogeneous landscape (Yuste et al., 2005).

The accumulated  $R_s$  of the CC1 site ( $497 \text{ g C m}^{-2} \text{ period}^{-1}$ ) was smaller than the MIX1 over the growing season (May–October 2016), while Reco was much higher (Table 3, Fig 3). The  $R_s/\text{Reco}$  ratio was 0.54 for the annual estimate as well as the growing season, falling within the range of previously published values (Davidson et al., 2006). A very similar seasonal cycle with a clear peak in July and August was observed for Reco,  $R_s$  and  $R_h$  (Fig. 5 in II, Fig. 4d, positive values).  $R_h/R_s$  ratio over the year was 0.7. The  $R_h$  is expected to be elevated on a clear-cut area due to the increased amount of detritus, more active decomposition and higher soil temperature (Grant et al., 2010; Radler, 2010; Vestin et al., 2020). Indeed, the value obtained in our study ( $420 \text{ g C m}^{-2} \text{ y}^{-1}$ ) was higher than the Bond-Lamberty model (Bond-Lamberty et al., 2004) estimate ( $354 \text{ g C m}^{-2} \text{ y}^{-1}$ ) for the forest ecosystem.

### 3.1.4. Environmental drivers of $\text{CO}_2$ fluxes

NEE represents the fluxes of  $\text{CO}_2$  on the ecosystem scale. In the absence of solar radiation during the night, the photosynthesis is zero, measured nighttime NEE represents nighttime Reco. Air temperature is the leading environmental driver of the ecosystem and soil respiration (Greco and Baldocchi, 1996; Lloyd and Taylor, 1994).

In the MIX1 site, temperature sensitivity ( $Q_{10}$  from Eq. 3) varied from  $1.93 \pm 0.14$  in December 2014 – February 2015 and  $1.94 \pm 0.09$  in September–December 2015 to  $2.75 \pm 0.19$  in March–May 2015. In June–August 2015, air temperature influence on Reco was absent (Fig. 6 in I). The reasons could include low soil moisture in July–September 2015 (Fig. 2D in I) and a small range of air temperatures. While the impact of air temperature on Reco in other periods was significant ( $p < 0.001$ ), air temperature described a very low portion of Reco variability (7–31%) at a half-hourly scale. Residual analysis indicated that the majority of outstanding values attributed to the low wind speed periods ( $< 1 \text{ m s}^{-1}$ ). Consequently, air mixing is another essential factor in ecosystem-scale flux analysis.

Reco at reference temperature (ER10) was the lowest in winter ( $1.03 \pm 0.07 \mu\text{mol m}^{-2} \text{s}^{-1}$ ) and the highest in summer 2014 ( $2.41 \pm 0.18 \mu\text{mol m}^{-2} \text{s}^{-1}$ ) in the MIX1 site. ER10 calculated from Lloyd and Taylor model for growing seasons 2017 and 2018 in the MIX2, CON, DEC, and CC2 sites can be found in Fig. 6 in **Article III**. The CON site ER10 was the lowest across the sites (2.50–2.59), in the same range as the MIX1 site in the summer months. The MIX2 site had the highest ER10 in 2017 ( $8.83 \mu\text{mol m}^{-2} \text{s}^{-1}$ ) out of all site-years. For the CC2 site, air temperature influence was not significant in 2017 and Lloyd and Taylor’s model described a very low part of the variability in 2018 ( $R^2 = 0.26$ ). The DEC site had the second-highest ER10 in 2017 ( $3.58 \mu\text{mol m}^{-2} \text{s}^{-1}$ ). Air temperature described a high portion of average Reco variability in 2017 in the MIX2 and DEC sites ( $R^2 = 0.90$ ), but much lower in the heatwave year (0.76 and 0.48 respectively), demonstrating the presence of a confounding factor (soil moisture).

The influence of soil temperature on Rs and Rh was assessed with the exponential equation for the MIX1 and CC1 sites. In the MIX1 site, Ts described 84% of Rs variation in 2014 but only 54% in 2015. The relationship was stronger for Rh (96% and 66% in 2014 and 2015, respectively). In the case of the CC1 site, soil temperature described 72% of the variation in Rs and 66% of the variation in Rh (Fig. 6 in **II**). We found no significant direct effect of soil moisture on the Rs or Rh in both sites.

Ecosystem respiration is the sum of above-ground plant and soil respiration, the latter consisting of heterotrophic and autotrophic components (Chapin et al., 2011). In the absence of drought stress, both of these components increase with air temperature (Wang et al., 2014). GPP modifies the response of root respiration to temperature through the allometric allocation of photosynthates (Schindlbacher et al., 2009). Heterotrophic respiration also depends on the fresh litter input, as short-lived fractions of SOM are preferable energy sources for microorganisms (Schimel et al., 1994; Schulze et al., 2000). Janssens et al. (2001) found that while the air temperature was the major factor on the site scale, productivity better explained the difference in Rs between different sites.

Solar radiation is the primary environmental driver of daytime NEE. We found that LRC parameters have a clear seasonality with the maximum in summer months, and their values differ for different ecosystems (Table 4 in **I**; Fig. 8 in **III**). In heterogeneous forests, parameters of LRC may vary depending on the footprint sector from which the signal originated. In the MIX1 site, different wind direction sectors yielded slightly varying LRC parameters, while the weather conditions in the data subsets were similar (Fig. S2 in **I**). In the case of the CC1 site, LRC curves of wind sectors with forested parts and pure clearcut area (Fig. 1 in **II**) were similar under warmer temperatures (Fig. 9 in **II**), but their parameters differed.

Weather conditions modify the impact of solar radiation on carbon fluxes. The influence of air temperature on the ecosystem photosynthetic capacity ( $\text{GPP}_{\text{max}}$ ) was studied in **Article III** for MIX2, CC2, CON and DEC sites.  $\text{GPP}_{\text{max}}$  increased with temperature, but the slope varied for different sites (Fig. 9 in **III**). The smallest slope for the growing season 2017 was observed for the CON site (1.44,

$R^2=0.68$ ,  $p<0.001$ ) and the biggest for the DEC site (4.37,  $R^2=0.57$ ,  $p<0.001$ ). The MIX2 and CC2 sites had similar slopes (1.94,  $R^2=0.75$ ,  $p<0.005$  for the MIX2 site and 2.02,  $R^2=0.74$ ,  $p<0.001$  for the CC2 site). For all the four study sites, the periods with high  $T_{\text{air}}$  and VPD (green to yellow colour in Fig. 9 in **III**) and low soil moisture (small circle size) were characterised by the reduction of  $GPP_{\text{max}}$ .

Plant photosynthesis increases with air temperature until a certain value ( $T_{\text{opt}}$ ) with a subsequent decrease (Fig. 7 in **III**) due to the elevated VPD that constrains stomatal conductance (Cowan and Farquhar, 1977; McAdam and Brodribb, 2015; Novick et al., 2016). Furthermore, temperature above  $T_{\text{opt}}$  affects maximum rates of carboxylation and electron transport (von Buttlar et al., 2018).  $T_{\text{opt}}$  of the CC2 site was the highest (27 °C) out of the four study sites, but the curve had the lowest upslope. The MIX2 site showed the lowest  $T_{\text{opt}}$  (20.5 °C), but the upslope was more considerable than that of the CC2 site. The upslope was the highest for the DEC site, with  $T_{\text{opt}}$  at 22.5–24.5 °C. The CON site  $T_{\text{opt}}$  varied between 21.5–22.5 °C. The values found for our forested ecosystems fall within the range reported previously for other forests at similar latitudes (Huang et al., 2019). Bennett et al. (2021) analysed  $T_{\text{opt}}$  for a wide variety of ecosystems in Australia. They found that the mean daily  $T_{\text{air}}$  and its daytime range, and maximum GPP were the main parameters impacting the  $T_{\text{opt}}$ . The curve upslope was influenced by downwelling shortwave radiation, and the VPD influenced the downslope. It has to be noted that GPP obtained by the daytime partitioning method, used for this analysis in **Article III** is modified to account for the possible decrease under the elevated VPD as part of the flux partitioning procedure (Lasslop et al., 2010)

### 3.1.5. The heatwave influence on CO<sub>2</sub> fluxes

The effect of heatwave 2018 on CO<sub>2</sub> fluxes was studied in four ecosystems in **Article III** (the CON and DEC sites are named the same, the MIX2 is MIX, and the CC2 is CC in **III**). Already in the spring months, the air temperature was higher than in previous years (Fig. 2b). At the same time, the amount of precipitation was much lower, especially in May 2018 (Fig. 2c). Nevertheless, the SWC was still moderately high in all the study sites due to the snowmelt in March and April (Fig. 2c in **III**). High air temperature led to elevated VPD in May 2018: higher values in sites with lower SWC, the CON and CC2 sites (Fig. 2d in **III**). June 2018 was a “usual” month by air temperature and precipitation (Fig. 2b,c), but the air temperature started to increase again in July. We identified the temperature anomaly (TA) period lasting nineteen consecutive days in the second part of July (Fig. 2b). The TA was accompanied by high VPD and low SWC in the upper horizon in all the sites (Table 2 in **III**). The lowest SWC during the TA was recorded for the CC2 site, the steepest decline was observed for the DEC site. The CON site featured a low SWC during all the study period due to the sandy podzolic soil and low groundwater table. The topographic position of a site

and soil structure play an essential role in the extent to which the forest carbon exchange may be affected by rainfall reduction and drought (Kljun et al., 2006).

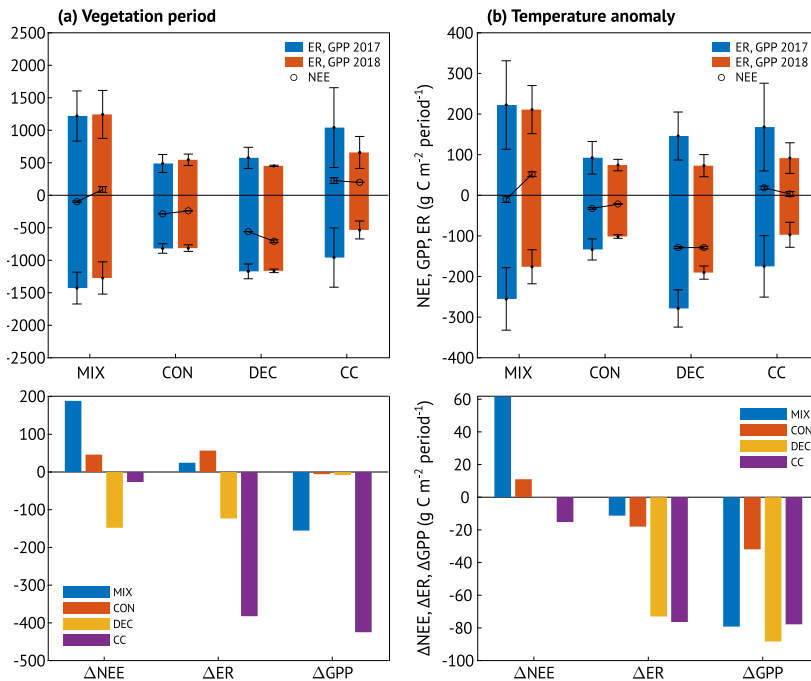


**Figure 5.** Upper panels: Accumulated net ecosystem exchange (NEE), gross primary production (GPP, negative values) and ecosystem respiration (ER, positive values) over the vegetation period (a) and temperature anomaly (b). Lower panels: the difference between the NEE, ER and GPP over the vegetation period (a) and temperature anomaly (b) in 2018 and the matching periods of 2017.

The diurnal cycle of NEE during the TA had a peak in carbon sequestration occurring earlier in the morning (Fig. 3 in **III**), as was previously observed for other ecosystems under drought conditions (Baldocchi, 1997). Such a diurnal cycle pattern persisted even after the temperature decreased for all sites except the CON site. The shape of the seasonal cycle also varied between the non-heat-wave (2017) and heatwave (2018) years for all four sites (Fig. 4 and Fig 4 in **III**).

The DEC site exhibited high GPP in spring – beginning of summer (compared to the previous year). At the same time, Reco was slightly higher in May but similar in June, leading to the higher net carbon uptake (more negative NEE) before the TA. Elevated carbon uptake in response to a warm spring was previously observed for deciduous forests in Canada (Barr et al., 2002; Black et al., 2000), various forests in the US (Wolf et al., 2016) and Europe (Smith et al., 2020). During the TA, both  $\Delta$ GPP and  $\Delta$ Reco were similar, thus gaining NEE in the same range as in the same period of the previous year (Fig. 5b). GPP and Reco remained smaller in August, but in September 2018, GPP was higher and Reco smaller than

in 2017, resulting in one more period of higher net carbon uptake. Consequently, over the growing season with the heatwave, the DEC site in our study was a stronger net carbon sink than in the previous year, gaining similar cumulative GPP but smaller Reco (Fig. 5a). The higher annual GPP and smaller Reco were also observed for an aspen forest in Canada during the first year of drought, resulting in the 2.5 times increase in net carbon uptake (Kljun et al., 2006). However, a beech forest in Denmark was characterised by a significant decrease of both GPP and Reco during the drought 2018, resulting in decreased net carbon uptake (Lindroth et al., 2020). Warmer spring conditions in the presence of available water could mitigate the effect of summer drought on the cumulative net carbon uptake (Pan and Schimel, 2016; Smith et al., 2020; Wolf et al., 2016). This effect may not be achieved as Reco also increases with temperature reducing the sink strength of the site (Barr et al., 2002).

In the case of the CON site, high temperatures of May 2018 stimulated Reco but only slightly increased GPP, thus reducing the net carbon uptake. Richardson et al. (2009) found the annual net carbon uptake increase due to the early spring to be twice higher for a deciduous-dominated forest than for a conifer-dominated one. Similar to our study, they observed that the higher spring temperature enhanced Reco in a coniferous forest more than in a deciduous forest. Both Reco and GPP in our study were reduced in July during the TA; net carbon uptake in this period was smaller as compared to the previous year (Fig 5b). However, unlike the DEC site, the CON site Reco was higher in the August and autumn months of 2018. GPP also recovered faster, and total monthly values after the TA were slightly higher than in the same months of 2017 (Fig. 4). Annual GPP was similar between the two years. As a result, the total net carbon uptake of the CON site was slightly smaller over the vegetation period and the calendar year due to the higher total Reco, while total GPP was similar to the previous year (Fig. 10c in **III**).

In the MIX2 site, both GPP and Reco were higher in May 2018 compared to 2017, but like in the CON site, Reco was more enhanced. As a result, the MIX2 site exhibited smaller net carbon uptake already in May and June 2018. Accumulated NEE of the MIX2 site during the TA period was positive, making it a net carbon source (while being net carbon sink during the same period in 2017). Both GPP and Reco were reduced, but  $\Delta$ GPP was much more prominent (Fig. 5b). After the TA, Reco gained higher monthly values in August–December 2018, while GPP was just slightly enhanced in September and October (Fig. 4). The MIX2 site was a net carbon source with higher NEE than the previous year during these months. Annually accumulated NEE was as well more elevated than over the 2017 due to lower GPP, while Reco was slightly higher (Fig. 10 in **III**). Mixed forests were previously shown to be more resilient to various biotic and abiotic disturbances (González et al., 2007; Griess and Knoke, 2011; Jactel et al., 2017; Pretzsch et al., 2013). Lower competition in the mixed forest is achieved by niche partitioning (Jucker et al., 2014) and facilitation (Ammer, 2019; Pretzsch et al., 2013; Steckel et al., 2020), especially in broadleaf-coniferous forests (Pardos et al., 2021). On the other hand, in the study of drought impact on mixed forests in

Eastern Finland, Grossiord et al. (2014) found lower soil moisture availability during the dry year in the stands composed of spruce, pine, and birch trees compared to pure coniferous forest stands. The birch competitiveness for the water resources could increase the drought exposure for spruce and pine trees. Another reason explaining the lower resistance of the mixed forest in this study could be the presence of clear-cuts. Judging by the shape of the NEE seasonal cycle (Fig 4b), their influence on the overall forest carbon balance might have been underestimated, especially in the second part of the year.

The CC2 site was a net carbon source during all months of 2017, while in June and July 2018, the total monthly NEE was negative (Fig 4b). Unlike the three forested sites in our study, the clear-cut area accumulated GPP and Reco were lower in all the months of 2018 compared to 2017. Warmer spring 2018 did not lead to the increase in either of the carbon balance components; a short net carbon uptake period in the end of May – the beginning of June was caused by the reduction of Reco (Fig. 4 in **III**). Already in spring 2018, SWC of the CC2 site was much lower than in other sites and went to near-zero values during the TA (Fig. 2 in **III**). Young trees plantation was previously shown to speed up the clear-cut recovery (Aguilos et al., 2014). In the absence of drought stress, temperature increase could positively affect the carbon uptake of the birch seedlings (Kellomäki and Wang, 2001; Pumpanen et al., 2012). However, water limitation and other stresses impact are more severe for young trees as they lack non-structural carbohydrates (Niinemets, 2010) and more shallow roots limit the access to deeper soil water table (Chan et al., 2018). Over the vegetation period, the CC2 site had the highest absolute  $\Delta$ GPP and  $\Delta$ Reco out of all the studied sites and thus was the most vulnerable to the heatwave impact (Fig 5).

Our findings describe the state of the ecosystems' carbon balance before and during the heatwave year. It was previously shown that the impact of the weather extremes is more severe during the time after the events took place (Kljun et al., 2006; van der Molen et al., 2011). Lower GPP leads to lower carbohydrate reserves in trees that can manifest in the decrease in plant growth, leaf area, and plant resilience to possible new disturbances over the upcoming years (Bréda et al., 2006)

We demonstrated that a broadleaf-coniferous mixed forest with clear-cuts within the hemiboreal zone might not be more resistant to the weather extremes than a pure coniferous forest. Heat-drought combination, in particular, may push it towards becoming a more substantial net source of CO<sub>2</sub>. A riparian alder forest could act as a booster for the net carbon uptake, albeit a short-lived one due to the usual life cycle and usage of such forest stands. Low but stable carbon sink might be supported by upland coniferous forests acclimated to low soil moisture in the upper soil level. We found a clear-cut, even with tree seedlings, to be the most vulnerable to the weather extremes; thus, the increase in forest harvesting of this type can be detrimental to balancing the hemiboreal zone carbon footprint.

### 3.2. Methane fluxes in a hemiboreal riparian forest (Article IV)

The study of CH<sub>4</sub> fluxes in a riparian alder forest (the DEC site) was conducted from September 2017 till the end of 2019 (soil and ecosystem (EC) fluxes) and published in **Article IV** (Mander et al., 2022). Stem fluxes were measured till the end of 2018. Environmental conditions in 2019 were milder compared to 2018, with lower air temperatures and higher precipitation (Fig. 6, upper panel). During the study period, the highest ecosystem CH<sub>4</sub> emission was observed in autumn-winter 2017/2018, when SWC was similarly elevated (Fig. 6). In late spring-summer 2018, when SWC was the lowest, ecosystem CH<sub>4</sub> flux remarkably varied with CH<sub>4</sub> consumption and release periods. It has to be noted that due to technical difficulties, a considerable portion of EC fluxes in the second part of summer 2018 (Fig. 8 in **IV**) was gap-filled (MDS methodology, Wutzler et al., 2018). On most days of the autumn 2018 – spring 2019, the forest was a net sink of methane, followed by much more variable but on average negative fluxes in summer and autumn 2019. Soil CH<sub>4</sub> fluxes followed a more apparent seasonal cycle, switching between a consistent source and sink periods (Fig. 6, lower panel). The stems were always a net methane source with a clear maximum in the wet period and close to zero values during the dry period and the rest of 2018.

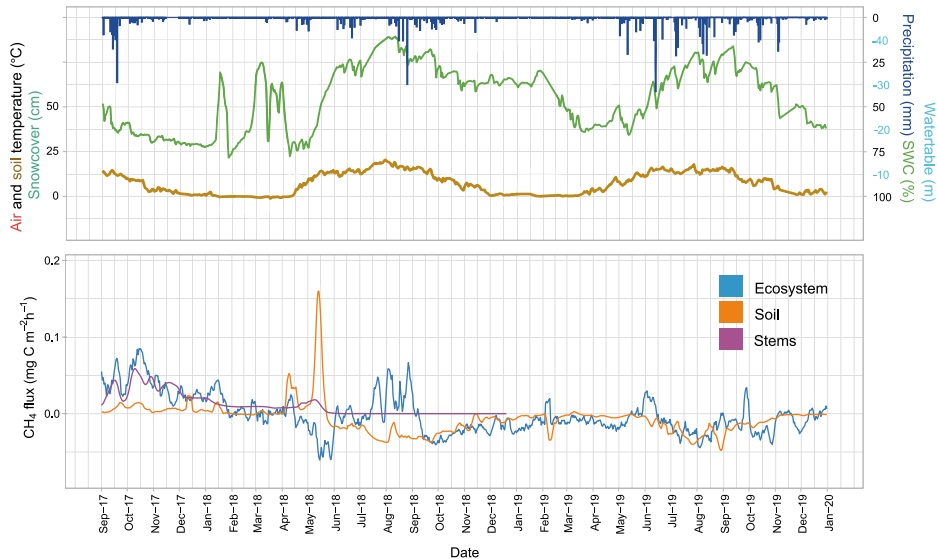


**Figure 6.** The dynamics of environmental characteristics (upper panel) and CH<sub>4</sub> fluxes from soil, stem and ecosystem level (lower panel) in the DEC site. Lines of CH<sub>4</sub> fluxes denote 5-day median values; the shaded area shows 25<sup>th</sup> and 75<sup>th</sup> percentiles. Source: Article IV, Figure 2.

Not all the variability in soil CH<sub>4</sub> fluxes was successfully “mapped” in the ecosystem scale flux. The most noticeable peak of soil CH<sub>4</sub> emission observed in spring 2018 was not reflected in ecosystem net flux; moreover, the average ecosystem flux during this period was negative (Figure , lower panel). One of the likely explanations is methodological constraints, as the corresponding period was characterised by the increased amount of “calm” nights when methane released from soil could stay undetected by the eddy-covariance system in the absence of sufficient mixing. Furthermore, the limitations of the chamber method described above (see Chapter 3.1.3) are also valid for methane flux chamber measurements. Microbial CH<sub>4</sub> consumption within the canopy (Putkinen et al., 2021) and canopy microclimatological conditions could contribute to this effect (Mikkelsen et al., 2011). Further detailed study of CH<sub>4</sub> flux movement under and within the canopy is needed (Rebmann et al., 2018).

On an annual scale, the riparian forest in our study was a minor net CH<sub>4</sub> sink, with the sum of the ecosystem-scale flux of  $-43$  and  $-96$  mg CH<sub>4</sub>-C m<sup>-2</sup> y<sup>-1</sup> in 2018 and 2019, respectively. These values are smaller than was previously reported for various forests (Flanagan et al., 2021; Nakai et al., 2020; Shoemaker et al., 2014 and Table S2 in IV). On the other hand, our site released 344 mg CH<sub>4</sub>-C m<sup>-2</sup> over the span of four months in September-December 2017. Accumulated soil methane flux for the same period was only 62 mg CH<sub>4</sub>-C m<sup>-2</sup> period<sup>-1</sup> while stems released a total of 285 mg CH<sub>4</sub>-C m<sup>-2</sup> period<sup>-1</sup>. Over 2018, soil methane uptake was  $-54$  mg CH<sub>4</sub>-C m<sup>-2</sup> year<sup>-1</sup> and stem flux methane release was 38 mg CH<sub>4</sub>-C m<sup>-2</sup> year<sup>-1</sup>. Total soil flux for 2019 was very close to ecosystem-scale flux ( $-91$  and  $-96$  mg CH<sub>4</sub>-C m<sup>-2</sup> y<sup>-1</sup> for soil and ecosystem fluxes, respectively).

According to the water regime, upland forest soils are usually methane sinks (Dlugokencky et al., 2011; Dutaur and Verchot, 2007; Saunio et al., 2020), while wetland forest soils are considerable sources of CH<sub>4</sub> (Covey and Megonigal, 2019; Salm et al., 2012; Turetsky et al., 2014). Riparian forests are located at the interface between aquatic and upland environments bearing the features of both (Gregory et al., 1991; Naiman and Décamps, 1997). Variation in aerobic and anaerobic conditions and a high supply of carbon from surface and ground water can result in methane hot spots formation (Hagedorn and Bellamy, 2011; McClain et al., 2003; Sommer, 2006). Consequently, the variability of CH<sub>4</sub> sinks and sources within an EC tower footprint area in a riparian forest could lead to a close to neutral annually accumulated net methane flux and reflect the discrepancy between the point-based measurements by chamber method and spatially integrated approach of EC technique.

Recently established methane exchange between forest plants and the atmosphere suggests that the net methane sink capacity of the forest might decrease (Covey and Megonigal, 2019; Feng et al., 2020; Pitz and Megonigal, 2017). Over the wet period in our study, stems CH<sub>4</sub> emissions exceeded soil fluxes and contributed 83% to the ecosystem flux. Flanagan et al. (2021) analysed soil, stem and ecosystem methane fluxes in a riparian forest in Canada. They found that the positive CH<sub>4</sub> emissions from stems offset the soil methane consumption. Although some studies suggest direct methane production in stems (Barba et al., 2021, 2019;

Yip et al., 2019), we found that CH<sub>4</sub> was more likely to be produced in soil and transported to the atmosphere through trees. This is further confirmed by a negative correlation between stem CH<sub>4</sub> fluxes and groundwater oxygen concentration and the decrease in stem flux with height (Fig. 7 in **IV**).

The soil water content was the main environmental factor that determined the fluxes of all the compartments with a strong positive correlation (Fig. 4 in **IV**). A high water table provides the anaerobic conditions required for methanogenesis in soil (Feng et al., 2020; Le Mer and Roger, 2001). The highest soil fluxes were observed in an SWC range of 0.4–0.5 m<sup>3</sup> m<sup>-3</sup>, while the optimum for the stems was around 0.6–0.7 m<sup>3</sup> m<sup>-3</sup> of SWC (Supplementary Fig. 4 in **IV**). This difference was reflected in the ecosystem scale flux with the maximum values in the SWC range of 0.45 to 0.65 m<sup>3</sup> m<sup>-3</sup> (Supplementary Fig. 5 in **IV**), illustrating a likely reciprocal alteration of the role of soil and tree stems in the total ecosystem flux depending on soil water conditions. Soil moisture was also previously found to be a major driver of soil CH<sub>4</sub> fluxes in both upland and wetland soils (del Grosso et al., 2000; Dutaur and Verchot, 2007; Jungkunst et al., 2008; Sakabe et al., 2018; Shoemaker et al., 2014; Smith et al., 2000), tree stems (Barba et al., 2019; Pitz et al., 2018; Schindler et al., 2020) and ecosystem-scale fluxes (Hommeltenberg et al., 2014; Iwata et al., 2015; Nakai et al., 2020; Wong et al., 2018).

The temperature was the second influencing factor for both soil and stems (negative correlation) with no impact on the ecosystem methane flux (Fig. 4 in **IV**). The increase in soil methane uptake with soil temperature is most likely related to the concurrent decrease in soil moisture and the rise in soil diffusivity (Dijkstra et al., 2012; Peterjohn et al., 1994; Sjögersten and Wookey, 2002). The lack of a strong correlation between half-hourly air temperature and ecosystem CH<sub>4</sub> flux was also previously shown for a larch forest in Siberia (Nakai et al., 2020) and a temperate forest in Canada (Wang et al., 2013).

The influence of temperature on ecosystem methane fluxes depends on the soil water content, season, and time scale. Iwata et al. (2015) found a significant positive correlation between soil temperature and ecosystem CH<sub>4</sub> fluxes observed for wet parts of a spruce forest in Alaska, while dry parts exhibited no influence. Similarly, Hommeltenberg et al. (2014) reported a positive correlation between CH<sub>4</sub> production and air temperature in the wetland forest in Germany, but only for periods with a high water table. Desai et al. (2015) studied CH<sub>4</sub> fluxes from a tall tower over a mixed landscape with forested areas and open wetlands in the US. They found no air temperature impact on the hourly and monthly scales but a strong positive impact on the daily and weekly values. Savi et al. (2016) demonstrated that the leading environmental drivers of the ecosystem CH<sub>4</sub> fluxes varied not only with the time scale but also with the season. In spring/summer, half-hourly fluxes in their study correlated the most with stomatal conductance and global radiation, while at the daily scale, the air temperature and RH were positively correlated in addition to stomatal conductance. On the other hand, in autumn/winter, VPD had the strongest positive correlation with CH<sub>4</sub> fluxes on both the half-hour and daily scales. The second strongest factor was SWC on a half-hourly scale and RH on a daily scale. The authors highlighted the fact the air

temperature on a daily scale had a positive correlation with ecosystem CH<sub>4</sub> during the spring/summer period and a negative correlation in autumn/winter, and suggested that water availability controls the sign of temperature influence.

Our study demonstrates that the ecosystem scale CH<sub>4</sub> flux in a riparian alder forest results from a complex array of plant and soil processes, varying greatly in both source and sink directions depending on the season and the combination of environmental conditions. A more comprehensive understanding of the forest CH<sub>4</sub> cycle, the interdependence of its compartments and their response to the environmental drivers is needed to forecast the possible variability in methane sink strength in light of the changing climate.

### **3.3. Nitrous oxide fluxes in a hemiboreal riparian forest (Article V)**

We studied N<sub>2</sub>O flux from the three compartments of the DEC site (soil, stems and ecosystem) from September 2017 till December 2019 (till December 2018 for the stem fluxes). The results are presented in **Article V** (Mander et al., 2021). Soil N<sub>2</sub>O fluxes were the most variable out of three compartments, with predominantly positive fluxes and prominent peaks of N<sub>2</sub>O emission (Fig. 7). McClain et al. (2003) termed such brief periods of time with disproportionately high reaction rates the “hot moments”. The highest and the most noticeable hot moment of soil N<sub>2</sub>O emission (almost eight times higher than the period average) was observed in May 2018. The increased soil N<sub>2</sub>O emission rates were measured from the majority of soil chambers (Supplementary Fig. 3 in **V**) during the onset of the drought in the absence of precipitation but were not reflected in the ecosystem scale. We found a strong negative correlation ( $r = -0.93$ ) between the speed of SWC decrease and soil N<sub>2</sub>O flux (Supplementary Fig. 7a in **V**) during this hot moment. The presence of peaks and hot moments in soil N<sub>2</sub>O fluxes in relation to changes in SWC was previously observed for various agricultural and forest soils (e.g. Anthony and Silver, 2021; Jungkunst et al., 2004; Parkin and Kaspar, 2006), the incubation (Harrison-Kirk et al., 2013) and plot experiments (Leitner et al., 2017). Temporary waterlogging, observed in our site in May 2018, and drying and rewetting cycles create beneficial conditions for the transition from microbial oxygen to NO<sub>3</sub> respiration (Barrat et al., 2020; Butterbach-Bahl et al., 2013; Groffman et al., 2009). Likewise, fluctuating SWC in the autumn months of 2017 created anaerobic conditions resulting in elevated N<sub>2</sub>O emission rates in both soil and ecosystem, although with smaller emission peaks if compared to May 2018 (Fig. 7).

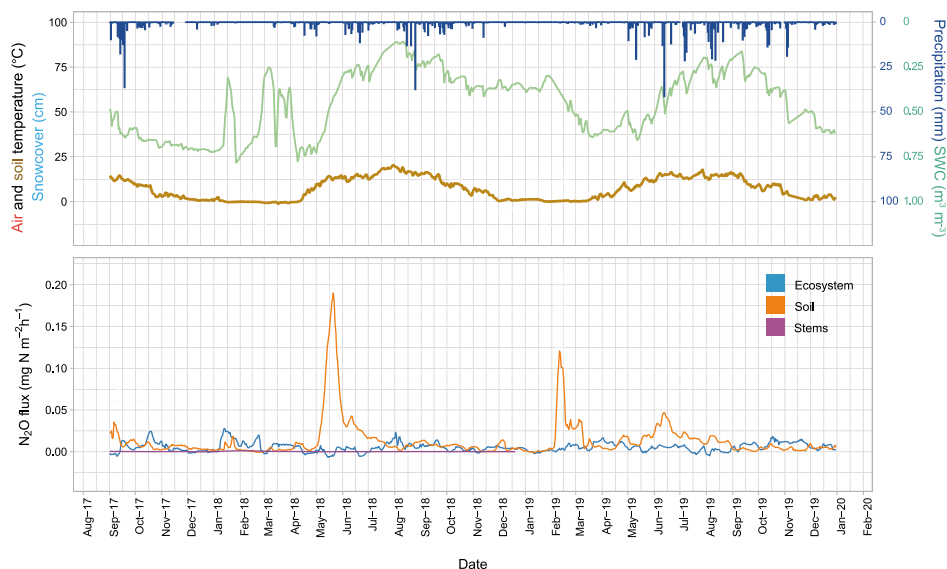


**Figure 7.** Dynamics of ecosystem-level  $\text{N}_2\text{O}$  fluxes in the riparian alder forest (the DEC site) during the study period Sep 2017–Dec 2019. Lines are 5-day median values, and shaded areas are 25th and 75th percentiles. The air temperature was measured at 50 cm from the soil surface, representing the near-ground air temperature. Note that the origins are on opposite ends of the left- and right-side axes. Source: Article V, Figure 1.

The second-largest observed soil  $\text{N}_2\text{O}$  emission hot moment was recorded in February 2019, when the air temperature varied around zero degrees C, resulting in the snow melting and SWC increase and freeze-thaw conditions (Fig. 7). The peaks in  $\text{N}_2\text{O}$  emission rates during freeze-thaw periods were previously reported for various ecosystems: croplands and arable fields (Johnson et al., 2010; Regina et al., 2004; Wagner-Riddle et al., 2017), grasslands and steppe (Holst et al., 2008; Müller et al., 2002; Wolf et al., 2010), wetlands (Yu et al., 2007) and forest soils (Guckland et al., 2010; Papen and Butterbach-Bahl, 1999; Wolf et al., 2010). In frozen soil, a part of soil water remains in liquid form, and the lack of oxygen supply creates favourable conditions for denitrification (Öquist et al., 2004). The disruption of soil aggregates during the freeze-thaw cycle exposes physically protected organic matter (Chen et al., 2020; Urakawa et al., 2014). Moreover, the death of fine roots and microorganisms creates additional rapidly decomposable organic matter (Christensen and Christensen, 1991; Christensen and Tiedje, 1990). Increased concentrations of soil  $\text{N}_2\text{O}$  trapped during freezing are released to the atmosphere when the ice is melting over a short period, resulting in a hot moment of  $\text{N}_2\text{O}$  emission (Teepe et al., 2001). Furthermore, our site exhibited increased soil  $\text{N}_2\text{O}$  emissions following the freeze-thaw peak in winter 2019. In a laboratory study, Öquist et al. (2004) discovered that denitrification processes still occurred in the anoxic parts of frozen boreal forest soils.

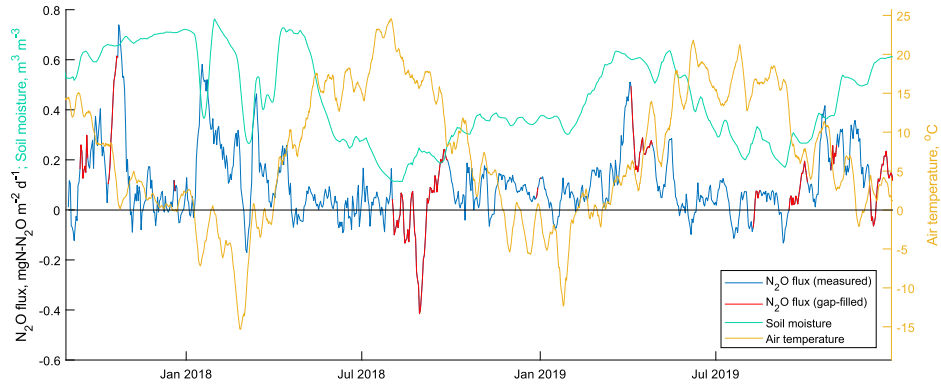


**Figure 8.** Temporal dynamics of ecosystem (eddy covariance) N<sub>2</sub>O flux, soil water content and air temperature in the Agali riparian grey alder forest from September 2017 to December 2019. 7-day running means are shown. Source: Article V, Supplementary figure 6.

Ecosystem N<sub>2</sub>O flux has not exhibited a distinguishable seasonal cycle but rather periods of increased emissions related to a combination of air temperature and SWC conditions (Fig. 8). Higher ecosystem fluxes were observed during the periods of changing air temperature (both increasing and decreasing), accompanied by the elevated SWC. Periods of low SWC and elevated air temperature (summer months of both study years) were characterised by near-zero N<sub>2</sub>O emissions. Nevertheless, we found no significant correlation between environmental parameters and ecosystem fluxes on a half-hourly scale over the whole measurement period.

The average yearly accumulated soil N<sub>2</sub>O flux was 208.65 mg N<sub>2</sub>O-N m<sup>-2</sup> y<sup>-1</sup> (over 2018 and 2019), almost one order of magnitude higher than the average annual ecosystem-scale N<sub>2</sub>O flux for the same period (27.7 mg N<sub>2</sub>O-N m<sup>-2</sup> y<sup>-1</sup>). The annual soil N<sub>2</sub>O flux was higher than previously reported for a temperate spruce forest in Germany (120 mg N<sub>2</sub>O-N m<sup>-2</sup> y<sup>-1</sup>, Wu et al., 2010), but more than two times smaller than soil N<sub>2</sub>O flux measured by Wen et al. (2017) in an alder forest over March–October 2015 (503.7 mg N<sub>2</sub>O-N m<sup>-2</sup> period<sup>-1</sup>). In a meta-analysis by Zhang et al. (2020), the average global forest N<sub>2</sub>O flux was reported 142.91 ± 14.1 mg N m<sup>-2</sup> year<sup>-1</sup>. Eddy covariance N<sub>2</sub>O fluxes were previously measured over agricultural lands (Hargreaves et al., 1996; Lognoul et al., 2019), grasslands (di Marco et al., 2005; Goodrich et al., 2021), mires (Hargreaves et al., 2001), and even over a rice-dominated landscape (Xie et al., 2022). Unfortunately, we found no studies of eddy-covariance N<sub>2</sub>O fluxes over similar forests for comparison with our study at the time of the manuscript preparation.

The stems were minor sources of N<sub>2</sub>O in the lower positions and small sinks in the upper ones. Compared to soil and ecosystem fluxes, stems N<sub>2</sub>O emissions were considerably smaller. Nevertheless, the periods of increased N<sub>2</sub>O emission from stems were observed in September–October 2017, January–February 2018 and June 2018 (Fig. 3 in V). Over September 2017–September 2018, stems N<sub>2</sub>O

emissions totalled  $3.64 \pm 0.18 \text{ mg N}_2\text{O-N m}^{-2} \text{ y}^{-1}$ , comprising 2% of total soil flux ( $215.5 \pm 7.7 \text{ mg N}_2\text{O-N m}^{-2} \text{ y}^{-1}$ ) and 13% of total ecosystem flux ( $28.8 \pm 5.22 \text{ mg N}_2\text{O-N m}^{-2} \text{ y}^{-1}$ ). Over the calendar year 2018, stems released  $1.97 \pm 0.11 \text{ mg N}_2\text{O-N m}^{-2} \text{ y}^{-1}$ , which was only 1% of total soil ( $196.3 \pm 7.1 \text{ mg N}_2\text{O-N m}^{-2} \text{ y}^{-1}$ ) and 8% of total ecosystem flux ( $24.30 \pm 4.07 \text{ mg N}_2\text{O-N m}^{-2} \text{ y}^{-1}$ ).

We expected ecosystem-scale measurements to represent the sum of its compartments or at least to be of the same scale of magnitude. This hypothesis was not confirmed, as soil fluxes exceeded ecosystem ones during continuous measurement periods. The notable intervals when ecosystem flux exceeded soil flux were observed in October 2017, January–February 2018, July 2018, March–April 2019, and all autumn months of 2019 (Figure 7). Neither of the soil flux hot moments described above was reflected in the ecosystem flux. A decoupling of the air masses above and below the canopy could be one of the likely explanations (Jocher et al., 2018). Such decoupling may be caused by canopy roughness and atmospheric stratification divergence across the canopy (Finnigan, 2000) as well as by the effect of a dense canopy that can suppress vertical mixing presenting a mechanical barrier (Jocher et al., 2018; Thomas et al., 2013; Wang et al., 2017). Therefore, during the periods of decoupling, an above-canopy EC system measures only a part of the total  $\text{N}_2\text{O}$  emission, while below canopy and soil emissions can be removed from the measurement volume by the horizontal advection (Belcher et al., 2008; Jocher et al., 2018; Thomas et al., 2013).

While our site is located on a relatively flat terrain, drainage flows are still possible during the low mixing periods. For example, the peaks of soil fluxes of  $\text{N}_2\text{O}$  (and  $\text{CH}_4$ , see Chapter 3.2) in May 2018 coincided with the periods of low wind speed and friction velocity. While the soil was emitting several times higher amounts of  $\text{N}_2\text{O}$ , the measured concentration above the canopy was not increased (Supplementary Fig. 8 in V). Under- and in-canopy wind measurements could be implemented to detect the decoupling periods (Thomas et al., 2013). Moreover, as canopies can alter air flows (Finnigan, 2000; Lee, 2000) and even exhibit counter gradient fluxes (Denmead and Bradley, 1985), the change in  $\text{N}_2\text{O}$  concentration in the volume below the EC system also has to be assessed in more detail, than a simplified one point-based approach (McHugh et al., 2017; Montagnani et al., 2018). Other causes, such as UV-induced photodissociation (Bao et al., 2018) and potential  $\text{N}_2\text{O}$  dissolution in atmospheric water, could also play a role. A better understanding of an  $\text{N}_2\text{O}$  budget in a riparian alder forest requires concentration profile measurements as well as canopy- and leaf-level studies.

### 3.4. Synthesis of the climate-forcing role of CO<sub>2</sub>, CH<sub>4</sub>, and N<sub>2</sub>O in hemiboreal forests

We studied GHG fluxes in a variety of forest ecosystems in the hemiboreal forest zone over the span of five years (2015–2019). The yearly accumulated fluxes represented in CO<sub>2</sub>-equivalents to assess the GHGs global warming potential over 100 years (GWP100=1 for CO<sub>2</sub>, GWP100=27.9 for CH<sub>4</sub>, and GWP100=273 for N<sub>2</sub>O; IPCC, 2021) are presented in Table 4. Carbon dioxide was the main driver of the GHG balance, with yearly values much higher than N<sub>2</sub>O and CH<sub>4</sub> of a riparian alder forest (the DEC site). While the two studied clear-cut areas (the CC1 and CC2 sites) and one mixed forest (the MIX2 site) were net annual CO<sub>2</sub> sources, their total climate forcing impact was still smaller than the joint net CO<sub>2</sub> sinks comprised of a mixed, coniferous and alder forests (the MIX1, CON, DEC sites). It has to be noted that the values under comparison are obtained from different years, one of which includes a heatwave.

**Table 4.** The annual balance of hemiboreal forests expressed in CO<sub>2</sub>-eq. (GWP100 = 1 for CO<sub>2</sub>, GWP100=27.9 for CH<sub>4</sub> and GWP100=273 for N<sub>2</sub>O; IPCC 2021). For the MIX2 and CON sites, the average values for the years 2017/2018 are presented

Site	Gas		Annual sum, g CO <sub>2</sub> -eq m <sup>-2</sup> year <sup>-1</sup>		
MIX1	CO <sub>2</sub>		-2143.60		
CC1	CO <sub>2</sub>		436.33		
CC2	CO <sub>2</sub>		1262.64		
MIX2	CO <sub>2</sub>		1066.82		
CON	CO <sub>2</sub>		-803.18		
DEC	CO <sub>2</sub>		-2326.13		
Site	Gas	Base	2018	2019	Average
DEC	CH <sub>4</sub>	EC-based	-1.60	-3.57	-2.59
		Chambers-based	-2.03	-3.41	-2.72
	N <sub>2</sub> O	EC-based	20.85	26.69	23.77
		Chambers-based	147.08	189.61	168.35

In 2018, a full calendar year of measurements was available for all three GHG in the DEC site (the 2019 CO<sub>2</sub> data of this site are subject to future publications and were not included in the thesis). The total carbon budget (all three GHGs) was -2306.89 g CO<sub>2</sub>-eq. m<sup>-2</sup> y<sup>-1</sup> for EC-based assessment of CH<sub>4</sub> and N<sub>2</sub>O, and -2181.08 g CO<sub>2</sub>-eq. m<sup>-2</sup> y<sup>-1</sup> if to use soil chambers-based CH<sub>4</sub> and N<sub>2</sub>O accumulated annual values. The DEC site was a net methane sink, but it contributed less than 0.1% to the CO<sub>2</sub>-based carbon uptake. In the case of N<sub>2</sub>O, the DEC site was a net source of nitrous oxide, but it was only 0.9% of the CO<sub>2</sub>-based sequestration. The chambers-based estimate of N<sub>2</sub>O was much higher, but it still was only 6% of CO<sub>2</sub>-based NEE. Most of the N<sub>2</sub>O emitted from the soil during the hot

moments (drought and freeze-thaw period) was not detected above the canopy, whereas the mechanisms are largely unclear (**Article V**). However, the riparian alder forest under study remained a strong net carbon sink in 2018, even when CH<sub>4</sub> and N<sub>2</sub>O fluxes were taken into account.

While a combined effect of all studied ecosystems is still below zero (i.e., carbon sequestration), clear-cutting weakens their joint sink strength. Moreover, a heatwave led to a decrease in the sink strength of the coniferous forest and an increase in source strength of the mixed one, adding to the vulnerability of the hemiboreal forests in the face of changing climate.

## 4. CONCLUSIONS

We studied six forest ecosystems varying in age (from 2–3-year-old clear-cut to a 200-year-old forest) and tree species composition (coniferous, deciduous and mixed) and growing in the geographical vicinity of a hemiboreal forest zone. A mixed spruce/birch forest (the MIX1 site) was the strongest net sink of CO<sub>2</sub>, followed closely by a riparian alder forest (the DEC site). The higher net carbon uptake resulted from lower Reco than that of the DEC site. Upland coniferous forest (the CON site) was a weaker net carbon sink and kept net carbon uptake even in the heatwave year. Both clear-cuts in our study were net sources of carbon with elevated respiration values. The mixed forest with the clear-cut areas in the footprint (the MIX2 site) exhibited similarly high Reco and a positive net result (net carbon source). The seasonal cycle of NEE was reminiscent of that of clear-cut areas, illustrating their high contribution to the forest carbon balance.

Air temperature is the primary factor affecting the ecosystem and soil respiration. The temperature response curve parameters vary between the forest ecosystems and years and exhibit apparent seasonal variability. Soil moisture conditions, especially drought, reduced the respiratory activity of all ecosystems. Solar radiation is the major driving factor of GPP, while air temperature modifies the parameters of light response curves. The ecosystem photosynthetic capacity is linearly increasing with temperature. High temperature values (above the temperature optima of the photosynthesis) accompanied by high VPD and low soil moisture lead to the GPP reduction. Light response curves parameters also differ between ecosystems and have a clear seasonality.

The studied hemiboreal forest ecosystems responded differently to the European heatwave 2018, with the photosynthesis (GPP) and respiration reduction of varying magnitude during the temperature anomaly being the only common trait. Our study demonstrated that mixed conifer-broadleaved forests might be more vulnerable to the heatwave than previously assumed, especially with clear-cut areas in the forest stand. More careful planning and forest management practices are needed in order to sustain them as carbon sinks under the influence of changing climate. Riparian alder forests could act as a shorter-term booster due to their high sink strength in combination with relatively small nitrous oxide emissions. However, they have a shorter storage capacity because of the typical lifecycle and usage of such forest stands in short-rotation forestry. The upland coniferous forest acclimated to the low soil moisture conditions is essential in sustaining a stable, albeit low, carbon sink regime. Clear-cut areas are the most vulnerable to the changes in temperature regime, especially in the absence of available soil water. A high reduction in GPP leads to the lack of carbohydrate reserves for the upcoming season and a possible increase in the number of years needed to reach the carbon compensation point. The rise of harvesting activities in the form of clear-cutting may alter the balancing of the hemiboreal zone carbon footprint.

A riparian alder forest (the DEC site) was an annual methane sink and a source of nitrous oxide, but the role of both GHG in the total climate forcing was minor

compared with the total CO<sub>2</sub> uptake. During the period of elevated soil moisture, tree stem CH<sub>4</sub> flux exceeded that of soil; the ecosystem CH<sub>4</sub> flux was equal to the sum of both, highlighting the importance of trees as conduits of soil-produced methane to the atmosphere. During the drought, the soil was a sink of methane and tree stem fluxes were close to zero; the canopy was the most likely source of CH<sub>4</sub>.

The annual dynamics of N<sub>2</sub>O was characterised by “hot moments” of gas emission comprising 56% of total soil N<sub>2</sub>O flux over 2.5 years of measurements. The change in soil water content and freeze-thaw cycles were indicated as the leading hot moments’ causes. The soil N<sub>2</sub>O variability was not reflected in ecosystem-scale flux, while stem fluxes were an order of magnitude smaller. Possible explanations include the decoupling between the under- and above the canopy processes, photochemical reactions and dissolution in canopy-space water. Complex simultaneous measurements of GHG fluxes in all compartments of a forest ecosystem are needed to fully assess the impact of N<sub>2</sub>O and CH<sub>4</sub> on the climate forcing.

In the following decades, we anticipate a global increase in the frequency of extreme weather events and disturbances causing alterations in the GHG balance of forest ecosystems. Hemiboreal forest zone has the potential for mitigating the negative impact due to the variability in forest types and their responses. However, the increase in clear-cutting is a worrying trend that can be detrimental to the whole hemiboreal zone.

## REFERENCES

- Aguilos, M., Takagi, K., Liang, N., Ueyama, M., Fukuzawa, K., Nomura, M., Kishida, O., Fukuzawa, T., Takahashi, H., Kotsuka, C., Sakai, R., Ito, K., Watanabe, Y., Fujinuma, Y., Takahashi, Y., Murayama, T., Saigusa, N., Sasa, K., 2014. Dynamics of ecosystem carbon balance recovering from a clear-cutting in a cool-temperate forest. *Agric. For. Meteorol.* 197, 26–39. <https://doi.org/10.1016/j.agrformet.2014.06.002>
- Ahti, T., Hämet-Ahti, L., Jalas, J., 1968. Vegetation zones and their sections in north-western Europe. *Ann. Bot. Fenn.* 5, 169–211.
- Allen, C.D., Breshears, D.D., McDowell, N.G., 2015. On underestimation of global vulnerability to tree mortality and forest die-off from hotter drought in the Anthropocene. *Ecosphere* 6, art129. <https://doi.org/10.1890/ES15-00203.1>
- Amiro, B.D., Barr, A.G., Barr, J.G., Black, T.A., Bracho, R., Brown, M., Chen, J., Clark, K.L., Davis, K.J., Desai, A.R., Dore, S., Engel, V., Fuentes, J.D., Goldstein, A.H., Goulden, M.L., Kolb, T.E., Lavigne, M.B., Law, B.E., Margolis, H.A., Martin, T., McCaughey, J.H., Misson, L., Montes-Helu, M., Noormets, A., Randerson, J.T., Starr, G., Xiao, J., 2010. Ecosystem carbon dioxide fluxes after disturbance in forests of North America. *J. Geophys. Res.* 115, G00K02. <https://doi.org/10.1029/2010JG001390>
- Ammer, C., 2019. Diversity and forest productivity in a changing climate. *New Phytol.* 221, 50–66. <https://doi.org/10.1111/nph.15263>
- Anthony, T.L., Silver, W.L., 2021. Hot moments drive extreme nitrous oxide and methane emissions from agricultural peatlands. *Glob. Change Biol.* 27, 5141–5153. <https://doi.org/10.1111/gcb.15802>
- Baldocchi, D., 2008. “Breathing” of the terrestrial biosphere: lessons learned from a global network of carbon dioxide flux measurement systems. *Aust. J. Bot.* 56, 1. <https://doi.org/10.1071/BT07151>
- Baldocchi, D., 1997. Measuring and modelling carbon dioxide and water vapour exchange over a temperate broad-leaved forest during the 1995 summer drought. *Plant Cell Environ.* 20, 1108–1122. <https://doi.org/10.1046/j.1365-3040.1997.d01-147.x>
- Baldocchi, D., Chu, H., Reichstein, M., 2018. Inter-annual variability of net and gross ecosystem carbon fluxes: A review. *Agric. For. Meteorol.* 249, 520–533. <https://doi.org/10.1016/j.agrformet.2017.05.015>
- Bao, T., Zhu, R., Wang, P., Ye, W., Ma, D., Xu, H., 2018. Potential effects of ultraviolet radiation reduction on tundra nitrous oxide and methane fluxes in maritime Antarctica. *Sci. Rep.* 8, 3716. <https://doi.org/10.1038/s41598-018-21881-1>
- Barba, J., Bradford, M.A., Brewer, P.E., Bruhn, D., Covey, K., van Haren, J., Megonigal, J.P., Mikkelsen, T.N., Pangala, S.R., Pihlatie, M., Poulter, B., Rivas-Ubach, A., Schadt, C.W., Terazawa, K., Warner, D.L., Zhang, Z., Vargas, R., 2019. Methane emissions from tree stems: a new frontier in the global carbon cycle. *New Phytol.* 222, 18–28. <https://doi.org/10.1111/nph.15582>
- Barba, J., Poyatos, R., Capocci, M., Vargas, R., 2021. Spatiotemporal variability and origin of CO<sub>2</sub> and CH<sub>4</sub> tree stem fluxes in an upland forest. *Glob. Change Biol.* 27, 4879–4893. <https://doi.org/10.1111/gcb.15783>
- Barr, A.G., Griffis, T.J., Black, T.A., Lee, X., Staebler, R.M., Fuentes, J.D., Chen, Z., Morgenstern, K., 2002. Comparing the carbon budgets of boreal and temperate deciduous forest stands. *Can. J. For. Res.* 32, 813–822. <https://doi.org/10.1139/x01-131>

- Barrat, H.A., Evans, J., Chadwick, D.R., Clark, I.M., Le Cocq, K., M. Cardenas, L., 2020. The impact of drought and rewetting on N<sub>2</sub>O emissions from soil in temperate and Mediterranean climates. *Eur. J. Soil Sci.* 72, 2504–2516. <https://doi.org/10.1111/ejss.13015>
- Barriopedro, D., Fischer, E.M., Luterbacher, J., Trigo, R.M., García-Herrera, R., 2011. The Hot Summer of 2010: Redrawing the Temperature Record Map of Europe. *Science* 332, 220–224. <https://doi.org/10.1126/science.1201224>
- Bastos, A., Ciais, P., Friedlingstein, P., Sitch, S., Pongratz, J., Fan, L., Wigneron, J.P., Weber, U., Reichstein, M., Fu, Z., Anthoni, P., Arneth, A., Haverd, V., Jain, A.K., Joetzjer, E., Knauer, J., Lienert, S., Loughran, T., McGuire, P.C., Tian, H., Viovy, N., Zaehle, S., 2020. Direct and seasonal legacy effects of the 2018 heat wave and drought on European ecosystem productivity. *Sci. Adv.* 6, eaba2724. <https://doi.org/10.1126/sciadv.aba2724>
- Belcher, S.E., Finnigan, J.J., Harman, I.N., 2008. Flows Through Forest Canopies in Complex Terrain. *Ecol. Appl.* 18, 1436–1453. <https://doi.org/10.1890/06-1894.1>
- Bennett, A.C., Arndt, S.K., Bennett, L.T., Knauer, J., Beringer, J., Griebel, A., Hinko-Najera, N., Liddell, M.J., Metzen, D., Pendall, E., Silberstein, R.P., Wardlaw, T.J., Woodgate, W., Haverd, V., 2021. Thermal optima of gross primary productivity are closely aligned with mean air temperatures across Australian wooded ecosystems. *Glob. Change Biol.* 27, 4727–4744. <https://doi.org/10.1111/gcb.15760>
- Bergeron, O., Margolis, H.A., Coursolle, C., Giasson, M.-A., 2008. How does forest harvest influence carbon dioxide fluxes of black spruce ecosystems in eastern North America? *Agric. For. Meteorol.* 148, 537–548. <https://doi.org/10.1016/j.agrformet.2007.10.012>
- Black, T.A., Chen, W.J., Barr, A.G., Arain, M.A., Chen, Z., Nesic, Z., Hogg, E.H., Neumann, H.H., Yang, P.C., 2000. Increased carbon sequestration by a boreal deciduous forest in years with a warm spring. *Geophys. Res. Lett.* 27, 1271–1274. <https://doi.org/10.1029/1999GL011234>
- Bond-Lamberty, B., Thomson, A., 2010. A global database of soil respiration data. *Biogeosciences* 7, 1915–1926. <https://doi.org/10.5194/bg-7-1915-2010>
- Bond-Lamberty, B., Wang, C., Gower, S.T., 2004. A global relationship between the heterotrophic and autotrophic components of soil respiration? *Glob. Change Biol.* 10, 1756–1766. <https://doi.org/10.1111/j.1365-2486.2004.00816.x>
- Bréda, N., Huc, R., Granier, A., Dreyer, E., 2006. Temperate forest trees and stands under severe drought: a review of ecophysiological responses, adaptation processes and long-term consequences. *Ann. For. Sci.* 63, 625–644. <https://doi.org/10.1051/forest:2006042>
- Buras, A., Rammig, A., Zang, C.S., 2020. Quantifying impacts of the 2018 drought on European ecosystems in comparison to 2003. *Biogeosciences* 17, 1655–1672. <https://doi.org/10.5194/bg-17-1655-2020>
- Butterbach-Bahl, K., Baggs, E.M., Dannenmann, M., Kiese, R., Zechmeister-Boltenstern, S., 2013. Nitrous oxide emissions from soils: how well do we understand the processes and their controls? *Philos. Trans. R. Soc. B Biol. Sci.* 368, 20130122. <https://doi.org/10.1098/rstb.2013.0122>
- Chan, F.C.C., Altaf Arain, M., Khomik, M., Brodeur, J.J., Peichl, M., Restrepo-Coupe, N., Thorne, R., Beamesderfer, E., McKenzie, S., Xu, B., Croft, H., Pejam, M., Trant, J., Kula, M., Skubel, R., 2018. Carbon, water and energy exchange dynamics of a young pine plantation forest during the initial fourteen years of growth. *For. Ecol. Manag.* 410, 12–26. <https://doi.org/10.1016/j.foreco.2017.12.024>

- Chapin, F.S., Matson, P.A., Vitousek, P.M., 2011. Principles of Terrestrial Ecosystem Ecology. Springer New York, New York, NY. <https://doi.org/10.1007/978-1-4419-9504-9>
- Chen, L., Chen, Z., Jia, G., Zhou, J., Zhao, J., Zhang, Z., 2020. Influences of forest cover on soil freeze-thaw dynamics and greenhouse gas emissions through the regulation of snow regimes: A comparison study of the farmland and forest plantation. *Sci. Total Environ.* 726, 138403. <https://doi.org/10.1016/j.scitotenv.2020.138403>
- Christensen, S., Christensen, B.T., 1991. Organic matter available for denitrification in different soil fractions: effect of freeze/thaw cycles and straw disposal. *J. Soil Sci.* 42, 637–647. <https://doi.org/10.1111/j.1365-2389.1991.tb00110.x>
- Christensen, S., Tiedje, J.M., 1990. Brief and vigorous N<sub>2</sub>O production by soil at spring thaw. *J. Soil Sci.* 41, 1–4. <https://doi.org/10.1111/j.1365-2389.1990.tb00039.x>
- Clough, T.J., Sherlock, R.R., Rolston, D.E., 2005. A Review of the Movement and Fate of N<sub>2</sub>O in the Subsoil. *Nutr. Cycl. Agroecosystems* 72, 3–11. <https://doi.org/10.1007/s10705-004-7349-z>
- Coursolle, C., Giasson, M.-A., Margolis, H.A., Bernier, P.Y., 2012. Moving towards carbon neutrality: CO<sub>2</sub> exchange of a black spruce forest ecosystem during the first 10 years of recovery after harvest. *Can. J. For. Res.* 42, 1908–1918. <https://doi.org/10.1139/x2012-133>
- Covey, K.R., Megonigal, J.P., 2019. Methane production and emissions in trees and forests. *New Phytol.* 222, 35–51. <https://doi.org/10.1111/nph.15624>
- Cowan, I.R., Farquhar, G.D., 1977. Stomatal function in relation to leaf metabolism and environment. *Symp. Soc. Exp. Biol.* 31, 471–505.
- Davidson, E.A., Keller, M., Erickson, H.E., Verchot, L.V., Veldkamp, E., 2000. Testing a Conceptual Model of Soil Emissions of Nitrous and Nitric Oxides. *BioScience* 50, 667–680. [https://doi.org/10.1641/0006-3568\(2000\)050\[0667:TACMOS\]2.0.CO;2](https://doi.org/10.1641/0006-3568(2000)050[0667:TACMOS]2.0.CO;2)
- Davidson, E.A., Richardson, A.D., Savage, K.E., Hollinger, D.Y., 2006. A distinct seasonal pattern of the ratio of soil respiration to total ecosystem respiration in a spruce-dominated forest. *Glob. Change Biol.* 12, 230–239. <https://doi.org/10.1111/j.1365-2486.2005.01062.x>
- del Grosso, S.J., Parton, W.J., Mosier, A.R., Ojima, D.S., Potter, C.S., Boroken, W., Brumme, R., Butterbach-Bahl, K., Crill, P.M., Dobbie, K., Smith, K.A., 2000. General CH<sub>4</sub> oxidation model and comparisons of CH<sub>4</sub> Oxidation in natural and managed systems. *Glob. Biogeochem. Cycles* 14, 999–1019. <https://doi.org/10.1029/1999GB001226>
- Denmead, O.T., Bradley, E.F., 1985. Flux-Gradient Relationships in a Forest Canopy, in: Hutchison, B.A., Hicks, B.B. (Eds.), *The Forest-Atmosphere Interaction: Proceedings of the Forest Environmental Measurements Conference Held at Oak Ridge, Tennessee, October 23–28, 1983*. Springer Netherlands, Dordrecht, pp. 421–442. [https://doi.org/10.1007/978-94-009-5305-5\\_27](https://doi.org/10.1007/978-94-009-5305-5_27)
- Desai, A.R., Xu, K., Tian, H., Weishampel, P., Thom, J., Baumann, D., Andrews, A.E., Cook, D.D., King, J.Y., Kolka, R., 2015. Landscape-level terrestrial methane flux observed from a very tall tower. *Agric. For. Meteorol.* 201 61–75 201, 61–75. <https://doi.org/10.1016/j.agrformet.2014.10.017>
- di Marco, C., Skiba, U., Weston, K., Hargreaves, K., Fowler, D., 2005. Field scale N<sub>2</sub>O flux measurements from grassland using eddy covariance. *Water Air Soil Pollut. Focus* 4, 143–149. <https://doi.org/10.1007/s11267-005-3024-x>

- Dijkstra, F.A., Prior, S.A., Runion, G.B., Torbert, H.A., Tian, H., Lu, C., Venterea, R.T., 2012. Effects of elevated carbon dioxide and increased temperature on methane and nitrous oxide fluxes: evidence from field experiments. *Front. Ecol. Environ.* 10, 520–527. <https://doi.org/10.1890/120059>
- Dlugokencky, E.J., Nisbet, E.G., Fisher, R., Lowry, D., 2011. Global atmospheric methane: budget, changes and dangers. *Philos. Trans. R. Soc. Math. Phys. Eng. Sci.* 369, 2058–2072. <https://doi.org/10.1098/rsta.2010.0341>
- Dutaur, L., Verchot, L.V., 2007. A global inventory of the soil CH<sub>4</sub> sink. *Glob. Biogeochem. Cycles* 21, n/a-n/a. <https://doi.org/10.1029/2006GB002734>
- Feng, H., Guo, J., Han, M., Wang, W., Peng, C., Jin, J., Song, X., Yu, S., 2020. A review of the mechanisms and controlling factors of methane dynamics in forest ecosystems. *For. Ecol. Manag.* 455, 117702. <https://doi.org/10.1016/j.foreco.2019.117702>
- Finnigan, J., 2000. Turbulence in Plant Canopies. *Annu. Rev. Fluid Mech.* 32, 519–571. <https://doi.org/10.1146/annurev.fluid.32.1.519>
- Flanagan, L.B., Nikkel, D.J., Scherloski, L.M., Tkach, R.E., Smits, K.M., Selinger, L.B., Rood, S.B., 2021. Multiple processes contribute to methane emission in a riparian cottonwood forest ecosystem. *New Phytol.* 229, 1970–1982. <https://doi.org/10.1111/nph.16977>
- Foken, T., Göockede, M., Mauder, M., Mahrt, L., Amiro, B., Munger, W., 2004. Post-Field Data Quality Control, in: Lee, X., Massman, W., Law, B. (Eds.), *Handbook of Micrometeorology: A Guide for Surface Flux Measurement and Analysis*, Atmospheric and Oceanographic Sciences Library. Springer Netherlands, Dordrecht, pp. 181–208. [https://doi.org/10.1007/1-4020-2265-4\\_9](https://doi.org/10.1007/1-4020-2265-4_9)
- Friedlingstein, P., O’Sullivan, M., Jones, M.W., Andrew, R.M., Hauck, J., Olsen, A., Peters, G.P., Peters, W., Pongratz, J., Sitch, S., Le Quéré, C., Canadell, J.G., Ciais, P., Jackson, R.B., Alin, S., Aragão, L.E.O.C., Arneeth, A., Arora, V., Bates, N.R., Becker, M., Benoit-Cattin, A., Bittig, H.C., Bopp, L., Bultan, S., Chandra, N., Chevallier, F., Chini, L.P., Evans, W., Florentie, L., Forster, P.M., Gasser, T., Gehlen, M., Gilfillan, D., Gkritzalis, T., Gregor, L., Gruber, N., Harris, I., Hartung, K., Haverd, V., Houghton, R.A., Ilyina, T., Jain, A.K., Joetzjer, E., Kadono, K., Kato, E., Kitidis, V., Korsbakken, J.I., Landschützer, P., Lefèvre, N., Lenton, A., Lienert, S., Liu, Z., Lombardozzi, D., Marland, G., Metzl, N., Munro, D.R., Nabel, J.E.M.S., Nakaoka, S.-I., Niwa, Y., O’Brien, K., Ono, T., Palmer, P.I., Pierrot, D., Poulter, B., Resplandy, L., Robertson, E., Rödenbeck, C., Schwinger, J., Séférian, R., Skjelvan, I., Smith, A.J.P., Sutton, A.J., Tanhua, T., Tans, P.P., Tian, H., Tilbrook, B., van der Werf, G., Vuichard, N., Walker, A.P., Wanninkhof, R., Watson, A.J., Willis, D., Wiltshire, A.J., Yuan, W., Yue, X., Zaehle, S., 2020. Global Carbon Budget 2020. *Earth Syst. Sci. Data* 12, 3269–3340. <https://doi.org/10.5194/essd-12-3269-2020>
- Froelich, N., Croft, H., Chen, J.M., Gonsamo, A., Staebler, R.M., 2015. Trends of carbon fluxes and climate over a mixed temperate–boreal transition forest in southern Ontario, Canada. *Agric. For. Meteorol.* 211–212, 72–84. <https://doi.org/10.1016/j.agrformet.2015.05.009>
- Gaumont-Guay, D., Black, T.A., Barr, A.G., Griffis, T.J., Jassal, R.S., Krishnan, P., Grant, N., Nescic, Z., 2014. Eight years of forest-floor CO<sub>2</sub> exchange in a boreal black spruce forest: Spatial integration and long-term temporal trends. *Agric. For. Meteorol.* 184, 25–35. <https://doi.org/10.1016/j.agrformet.2013.08.010>
- González, J.R., Trasobares, A., Palahí, M., Pukkala, T., 2007. Predicting stand damage and tree survival in burned forests in Catalonia (North-East Spain). *Ann. For. Sci.* 64, 733–742. <https://doi.org/10.1051/forest:2007053>

- Goodrich, J.P., Wall, A.M., Campbell, D.I., Fletcher, D., Wecking, A.R., Schipper, L.A., 2021. Improved gap filling approach and uncertainty estimation for eddy covariance N<sub>2</sub>O fluxes. *Agric. For. Meteorol.* 297, 108280. <https://doi.org/10.1016/j.agrformet.2020.108280>
- Grant, R.F., Barr, A.G., Black, T.A., Margolis, H.A., Mccaughey, J.H., Trofymow, J.A., 2010. Net ecosystem productivity of temperate and boreal forests after clearcutting—a Fluxnet-Canada measurement and modelling synthesis. *Tellus B Chem. Phys. Meteorol.* 62, 475–496. <https://doi.org/10.1111/j.1600-0889.2010.00500.x>
- Grant, R.F., Black, T.A., Humphreys, E.R., Morgenstern, K., 2007. Changes in net ecosystem productivity with forest age following clearcutting of a coastal Douglas-fir forest: testing a mathematical model with eddy covariance measurements along a forest chronosequence. *Tree Physiol.* 27, 115–131. <https://doi.org/10.1093/treephys/27.1.115>
- Greco, S., Baldocchi, D.D., 1996. Seasonal variations of CO<sub>2</sub> and water vapour exchange rates over a temperate deciduous forest. *Glob. Change Biol.* 2, 183–197. <https://doi.org/10.1111/j.1365-2486.1996.tb00071.x>
- Gregory, S.V., Swanson, F.J., McKee, W.A., Cummins, K.W., 1991. An Ecosystem Perspective of Riparian Zones: Focus on links between land and water. *BioScience* 41, 540–551. <https://doi.org/10.2307/1311607>
- Griess, V.C., Knoke, T., 2011. Growth performance, windthrow, and insects: meta-analyses of parameters influencing performance of mixed-species stands in boreal and northern temperate biomes. *Can. J. For. Res.* 41, 1141–1159. <https://doi.org/10.1139/x11-042>
- Groffman, P.M., Butterbach-Bahl, K., Fulweiler, R.W., Gold, A.J., Morse, J.L., Stander, E.K., Tague, C., Tonitto, C., Vidon, P., 2009. Challenges to incorporating spatially and temporally explicit phenomena (hotspots and hot moments) in denitrification models. *Biogeochemistry* 93, 49–77. <https://doi.org/10.1007/s10533-008-9277-5>
- Grünwald, T., Bernhofer, C., 2007. A decade of carbon, water and energy flux measurements of an old spruce forest at the Anchor Station Tharandt. *Tellus B Chem. Phys. Meteorol.* 59, 387–396. <https://doi.org/10.1111/j.1600-0889.2007.00259.x>
- Guckland, A., Corre, M.D., Flessa, H., 2010. Variability of soil N cycling and N<sub>2</sub>O emission in a mixed deciduous forest with different abundance of beech. *Plant Soil* 336, 25–38. <https://doi.org/10.1007/s11104-010-0437-8>
- Gundersen, P., Thybring, E.E., Nord-Larsen, T., Vesterdal, L., Nadelhoffer, K.J., Johannsen, V.K., 2021. Old-growth forest carbon sinks overestimated. *Nature* 591, E21–E23. <https://doi.org/10.1038/s41586-021-03266-z>
- Hadden, D., Grelle, A., 2017. Net CO<sub>2</sub> emissions from a primary boreo-nemoral forest over a 10 year period. *For. Ecol. Manag.* 398, 164–173. <https://doi.org/10.1016/j.foreco.2017.05.008>
- Hadden, D., Grelle, A., 2016. Changing temperature response of respiration turns boreal forest from carbon sink into carbon source. *Agric. For. Meteorol.* 223, 30–38. <https://doi.org/10.1016/j.agrformet.2016.03.020>
- Hagedorn, F., Bellamy, P., 2011. Hot Spots and Hot Moments for Greenhouse Gas Emissions from Soils, in: Jandl, R., Rodeghiero, M., Olsson, M. (Eds.), *Soil Carbon in Sensitive European Ecosystems*. John Wiley & Sons, Ltd, Chichester, UK, pp. 13–32. <https://doi.org/10.1002/9781119970255.ch2>
- Hargreaves, K.J., Fowler, D., Pitcairn, C.E.R., Aurela, M., 2001. Annual methane emission from Finnish mires estimated from eddy covariance campaign measurements. *Theor. Appl. Climatol.* 70, 203–213. <https://doi.org/10.1007/s007040170015>

- Hargreaves, K.J., Wienhold, F.G., Klemedtsson, L., Arah, J.R.M., Beverland, I.J., Fowler, D., Galle, B., Griffith, D.W.T., Skiba, U., Smith, K.A., Welling, M., Harris, G.W., 1996. Measurement of nitrous oxide emission from agricultural land using micrometeorological methods. *Atmos. Environ., Joint 8th CAGCP and 2nd IGAC Conference on Global Atmospheric Chemistry* 30, 1563–1571.  
[https://doi.org/10.1016/1352-2310\(95\)00468-8](https://doi.org/10.1016/1352-2310(95)00468-8)
- Harris, N.L., Gibbs, D.A., Baccini, A., Birdsey, R.A., de Bruin, S., Farina, M., Fatoyinbo, L., Hansen, M.C., Herold, M., Houghton, R.A., Potapov, P.V., Suarez, D.R., Roman-Cuesta, R.M., Saatchi, S.S., Slay, C.M., Turubanova, S.A., Tyukavina, A., 2021. Global maps of twenty-first century forest carbon fluxes. *Nat. Clim. Change* 11, 234–240. <https://doi.org/10.1038/s41558-020-00976-6>
- Harrison-Kirk, T., Beare, M.H., Meenken, E.D., Condron, L.M., 2013. Soil organic matter and texture affect responses to dry/wet cycles: Effects on carbon dioxide and nitrous oxide emissions. *Soil Biol. Biochem.* 57, 43–55.  
<https://doi.org/10.1016/j.soilbio.2012.10.008>
- Hickler, T., Vohland, K., Feehan, J., Miller, P.A., Smith, B., Costa, L., Giesecke, T., Fronzek, S., Carter, T.R., Cramer, W., Kühn, I., Sykes, M.T., 2012. Projecting the future distribution of European potential natural vegetation zones with a generalized, tree species-based dynamic vegetation model: Future changes in European vegetation zones. *Glob. Ecol. Biogeogr.* 21, 50–63.  
<https://doi.org/10.1111/j.1466-8238.2010.00613.x>
- Hiltbrunner, D., Zimmermann, S., Karbin, S., Hagedorn, F., Niklaus, P.A., 2012. Increasing soil methane sink along a 120-year afforestation chronosequence is driven by soil moisture. *Glob. Change Biol.* 18, 3664–3671.  
<https://doi.org/10.1111/j.1365-2486.2012.02798.x>
- Hollinger, D.Y., Kelliher, F.M., Byers, J.N., Hunt, J.E., McSeveny, T.M., Weir, P.L., 1994. Carbon Dioxide Exchange between an Undisturbed Old-Growth Temperate Forest and the Atmosphere. *Ecology* 75, 134–150. <https://doi.org/10.2307/1939390>
- Holst, J., Liu, C., Yao, Z., Brüggemann, N., Zheng, X., Giese, M., Butterbach-Bahl, K., 2008. Fluxes of nitrous oxide, methane and carbon dioxide during freezing–thawing cycles in an Inner Mongolian steppe. *Plant Soil* 308, 105–117.  
<https://doi.org/10.1007/s11104-008-9610-8>
- Hommeltenberg, J., Mauder, M., Drösler, M., Heidbach, K., Werle, P., Schmid, H.P., 2014. Ecosystem scale methane fluxes in a natural temperate bog-pine forest in southern Germany. *Agric. For. Meteorol.* 198–199, 273–284.  
<https://doi.org/10.1016/j.agrformet.2014.08.017>
- Huang, M., Piao, S., Ciais, P., Peñuelas, J., Wang, X., Keenan, T.F., Peng, S., Berry, J.A., Wang, K., Mao, J., Alkama, R., Cescatti, A., Cuntz, M., De Deurwaerder, H., Gao, M., He, Y., Liu, Y., Luo, Y., Myneni, R.B., Niu, S., Shi, X., Yuan, W., Verbeeck, H., Wang, T., Wu, J., Janssens, I.A., 2019. Air temperature optima of vegetation productivity across global biomes. *Nat. Ecol. Evol.* 3, 772–779.  
<https://doi.org/10.1038/s41559-019-0838-x>
- Humphreys, E.R., Andrew Black, T., Morgenstern, K., Li, Z., Nestic, Z., 2005. Net ecosystem production of a Douglas-fir stand for 3 years following clearcut harvesting. *Glob. Change Biol.* 11, 450–464. <https://doi.org/10.1111/j.1365-2486.2005.00914.x>
- Ilvesniemi, H., Levula, J., Ojansuu, R., Kolari, P., Kulmala, L., Pumpanen, J., Launiainen, S., Vesala, T., Nikinmaa, E., 2009. Long-term measurements of the carbon balance of a boreal Scots pine dominated forest ecosystem. *Boreal Environ. Res.* 14, 731–753.

- IPCC, 2021. IPCC, 2021: Climate Change 2021: The Physical Science Basis. Contribution of Working Group I to the Sixth Assessment Report of the Intergovernmental Panel on Climate Change. Cambridge University Press.
- Iwata, H., Harazono, Y., Ueyama, M., Sakabe, A., Nagano, H., Kosugi, Y., Takahashi, K., Kim, Y., 2015. Methane exchange in a poorly-drained black spruce forest over permafrost observed using the eddy covariance technique. *Agric. For. Meteorol.* 214–215, 157–168. <https://doi.org/10.1016/j.agrformet.2015.08.252>
- Jactel, H., Bauhus, J., Boberg, J., Bonal, D., Castagnyrol, B., Gardiner, B., Gonzalez-Olabarria, J.R., Koricheva, J., Meurisse, N., Brockerhoff, E.G., 2017. Tree Diversity Drives Forest Stand Resistance to Natural Disturbances. *Curr. For. Rep.* 3, 223–243. <https://doi.org/10.1007/s40725-017-0064-1>
- Janssens, I.A., Lankreijer, H., Matteucci, G., Kowalski, A.S., Buchmann, N., Epron, D., Pilegaard, K., Kutsch, W., Longdoz, B., Grünwald, T., Montagnani, L., Dore, S., Rebmann, C., Moors, E.J., Grelle, A., Rannik, Ü., Morgenstern, K., Oltchev, S., Clement, R., Guðmundsson, J., Minerbi, S., Berbigier, P., Ibrom, A., Moncrieff, J., Aubinet, M., Bernhofer, C., Jensen, N.O., Vesala, T., Granier, A., Schulze, E.-D., Lindroth, A., Dolman, A.J., Jarvis, P.G., Ceulemans, R., Valentini, R., 2001. Productivity overshadows temperature in determining soil and ecosystem respiration across European forests. *Glob. Change Biol.* 7, 269–278. <https://doi.org/10.1046/j.1365-2486.2001.00412.x>
- Jensen, R., Herbst, M., Friborg, T., 2017. Direct and indirect controls of the interannual variability in atmospheric CO<sub>2</sub> exchange of three contrasting ecosystems in Denmark. *Agric. For. Meteorol.* 233, 12–31. <https://doi.org/10.1016/j.agrformet.2016.10.023>
- Jocher, G., Marshall, J., Nilsson, M.B., Linder, S., De Simon, G., Hörnlund, T., Lundmark, T., Näsholm, T., Ottosson Löfvenius, M., Tarvainen, L., Wallin, G., Peichl, M., 2018. Impact of Canopy Decoupling and Subcanopy Advection on the Annual Carbon Balance of a Boreal Scots Pine Forest as Derived From Eddy Covariance. *J. Geophys. Res. Biogeosciences* 123, 303–325. <https://doi.org/10.1002/2017JG003988>
- Johnson, J.M.F., Archer, D., Barbour, N., 2010. Greenhouse Gas Emission from Contrasting Management Scenarios in the Northern Corn Belt. *Soil Sci. Soc. Am. J.* 74, 396–406. <https://doi.org/10.2136/sssaj2009.0008>
- Jucker, T., Bouriaud, O., Avacaritei, D., Dănilă, I., Duduman, G., Valladares, F., Coomes, D.A., 2014. Competition for light and water play contrasting roles in driving diversity–productivity relationships in Iberian forests. *J. Ecol.* 102, 1202–1213. <https://doi.org/10.1111/1365-2745.12276>
- Jungkunst, H.F., Fiedler, S., Stahr, K., 2004. N<sub>2</sub>O emissions of a mature Norway spruce (*Picea abies*) stand in the Black Forest (southwest Germany) as differentiated by the soil pattern. *J. Geophys. Res. Atmospheres* 109. <https://doi.org/10.1029/2003JD004344>
- Jungkunst, H.F., Flessa, H., Scherber, C., Fiedler, S., 2008. Groundwater level controls CO<sub>2</sub>, N<sub>2</sub>O and CH<sub>4</sub> fluxes of three different hydromorphic soil types of a temperate forest ecosystem. *Soil Biol. Biochem.* 40, 2047–2054. <https://doi.org/10.1016/j.soilbio.2008.04.015>
- Kellomäki, S., Wang, K.-Y., 2001. Growth and Resource Use of Birch Seedlings Under Elevated Carbon Dioxide and Temperature. *Ann. Bot.* 87, 669–682. <https://doi.org/10.1006/anbo.2001.1393>

- Kirschke, S., Bousquet, P., Ciais, P., Saunois, M., Canadell, J.G., Dlugokencky, E.J., Bergamaschi, P., Bergmann, D., Blake, D.R., Bruhwiler, L., Cameron-Smith, P., Castaldi, S., Chevallier, F., Feng, L., Fraser, A., Heimann, M., Hodson, E.L., Houweling, S., Josse, B., Fraser, P.J., Krummel, P.B., Lamarque, J.-F., Langenfelds, R.L., Le Quéré, C., Naik, V., O'Doherty, S., Palmer, P.I., Pison, I., Plummer, D., Poulter, B., Prinn, R.G., Rigby, M., Ringeval, B., Santini, M., Schmidt, M., Shindell, D.T., Simpson, I.J., Spahni, R., Steele, L.P., Strode, S.A., Sudo, K., Szopa, S., van der Werf, G.R., Voulgarakis, A., van Weele, M., Weiss, R.F., Williams, J.E., Zeng, G., 2013. Three decades of global methane sources and sinks. *Nat. Geosci.* 6, 813–823. <https://doi.org/10.1038/ngeo1955>
- Kljun, N., Black, T.A., Griffis, T.J., Barr, A.G., Gaumont-Guay, D., Morgenstern, K., McCaughey, J.H., Nesic, Z., 2006. Response of Net Ecosystem Productivity of Three Boreal Forest Stands to Drought. *Ecosystems* 9, 1128–1144. <https://doi.org/10.1007/s10021-005-0082-x>
- Kljun, N., Calanca, P., Rotach, M.W., Schmid, H.P., 2015. A simple two-dimensional parameterisation for Flux Footprint Prediction (FFP). *Geosci. Model Dev.* 8, 3695–3713. <https://doi.org/10.5194/gmd-8-3695-2015>
- Knohl, A., Sør, A.R.B., Kutsch, W.L., Göckede, M., Buchmann, N., 2008. Representative estimates of soil and ecosystem respiration in an old beech forest. *Plant Soil* 302, 189–202. <https://doi.org/10.1007/s11104-007-9467-2>
- Kolari, P., Pumpanen, J., Rannik, Ü., Ilvesniemi, H., Hari, P., Berninger, F., 2004. Carbon balance of different aged Scots pine forests in Southern Finland: Carbon Balance In Boreal Scots Pine Forests. *Glob. Change Biol.* 10, 1106–1119. <https://doi.org/10.1111/j.1529-8817.2003.00797.x>
- Krasnova, A., Kukumägi, M., Mander, Ü., Torga, R., Krasnov, D., Noe, S.M., Ostonen, I., Püttsepp, Ü., Killian, H., Uri, V., Lõhmus, K., Söber, J., Soosaar, K., 2019. Carbon exchange in a hemiboreal mixed forest in relation to tree species composition. *Agric. For. Meteorol.* 275, 11–23. <https://doi.org/10.1016/j.agrformet.2019.05.007>
- Krasnova, A., Mander, Ü., Noe, S.M., Uri, V., Krasnov, D., Soosaar, K., 2022. Hemiboreal forests' CO<sub>2</sub> fluxes response to the European 2018 heatwave. *Agric. For. Meteorol.*
- Kukumägi, M., Ostonen, I., Uri, V., Helmisaari, H.-S., Kanal, A., Kull, O., Lõhmus, K., 2017. Variation of soil respiration and its components in hemiboreal Norway spruce stands of different ages. *Plant Soil* 414, 265–280. <https://doi.org/10.1007/s11104-016-3133-5>
- Lasslop, G., Reichstein, M., Papale, D., Richardson, A.D., Arneeth, A., Barr, A., Stoy, P., Wohlfahrt, G., 2010. Separation of net ecosystem exchange into assimilation and respiration using a light response curve approach: critical issues and global evaluation: SEPARATION OF NEE INTO GPP AND RECO. *Glob. Change Biol.* 16, 187–208. <https://doi.org/10.1111/j.1365-2486.2009.02041.x>
- Le Mer, J., Roger, P., 2001. Production, oxidation, emission and consumption of methane by soils: A review. *Eur. J. Soil Biol.* 37, 25–50. [https://doi.org/10.1016/S1164-5563\(01\)01067-6](https://doi.org/10.1016/S1164-5563(01)01067-6)
- Lee, X., 2000. Air motion within and above forest vegetation in non-ideal conditions. *For. Ecol. Manag.* 135, 3–18. [https://doi.org/10.1016/S0378-1127\(00\)00294-2](https://doi.org/10.1016/S0378-1127(00)00294-2)
- Leitner, S., Homyak, P.M., Blankinship, J.C., Eberwein, J., Jenerette, G.D., Zechmeister-Boltenstern, S., Schimel, J.P., 2017. Linking NO and N<sub>2</sub>O emission pulses with the mobilization of mineral and organic N upon rewetting dry soils. *Soil Biol. Biochem.* 115, 461–466. <https://doi.org/10.1016/j.soilbio.2017.09.005>

- Leon, E., Vargas, R., Bullock, S., Lopez, E., Panosso, A.R., La Scala, N., 2014. Hot spots, hot moments, and spatio-temporal controls on soil CO<sub>2</sub> efflux in a water-limited ecosystem. *Soil Biol. Biochem.* 77, 12–21.  
<https://doi.org/10.1016/j.soilbio.2014.05.029>
- Lindroth, A., Holst, J., Heliasz, M., Vestin, P., Lagergren, F., Biermann, T., Cai, Z., Mölder, M., 2018. Effects of low thinning on carbon dioxide fluxes in a mixed hemiboreal forest. *Agric. For. Meteorol.* 262, 59–70.  
<https://doi.org/10.1016/j.agrformet.2018.06.021>
- Lindroth, A., Holst, J., Linderson, M.-L., Aurela, M., Biermann, T., Heliasz, M., Chi, J., Ibrom, A., Kolari, P., Klemedtsson, L., Krasnova, A., Laurila, T., Lehner, I., Lohila, A., Mammarella, I., Mölder, M., Löfvenius, M.O., Peichl, M., Pilegaard, K., Soosaar, K., Vesala, T., Vestin, P., Weslien, P., Nilsson, M., 2020. Effects of drought and meteorological forcing on carbon and water fluxes in Nordic forests during the dry summer of 2018. *Philos. Trans. R. Soc. B Biol. Sci.* 375, 20190516.  
<https://doi.org/10.1098/rstb.2019.0516>
- Liu, X., Dong, W., Wood, J.D., Wang, Y., Li, X., Zhang, Y., Hu, C., Gu, L., 2022. Aboveground and belowground contributions to ecosystem respiration in a temperate deciduous forest. *Agric. For. Meteorol.* 314, 108807.  
<https://doi.org/10.1016/j.agrformet.2022.108807>
- Livingston, G.P., Hutchinson, G.L., 1995. Enclosure-based measurement of trace gas exchange: Applications and sources of error, in: Matson, P.A., Harriss, R.C. (Eds.), *Biogenic Trace Gases: Measuring Emissions from Soil and Water*. Blackwell Science Ltd, Oxford, UK, pp. 14–51.
- Lloyd, J., Taylor, J.A., 1994. On the Temperature Dependence of Soil Respiration. *Funct. Ecol.* 8, 315. <https://doi.org/10.2307/2389824>
- Lognoul, M., Debaq, A., De Ligne, A., Dumont, B., Manise, T., Bodson, B., Heinesch, B., Aubinet, M., 2019. N<sub>2</sub>O flux short-term response to temperature and topsoil disturbance in a fertilized crop: An eddy covariance campaign. *Agric. For. Meteorol.* 271, 193–206. <https://doi.org/10.1016/j.agrformet.2019.02.033>
- Lõhmus, A., Kraut, A., 2010. Stand structure of hemiboreal old-growth forests: Characteristic features, variation among site types, and a comparison with FSC-certified mature stands in Estonia. *For. Ecol. Manag.* 260, 155–165.  
<https://doi.org/10.1016/j.foreco.2010.04.018>
- Luyssaert, S., Ciais, P., Piao, S.L., Schulze, E.-D., Jung, M., Zaehle, S., Schelhaas, M.J., Reichstein, M., Churkina, G., Papale, D., Abril, G., Beer, C., Grace, J., Loustau, D., Matteucci, G., Magnani, F., Nabuurs, G.J., Verbeeck, H., Sulkava, M., van der Werf, G.R., Janssens, I.A., members of the CARBOEUROPE-IP SYNTHESIS TEAM, 2010. The European carbon balance. Part 3: forests. *Glob. Change Biol.* 16, 1429–1450. <https://doi.org/10.1111/j.1365-2486.2009.02056.x>
- Luyssaert, S., Schulze, E.-D., Börner, A., Knohl, A., Hessenmöller, D., Law, B.E., Ciais, P., Grace, J., 2008. Old-growth forests as global carbon sinks. *Nature* 455, 213–215. <https://doi.org/10.1038/nature07276>
- Machacova, K., Bäck, J., Vanhatalo, A., Halmeenmäki, E., Kolari, P., Mammarella, I., Pumpanen, J., Acosta, M., Urban, O., Pihlatie, M., 2016. *Pinus sylvestris* as a missing source of nitrous oxide and methane in boreal forest. *Sci. Rep.* 6, 23410.  
<https://doi.org/10.1038/srep23410>
- Machacova, K., Maier, M., Svobodova, K., Lang, F., Urban, O., 2017. Cryptogamic stem covers may contribute to nitrous oxide consumption by mature beech trees. *Sci. Rep.* 7, 13243. <https://doi.org/10.1038/s41598-017-13781-7>

- Mamkin, V., Kurbatova, J., Avilov, V., Ivanov, D., Kuricheva, O., Varlagin, A., Yaseneva, I., Olchev, A., 2019. Energy and CO<sub>2</sub> exchange in an undisturbed spruce forest and clear-cut in the Southern Taiga. *Agric. For. Meteorol.* 265, 252–268. <https://doi.org/10.1016/j.agrformet.2018.11.018>
- Mander, Ü., Krasnova, A., Escuer-Gatius, J., Espenberg, M., Schindler, T., Machacova, K., Pärn, J., Maddison, M., Megonigal, J.P., Pihlatie, M., Kasak, K., Niinemets, Ü., Junninen, H., Soosaar, K., 2021. Forest canopy mitigates soil N<sub>2</sub>O emission during hot moments. *Npj Clim. Atmospheric Sci.* 4, 39. <https://doi.org/10.1038/s41612-021-00194-7>
- Mander, Ü., Krasnova, A., Schindler, T., Megonigal, J.P., Escuer-Gatius, J., Espenberg, M., Machacova, K., Maddison, M., Pärn, J., Ranniku, R., Pihlatie, M., Kasak, K., Niinemets, Ü., Soosaar, K., 2022. Long-term dynamics of soil, tree stem and ecosystem methane fluxes in a riparian forest. *Sci. Total Environ.* 809, 151723. <https://doi.org/10.1016/j.scitotenv.2021.151723>
- Mander, Ü., Löhmus, K., Teiter, S., Uri, V., Augustin, J., 2008. Gaseous nitrogen and carbon fluxes in riparian alder stands. *Boreal Environ. Res.* 13, 231–241.
- Martin, T.L., Kaushik, N.K., Trevors, J.T., Whiteley, H.R., 1999. Review: Denitrification in temperate climate riparian zones. *Water. Air. Soil Pollut.* 111, 171–186. <https://doi.org/10.1023/A:1005015400607>
- Mauder, M., Cuntz, M., Drüe, C., Graf, A., Rebmann, C., Schmid, H.P., Schmidt, M., Steinbrecher, R., 2013. A strategy for quality and uncertainty assessment of long-term eddy-covariance measurements. *Agric. For. Meteorol.* 169, 122–135. <https://doi.org/10.1016/j.agrformet.2012.09.006>
- McAdam, S.A.M., Brodribb, T.J., 2015. The evolution of mechanisms driving the stomatal response to vapor pressure deficit. *Plant Physiol.* 167, 833–843. <https://doi.org/10.1104/pp.114.252940>
- McClain, M.E., Boyer, E.W., Dent, C.L., Gergel, S.E., Grimm, N.B., Groffman, P.M., Hart, S.C., Harvey, J.W., Johnston, C.A., Mayorga, E., McDowell, W.H., Pinay, G., 2003. Biogeochemical Hot Spots and Hot Moments at the Interface of Terrestrial and Aquatic Ecosystems. *Ecosystems* 6, 301–312. <https://doi.org/10.1007/s10021-003-0161-9>
- McHugh, I.D., Beringer, J., Cunningham, S.C., Baker, P.J., Cavagnaro, T.R., Mac Nally, R., Thompson, R.M., 2017. Interactions between nocturnal turbulent flux, storage and advection at an “ideal” eucalypt woodland site. *Biogeosciences* 14, 3027–3050. <https://doi.org/10.5194/bg-14-3027-2017>
- Mikkelsen, T.N., Bruhn, D., Ambus, P., Larsen, K.S., Ibrom, I., Pilegaard, K., 2011. Is methane released from the forest canopy? *IForest – Biogeosciences For.* 4, 200. <https://doi.org/10.3832/ifor0591-004>
- Mkhabela, M.S., Amiro, B.D., Barr, A.G., Black, T.A., Hawthorne, I., Kidston, J., McCaughey, J.H., Orchansky, A.L., Nesic, Z., Sass, A., Shashkov, A., Zha, T., 2009. Comparison of carbon dynamics and water use efficiency following fire and harvesting in Canadian boreal forests. *Agric. For. Meteorol.* 149, 783–794. <https://doi.org/10.1016/j.agrformet.2008.10.025>
- Montagnani, L., Grünwald, T., Kowalski, A., Mammarella, I., Merbold, L., Metzger, S., Sedláč, P., Siebicke, L., 2018. Estimating the storage term in eddy covariance measurements: the ICOS methodology. *Int. Agrophysics* 32, 551–567. <https://doi.org/10.1515/intag-2017-0037>

- Müller, C., Martin, M., Stevens, R.J., Laughlin, R.J., Kammann, C., Ottow, J.C.G., Jäger, H.-J., 2002. Processes leading to N<sub>2</sub>O emissions in grassland soil during freezing and thawing. *Soil Biol. Biochem.* 34, 1325–1331.  
[https://doi.org/10.1016/S0038-0717\(02\)00076-7](https://doi.org/10.1016/S0038-0717(02)00076-7)
- Murphy, R.M., Richards, K.G., Krol, D.J., Gebremichael, A.W., Lopez-Sangil, L., Rambaud, J., Cowan, N., Lanigan, G.J., Saunders, M., 2022. Assessing nitrous oxide emissions in time and space with minimal uncertainty using static chambers and eddy covariance from a temperate grassland. *Agric. For. Meteorol.* 313, 108743.  
<https://doi.org/10.1016/j.agrformet.2021.108743>
- Naiman, R.J., Décamps, H., 1997. The Ecology of Interfaces: Riparian Zones. *Annu. Rev. Ecol. Syst.* 28, 621–658. <https://doi.org/10.1146/annurev.ecolsys.28.1.621>
- Nakai, T., Hiyama, T., Petrov, R.E., Kotani, A., Ohta, T., Maximov, T.C., 2020. Application of an open-path eddy covariance methane flux measurement system to a larch forest in eastern Siberia. *Agric. For. Meteorol.* 282–283, 107860.  
<https://doi.org/10.1016/j.agrformet.2019.107860>
- Ney, P., Graf, A., Bogena, H., Diekkrüger, B., Drüe, C., Esser, O., Heinemann, G., Klosterhalfen, A., Pick, K., Pütz, T., Schmidt, M., Valler, V., Vereecken, H., 2019. CO<sub>2</sub> fluxes before and after partial deforestation of a Central European spruce forest. *Agric. For. Meteorol.* 274, 61–74. <https://doi.org/10.1016/j.agrformet.2019.04.009>
- Ni, X., Groffman, P.M., 2018. Declines in methane uptake in forest soils. *Proc. Natl. Acad. Sci.* 115, 8587–8590. <https://doi.org/10.1073/pnas.1807377115>
- Niinemets, Ü., 2010. Responses of forest trees to single and multiple environmental stresses from seedlings to mature plants: Past stress history, stress interactions, tolerance and acclimation. *For. Ecol. Manag.* 260, 1623–1639.  
<https://doi.org/10.1016/j.foreco.2010.07.054>
- Noe, S.M., Niinemets, Ü., Krasnova, A., Krasnov, D., Motallebi, A., Kängsepp, V., Jögiste, K., Hörrak, U., Komsaare, K., Mirme, S., Vana, M., Tammet, H., Bäck, J., Vesala, T., Kulmala, M., Petäjä, T., Kangur, A., 2015. SMEAR Estonia: Perspectives of a large-scale forest ecosystem – atmosphere research infrastructure. *For. Stud.* 63, 56–84. <https://doi.org/10.1515/fsmu-2015-0009>
- Noormets, A., Epron, D., Domec, J.C., McNulty, S.G., Fox, T., Sun, G., King, J.S., 2015. Effects of forest management on productivity and carbon sequestration: A review and hypothesis. *For. Ecol. Manag.* 355, 124–140.  
<https://doi.org/10.1016/j.foreco.2015.05.019>
- Novick, K.A., Ficklin, D.L., Stoy, P.C., Williams, C.A., Bohrer, G., Oishi, A.C., Papuga, S.A., Blanken, P.D., Noormets, A., Sulman, B.N., Scott, R.L., Wang, L., Phillips, R.P., 2016. The increasing importance of atmospheric demand for ecosystem water and carbon fluxes. *Nat. Clim. Change* 6, 1023–1027.  
<https://doi.org/10.1038/nclimate3114>
- Öquist, M.G., Nilsson, M., Sörensson, F., Kasimir-Klemetsson, Å., Persson, T., Westli, P., Klemetsson, L., 2004. Nitrous oxide production in a forest soil at low temperatures – processes and environmental controls. *FEMS Microbiol. Ecol.* 49, 371–378. <https://doi.org/10.1016/j.femsec.2004.04.006>
- Pachauri, R.K., Mayer, L., Intergovernmental Panel on Climate Change (Eds.), 2015. *Climate change 2014: synthesis report*. Intergovernmental Panel on Climate Change, Geneva, Switzerland.
- Pan, Y., Schimel, D., 2016. Synergy of a warm spring and dry summer. *Nature* 534, 483–484. <https://doi.org/10.1038/nature18450>

- Papale, D., Reichstein, M., Aubinet, M., Canfora, E., Bernhofer, C., Kutsch, W., Longdoz, B., Rambal, S., Valentini, R., Vesala, T., Yakir, D., 2006. Towards a standardized processing of Net Ecosystem Exchange measured with eddy covariance technique: algorithms and uncertainty estimation. *Biogeosciences* 3, 571–583. <https://doi.org/10.5194/bg-3-571-2006>
- Papen, H., Butterbach-Bahl, K., 1999. A 3-year continuous record of nitrogen trace gas fluxes from untreated and limed soil of a N-saturated spruce and beech forest ecosystem in Germany: 1. N<sub>2</sub>O emissions. *J. Geophys. Res. Atmospheres* 104, 18487–18503. <https://doi.org/10.1029/1999JD900293>
- Pardos, M., del Río, M., Pretzsch, H., Jactel, H., Bielak, K., Bravo, F., Brazaitis, G., Defosse, E., Engel, M., Godvod, K., Jacobs, K., Jansone, L., Jansons, A., Morin, X., Nothdurft, A., Oreti, L., Ponette, Q., Pach, M., Riofrío, J., Ruíz-Peinado, R., Tomao, A., Uhl, E., Calama, R., 2021. The greater resilience of mixed forests to drought mainly depends on their composition: Analysis along a climate gradient across Europe. *For. Ecol. Manag.* 481, 118687. <https://doi.org/10.1016/j.foreco.2020.118687>
- Parkin, T.B., Kaspar, T.C., 2006. Nitrous Oxide Emissions from Corn–Soybean Systems in the Midwest. *J. Environ. Qual.* 35, 1496–1506. <https://doi.org/10.2134/jeq2005.0183>
- Peichl, M., Arain, M.A., Brodeur, J.J., 2010. Age effects on carbon fluxes in temperate pine forests. *Agric. For. Meteorol.* 150, 1090–1101. <https://doi.org/10.1016/j.agrformet.2010.04.008>
- Perkins, S.E., Alexander, L.V., 2013. On the Measurement of Heat Waves. *J. Clim.* 26, 4500–4517. <https://doi.org/10.1175/JCLI-D-12-00383.1>
- Perkins-Kirkpatrick, S.E., Gibson, P.B., 2017. Changes in regional heatwave characteristics as a function of increasing global temperature. *Sci. Rep.* 7, 12256. <https://doi.org/10.1038/s41598-017-12520-2>
- Peterjohn, W.T., Melillo, J.M., Steudler, P.A., Newkirk, K.M., Bowles, F.P., Aber, J.D., 1994. Responses of Trace Gas Fluxes and N Availability to Experimentally Elevated Soil Temperatures. *Ecol. Appl.* 4, 617–625. <https://doi.org/10.2307/1941962>
- Peters, W., Bastos, A., Ciais, P., Vermeulen, A., 2020. A historical, geographical and ecological perspective on the 2018 European summer drought. *Philos. Trans. R. Soc. B Biol. Sci.* 375, 20190505. <https://doi.org/10.1098/rstb.2019.0505>
- Pihlatie, M., Ambus, P., Rinne, J., Pilegaard, K., Vesala, T., 2005. Plant-mediated nitrous oxide emissions from beech (*Fagus sylvatica*) leaves. *New Phytol.* 168, 93–98. <https://doi.org/10.1111/j.1469-8137.2005.01542.x>
- Pitz, S., Megonigal, J.P., 2017. Temperate forest methane sink diminished by tree emissions. *New Phytol.* 214, 1432–1439. <https://doi.org/10.1111/nph.14559>
- Pitz, S.L., Megonigal, J.P., Chang, C.-H., Szlavecz, K., 2018. Methane fluxes from tree stems and soils along a habitat gradient. *Biogeochemistry* 137, 307–320. <https://doi.org/10.1007/s10533-017-0400-3>
- Pretzsch, H., Schütze, G., Uhl, E., 2013. Resistance of European tree species to drought stress in mixed *versus* pure forests: evidence of stress release by inter-specific facilitation: Drought stress release by inter-specific facilitation. *Plant Biol.* 15, 483–495. <https://doi.org/10.1111/j.1438-8677.2012.00670.x>
- Pumpanen, J., Heinonsalo, J., Rasilo, T., Villemot, J., Ilvesniemi, H., 2012. The effects of soil and air temperature on CO<sub>2</sub> exchange and net biomass accumulation in Norway spruce, Scots pine and Silver birch seedlings. *Tree Physiol.* 32, 724–736. <https://doi.org/10.1093/treephys/tps007>

- Putkinen, A., Siljanen, H.M.P., Laihonon, A., Paasisalo, I., Porkka, K., Tiirola, M., Haikarainen, I., Tenhoviirta, S., Pihlatie, M., 2021. New insight to the role of microbes in the methane exchange in trees: evidence from metagenomic sequencing. *New Phytol.* 231, 524–536. <https://doi.org/10.1111/nph.17365>
- Radler, K., 2010. Radiation and Temperature Responses to a Small Clear-Cut in a Spruce Forest. *Open Geogr. J.* 3, 103–114. <https://doi.org/10.2174/1874923201003010103>
- Rebmann, C., Aubinet, M., Schmid, H., Arriga, N., Aurela, M., Burba, G., Clement, R., De Ligne, A., Fratini, G., Gielen, B., Grace, J., Graf, A., Gross, P., Haapanala, S., Herbst, M., Hörtnagl, L., Ibrom, A., Joly, L., Kljun, N., Kolle, O., Kowalski, A., Lindroth, A., Loustau, D., Mammarella, I., Mauder, M., Merbold, L., Metzger, S., Mölder, M., Montagnani, L., Papale, D., Pavelka, M., Peichl, M., Roland, M., Serrano-Ortiz, P., Siebicke, L., Steinbrecher, R., Tuovinen, J.-P., Vesala, T., Wohlfahrt, G., Franz, D., 2018. ICOS eddy covariance flux-station site setup: a review. *Int. Agrophysics* 32, 471–494. <https://doi.org/10.1515/intag-2017-0044>
- Regina, K., Syväsalö, E., Hannukkala, A., Esala, M., 2004. Fluxes of N<sub>2</sub>O from farmed peat soils in Finland. *Eur. J. Soil Sci.* 55, 591–599. <https://doi.org/10.1111/j.1365-2389.2004.00622.x>
- Reichstein, M., Falge, E., Baldocchi, D., Papale, D., Aubinet, M., Berbigier, P., Bernhofer, C., Buchmann, N., Gilmanov, T., Granier, A., Grunwald, T., Havrankova, K., Ilvesniemi, H., Janous, D., Knohl, A., Laurila, T., Lohila, A., Loustau, D., Matteucci, G., Meyers, T., Miglietta, F., Ourcival, J.-M., Pumpanen, J., Rambal, S., Rotenberg, E., Sanz, M., Tenhunen, J., Seufert, G., Vaccari, F., Vesala, T., Yakir, D., Valentini, R., 2005. On the separation of net ecosystem exchange into assimilation and ecosystem respiration: review and improved algorithm. *Glob. Change Biol.* 11, 1424–1439. <https://doi.org/10.1111/j.1365-2486.2005.001002.x>
- Richardson, A.D., Hollinger, D.Y., Dail, D.B., Lee, J.T., Munger, J.W., O’keefe, J., 2009. Influence of spring phenology on seasonal and annual carbon balance in two contrasting New England forests. *Tree Physiol.* 29, 321–331. <https://doi.org/10.1093/treephys/tpn040>
- Roy, S., Khasa, D.P., Greer, C.W., 2007. Combining alders, frankia, and mycorrhizae for the revegetation and remediation of contaminated ecosystems. *Can. J. Bot.* 85, 237–251. <https://doi.org/10.1139/B07-017>
- Saetersdal, M., Birks, H.J.B., Peglar, S., 1998. Predicting changes in Fennoscandian vascular-plant species richness as a result of future climatic change. *J. Biogeogr.* 25, 111–112. <https://doi.org/10.1046/j.1365-2699.1998.251192.x>
- Saikawa, E., Prinn, R.G., Dlugokencky, E., Ishijima, K., Dutton, G.S., Hall, B.D., Langenfelds, R., Tohjima, Y., Machida, T., Manizza, M., Rigby, M., O’Doherty, S., Patra, P.K., Harth, C.M., Weiss, R.F., Krummel, P.B., van der Schoot, M., Fraser, P.J., Steele, L.P., Aoki, S., Nakazawa, T., Elkins, J.W., 2014. Global and regional emissions estimates for N<sub>2</sub>O. *Atmospheric Chem. Phys.* 14, 4617–4641. <https://doi.org/10.5194/acp-14-4617-2014>
- Sakabe, A., Itoh, M., Hirano, T., Kusin, K., 2018. Ecosystem-scale methane flux in tropical peat swamp forest in Indonesia. *Glob. Change Biol.* 24, 5123–5136. <https://doi.org/10.1111/gcb.14410>
- Salm, J.-O., Maddison, M., Tammik, S., Soosaar, K., Truu, J., Mander, Ü., 2012. Emissions of CO<sub>2</sub>, CH<sub>4</sub> and N<sub>2</sub>O from undisturbed, drained and mined peatlands in Estonia. *Hydrobiologia* 692, 41–55. <https://doi.org/10.1007/s10750-011-0934-7>

- Saunio, M., Stavert, A.R., Poulter, B., Bousquet, P., Canadell, J.G., Jackson, R.B., Raymond, P.A., Dlugokencky, E.J., Houweling, S., Patra, P.K., Ciais, P., Arora, V.K., Bastviken, D., Bergamaschi, P., Blake, D.R., Brailsford, G., Bruhwiler, L., Carlson, K.M., Carrol, M., Castaldi, S., Chandra, N., Crevoisier, C., Crill, P.M., Covey, K., Curry, C.L., Etiope, G., Frankenberg, C., Gedney, N., Hegglin, M.I., Höglund-Isaksson, L., Hugelius, G., Ishizawa, M., Ito, A., Janssens-Maenhout, G., Jensen, K.M., Joos, F., Kleinen, T., Krummel, P.B., Langenfelds, R.L., Laruelle, G.G., Liu, L., Machida, T., Maksyutov, S., McDonald, K.C., McNorton, J., Miller, P.A., Melton, J.R., Morino, I., Müller, J., Murguia-Flores, F., Naik, V., Niwa, Y., Noce, S., O'Doherty, S., Parker, R.J., Peng, C., Peng, S., Peters, G.P., Prigent, C., Prinn, R., Ramonet, M., Regnier, P., Riley, W.J., Rosentreter, J.A., Segers, A., Simpson, I.J., Shi, H., Smith, S.J., Steele, L.P., Thornton, B.F., Tian, H., Tohjima, Y., Tubiello, F.N., Tsuruta, A., Viovy, N., Voulgarakis, A., Weber, T.S., van Weele, M., van der Werf, G.R., Weiss, R.F., Worthy, D., Wunch, D., Yin, Y., Yoshida, Y., Zhang, W., Zhang, Z., Zhao, Y., Zheng, B., Zhu, Qing, Zhu, Qian, Zhuang, Q., 2020. The Global Methane Budget 2000–2017. *Earth Syst. Sci. Data* 12, 1561–1623. <https://doi.org/10.5194/essd-12-1561-2020>
- Savi, F., Di Bene, C., Canfora, L., Mondini, C., Fares, S., 2016. Environmental and biological controls on CH<sub>4</sub> exchange over an evergreen Mediterranean forest. *Agric. For. Meteorol.* 226–227, 67–79. <https://doi.org/10.1016/j.agrformet.2016.05.014>
- Schär, C., Vidale, P.L., Lüthi, D., Frei, C., Häberli, C., Liniger, M.A., Appenzeller, C., 2004. The role of increasing temperature variability in European summer heatwaves. *Nature* 427, 332–336. <https://doi.org/10.1038/nature02300>
- Schimel, D.S., Braswell, B.H., Holland, E.A., McKeown, R., Ojima, D.S., Painter, T.H., Parton, W.J., Townsend, A.R., 1994. Climatic, edaphic, and biotic controls over storage and turnover of carbon in soils. *Glob. Biogeochem. Cycles* 8, 279–293. <https://doi.org/10.1029/94GB00993>
- Schindlbacher, A., Zechmeister-Boltenstern, S., Jandl, R., 2009. Carbon losses due to soil warming: Do autotrophic and heterotrophic soil respiration respond equally? *Glob. Change Biol.* 15, 901–913. <https://doi.org/10.1111/j.1365-2486.2008.01757.x>
- Schindler, T., Mander, Ü., Machacova, K., Espenberg, M., Krasnov, D., Escuer-Gatius, J., Veber, G., Pärn, J., Soosaar, K., 2020. Short-term flooding increases CH<sub>4</sub> and N<sub>2</sub>O emissions from trees in a riparian forest soil-stem continuum. *Sci. Rep.* 10, 3204. <https://doi.org/10.1038/s41598-020-60058-7>
- Schulze, E.-D., Höglberg, P., van Oene, H., Persson, T., Harrison, A.F., Read, D., Kjølter, A., Matteucci, G., 2000. Interactions Between the Carbon and Nitrogen Cycles and the Role of Biodiversity: A Synopsis of a Study Along a North-South Transect Through Europe, in: Schulze, Ernst-Detlef (Ed.), *Carbon and Nitrogen Cycling in European Forest Ecosystems*, Ecological Studies. Springer, Berlin, Heidelberg, pp. 468–491. [https://doi.org/10.1007/978-3-642-57219-7\\_21](https://doi.org/10.1007/978-3-642-57219-7_21)
- Shoemaker, J.K., Keenan, T.F., Hollinger, D.Y., Richardson, A.D., 2014. Forest ecosystem changes from annual methane source to sink depending on late summer water balance: Ecosystem-scale forest methane fluxes. *Geophys. Res. Lett.* 41, 673–679. <https://doi.org/10.1002/2013GL058691>
- Shorohova, E., Kuuluvainen, T., Kangur, A., Jögiste, K., 2009. Natural stand structures, disturbance regimes and successional dynamics in the Eurasian boreal forests: a review with special reference to Russian studies. *Ann. For. Sci.* 66, 201–201. <https://doi.org/10.1051/forest/2008083>

- Sjögersten, S., Wookey, P.A., 2002. Spatio-temporal variability and environmental controls of methane fluxes at the forest–tundra ecotone in the Fennoscandian mountains. *Glob. Change Biol.* 8, 885–894.  
<https://doi.org/10.1046/j.1365-2486.2002.00522.x>
- Smith, K.A., Dobbie, K.E., Ball, B.C., Bakken, L.R., Sitaula, B.K., Hansen, S., Brumme, R., Borken, W., Christensen, S., Priemé, A., Fowler, D., Macdonald, J.A., Skiba, U., Klemedtsson, L., Kasimir-Klemedtsson, A., Degórska, A., Orlanski, P., 2000. Oxidation of atmospheric methane in Northern European soils, comparison with other ecosystems, and uncertainties in the global terrestrial sink: METHANE OXIDATION IN SOILS. *Glob. Change Biol.* 6, 791–803.  
<https://doi.org/10.1046/j.1365-2486.2000.00356.x>
- Smith, N.E., Kooijmans, L.M.J., Koren, G., van Schaik, E., van der Woude, A.M., Wanders, N., Ramonet, M., Xueref-Remy, I., Siebicke, L., Manca, G., Brümmner, C., Baker, I.T., Haynes, K.D., Luijckx, I.T., Peters, W., 2020. Spring enhancement and summer reduction in carbon uptake during the 2018 drought in northwestern Europe. *Philos. Trans. R. Soc. B Biol. Sci.* 375, 20190509.  
<https://doi.org/10.1098/rstb.2019.0509>
- Soloway, A.D., Amiro, B.D., Dunn, A.L., Wofsy, S.C., 2017. Carbon neutral or a sink? Uncertainty caused by gap-filling long-term flux measurements for an old-growth boreal black spruce forest. *Agric. For. Meteorol.* 233, 110–121.  
<https://doi.org/10.1016/j.agrformet.2016.11.005>
- Sommer, M., 2006. Influence of soil pattern on matter transport in and from terrestrial biogeosystems—A new concept for landscape pedology. *Geoderma, Advances in landscape-scale soil research* 133, 107–123.  
<https://doi.org/10.1016/j.geoderma.2006.03.040>
- Steckel, M., del Río, M., Heym, M., Aldea, J., Bielak, K., Brazaitis, G., Černý, J., Coll, L., Collet, C., Ehbrecht, M., Jansons, A., Nothdurft, A., Pach, M., Pardos, M., Ponette, Q., Reventlow, D.O.J., Sitko, R., Svoboda, M., Vallet, P., Wolff, B., Pretzsch, H., 2020. Species mixing reduces drought susceptibility of Scots pine (*Pinus sylvestris* L.) and oak (*Quercus robur* L., *Quercus petraea* (Matt.) Liebl.) – Site water supply and fertility modify the mixing effect. *For. Ecol. Manag.* 461, 117908.  
<https://doi.org/10.1016/j.foreco.2020.117908>
- Subke, J.-A., Inglima, I., Francesca Cotrufo, M., 2006. Trends and methodological impacts in soil CO<sub>2</sub> efflux partitioning: A metaanalytical review: SOIL CO<sub>2</sub> EFFLUX PARTITIONING – METAANALYSIS. *Glob. Change Biol.* 12, 921–943.  
<https://doi.org/10.1111/j.1365-2486.2006.01117.x>
- Teepe, R., Brumme, R., Beese, F., 2001. Nitrous oxide emissions from soil during freezing and thawing periods. *Soil Biol. Biochem.* 33, 1269–1275.  
[https://doi.org/10.1016/S0038-0717\(01\)00084-0](https://doi.org/10.1016/S0038-0717(01)00084-0)
- Thomas, C.K., Martin, J.G., Law, B.E., Davis, K., 2013. Toward biologically meaningful net carbon exchange estimates for tall, dense canopies: Multi-level eddy covariance observations and canopy coupling regimes in a mature Douglas-fir forest in Oregon. *Agric. For. Meteorol.* 173, 14–27. <https://doi.org/10.1016/j.agrformet.2013.01.001>
- Turetsky, M.R., Kotowska, A., Bubier, J., Dise, N.B., Crill, P., Hornibrook, E.R.C., Minkinen, K., Moore, T.R., Myers-Smith, I.H., Nykänen, H., Olefeldt, D., Rinne, J., Saarnio, S., Shurpali, N., Tuittila, E.-S., Waddington, J.M., White, J.R., Wickland, K.P., Wilming, M., 2014. A synthesis of methane emissions from 71 northern, temperate, and subtropical wetlands. *Glob. Change Biol.* 20, 2183–2197.  
<https://doi.org/10.1111/gcb.12580>

- Urakawa, R., Shibata, H., Kuroiwa, M., Inagaki, Y., Tateno, R., Hishi, T., Fukuzawa, K., Hirai, K., Toda, H., Oyanagi, N., Nakata, M., Nakanishi, A., Fukushima, K., Enoki, T., Suwa, Y., 2014. Effects of freeze–thaw cycles resulting from winter climate change on soil nitrogen cycling in ten temperate forest ecosystems throughout the Japanese archipelago. *Soil Biol. Biochem.* 74, 82–94.  
<https://doi.org/10.1016/j.soilbio.2014.02.022>
- Uri, V., Kukumägi, M., Aosaar, J., Varik, M., Becker, H., Aun, K., Krasnova, A., Morozov, G., Ostonen, I., Mander, Ü., Lõhmus, K., Rosenvald, K., Kriiska, K., Soosaar, K., 2019. The carbon balance of a six-year-old Scots pine (*Pinus sylvestris* L.) ecosystem estimated by different methods. *For. Ecol. Manag.* 433, 248–262.  
<https://doi.org/10.1016/j.foreco.2018.11.012>
- van der Molen, M.K., Dolman, A.J., Ciais, P., Eglin, T., Gobron, N., Law, B.E., Meir, P., Peters, W., Phillips, O.L., Reichstein, M., Chen, T., Dekker, S.C., Doubková, M., Friedl, M.A., Jung, M., van den Hurk, B.J.J.M., de Jeu, R.A.M., Kruijt, B., Ohta, T., Rebel, K.T., Plummer, S., Seneviratne, S.I., Sitch, S., Teuling, A.J., van der Werf, G.R., Wang, G., 2011. Drought and ecosystem carbon cycling. *Agric. For. Meteorol.* 151, 765–773. <https://doi.org/10.1016/j.agrformet.2011.01.018>
- van't Hoff, J.H., 1898. *Lectures on Theoretical and Physical Chemistry: Part 1. Chemical dynamics.* Edward Arnold.
- Vestin, P., Mölder, M., Kljun, N., Cai, Z., Hasan, A., Holst, J., Klemetsson, L., Lindroth, A., 2020. Impacts of Clear-Cutting of a Boreal Forest on Carbon Dioxide, Methane and Nitrous Oxide Fluxes. *Forests* 11, 961.  
<https://doi.org/10.3390/f11090961>
- Vickers, D., Mahrt, L., 1997. Quality Control and Flux Sampling Problems for Tower and Aircraft Data. *J. Atmospheric Ocean. Technol.* 14, 512–526.  
[https://doi.org/10.1175/1520-0426\(1997\)014<0512:QCAFSP>2.0.CO;2](https://doi.org/10.1175/1520-0426(1997)014<0512:QCAFSP>2.0.CO;2)
- Vogel, C.S., Curtis, P.S., Thomas\*, R.B., 1997. Growth and nitrogen accretion of dinitrogen-fixing *Alnus glutinosa* (L.) Gaertn. under elevated carbon dioxide. *Plant Ecol.* 130, 63–70. <https://doi.org/10.1023/A:1009783625188>
- von Buttlar, J., Zscheischler, J., Rammig, A., Sippel, S., Reichstein, M., Knohl, A., Jung, M., Menzer, O., Arain, M.A., Buchmann, N., Cescatti, A., Gianelle, D., Kiely, G., Law, B.E., Magliulo, V., Margolis, H., McCaughey, H., Merbold, L., Migliavacca, M., Montagnani, L., Oechel, W., Pavelka, M., Peichl, M., Rambal, S., Raschi, A., Scott, R.L., Vaccari, F.P., van Gorsel, E., Varlagin, A., Wohlfahrt, G., Mahecha, M.D., 2018. Impacts of droughts and extreme-temperature events on gross primary production and ecosystem respiration: a systematic assessment across ecosystems and climate zones. *Biogeosciences* 15, 1293–1318. <https://doi.org/10.5194/bg-15-1293-2018>
- Wagner-Riddle, C., Congreves, K.A., Abalos, D., Berg, A.A., Brown, S.E., Ambadan, J.T., Gao, X., Tenuta, M., 2017. Globally important nitrous oxide emissions from croplands induced by freeze–thaw cycles. *Nat. Geosci.* 10, 279–283.  
<https://doi.org/10.1038/ngeo2907>
- Wang, J.M., Murphy, J.G., Geddes, J.A., Winsborough, C.L., Basiliko, N., Thomas, S.C., 2013. Methane fluxes measured by eddy covariance and static chamber techniques at a temperate forest in central Ontario, Canada. *Biogeosciences* 10, 4371–4382.  
<https://doi.org/10.5194/bg-10-4371-2013>
- Wang, X., Liu, L., Piao, S., Janssens, I.A., Tang, J., Liu, W., Chi, Y., Wang, J., Xu, S., 2014. Soil respiration under climate warming: differential response of heterotrophic and autotrophic respiration. *Glob. Change Biol.* 20, 3229–3237.  
<https://doi.org/10.1111/gcb.12620>

- Wang, X., Wang, C., Bond-Lamberty, B., 2017. Quantifying and reducing the differences in forest CO<sub>2</sub>-fluxes estimated by eddy covariance, biometric and chamber methods: A global synthesis. *Agric. For. Meteorol.* 247, 93–103.  
<https://doi.org/10.1016/j.agrformet.2017.07.023>
- Weber, A., Smolander, A., Nurmiaho-Lassila, E.-L., Sundman, V., 1988. Isolation and Characterization of Frankia Strains from *Alnus incana* and *Alnus glutinosa* in Finland. *Symbiosis* 97–116.
- Wei, W., Weile, C., Shaopeng, W., 2010. Forest soil respiration and its heterotrophic and autotrophic components: Global patterns and responses to temperature and precipitation. *Soil Biol. Biochem.* 42, 1236–1244.  
<https://doi.org/10.1016/j.soilbio.2010.04.013>
- Wen, Y., Corre, M.D., Rachow, C., Chen, L., Veldkamp, E., 2017. Nitrous oxide emissions from stems of alder, beech and spruce in a temperate forest. *Plant Soil* 420, 423–434. <https://doi.org/10.1007/s11104-017-3416-5>
- Wolf, B., Zheng, X., Brüggemann, N., Chen, W., Dannemann, M., Han, X., Sutton, M.A., Wu, H., Yao, Z., Butterbach-Bahl, K., 2010. Grazing-induced reduction of natural nitrous oxide release from continental steppe. *Nature* 464, 881–884.  
<https://doi.org/10.1038/nature08931>
- Wolf, S., Keenan, T.F., Fisher, J.B., Baldocchi, D.D., Desai, A.R., Richardson, A.D., Scott, R.L., Law, B.E., Litvak, M.E., Brunsell, N.A., Peters, W., van der Laan-Luijkx, I.T., 2016. Warm spring reduced carbon cycle impact of the 2012 US summer drought. *Proc. Natl. Acad. Sci.* 113, 5880–5885.  
<https://doi.org/10.1073/pnas.1519620113>
- Wong, G.X., Hirata, R., Hirano, T., Kiew, F., Aeries, E.B., Musin, K.K., Waili, J.W., Lo, K.S., Melling, L., 2018. Micrometeorological measurement of methane flux above a tropical peat swamp forest. *Agric. For. Meteorol.* 256–257, 353–361.  
<https://doi.org/10.1016/j.agrformet.2018.03.025>
- Wu, X., Brüggemann, N., Gasche, R., Shen, Z., Wolf, B., Butterbach-Bahl, K., 2010. Environmental controls over soil-atmosphere exchange of N<sub>2</sub>O, NO, and CO<sub>2</sub> in a temperate Norway spruce forest. *Glob. Biogeochem. Cycles* 24.  
<https://doi.org/10.1029/2009GB003616>
- Wutzler, T., Lucas-Moffat, A., Migliavacca, M., Knauer, J., Sickel, K., Šigut, L., Menzer, O., Reichstein, M., 2018. Basic and extensible post-processing of eddy covariance flux data with REddyProc. *Biogeosciences* 15, 5015–5030.  
<https://doi.org/10.5194/bg-15-5015-2018>
- Xiao, J., Zhuang, Q., Baldocchi, D.D., Law, B.E., Richardson, A.D., Chen, J., Oren, R., Starr, G., Noormets, A., Ma, S., Verma, S.B., Wharton, S., Wofsy, S.C., Bolstad, P.V., Burns, S.P., Cook, D.R., Curtis, P.S., Drake, B.G., Falk, M., Fischer, M.L., Foster, D.R., Gu, L., Hadley, J.L., Hollinger, D.Y., Katul, G.G., Litvak, M., Martin, T.A., Matamala, R., McNulty, S., Meyers, T.P., Monson, R.K., Munger, J.W., Oechel, W.C., Paw U, K.T., Schmid, H.P., Scott, R.L., Sun, G., Suyker, A.E., Torn, M.S., 2008. Estimation of net ecosystem carbon exchange for the conterminous United States by combining MODIS and AmeriFlux data. *Agric. For. Meteorol.* 148, 1827–1847. <https://doi.org/10.1016/j.agrformet.2008.06.015>
- Xie, Y., Zhang, M., Xiao, W., Zhao, J., Huang, W., Zhang, Z., Hu, Y., Qin, Z., Jia, L., Pu, Y., Chu, H., Wang, J., Shi, J., Liu, S., Lee, X., 2022. Nitrous oxide flux observed with tall-tower eddy covariance over a heterogeneous rice cultivation landscape. *Sci. Total Environ.* 810, 152210. <https://doi.org/10.1016/j.scitotenv.2021.152210>

- Yip, D.Z., Veach, A.M., Yang, Z.K., Cregger, M.A., Schadt, C.W., 2019. Methanogenic Archaea dominate mature heartwood habitats of Eastern Cottonwood (*Populus deltoides*). *New Phytol.* 222, 115–121. <https://doi.org/10.1111/nph.15346>
- Yu, J., Sun, W., Liu, J., Wang, J., Yang, J., Meixner, F.X., 2007. Enhanced net formations of nitrous oxide and methane underneath the frozen soil in Sanjiang wetland, northeastern China. *J. Geophys. Res. Atmospheres* 112. <https://doi.org/10.1029/2006JD008025>
- Yuste, J.C., Nagy, M., Janssens, I.A., Carrara, A., Ceulemans, R., 2005. Soil respiration in a mixed temperate forest and its contribution to total ecosystem respiration. *Tree Physiol.* 25, 609–619. <https://doi.org/10.1093/treephys/25.5.609>
- Zhang, K., Wu, H., Li, M., Yan, Z., Li, Y., Wang, J., Zhang, X., Yan, L., Kang, X., 2020. Magnitude and Edaphic Controls of Nitrous Oxide Fluxes in Natural Forests at Different Scales. *Forests* 11, 251. <https://doi.org/10.3390/f11030251>
- Ziemblińska, K., Urbaniak, M., Chojnicki, B.H., Black, T.A., Niu, S., Olejnik, J., 2016. Net ecosystem productivity and its environmental controls in a mature Scots pine stand in north-western Poland. *Agric. For. Meteorol.* 228–229, 60–72. <https://doi.org/10.1016/j.agrformet.2016.05.022>

## SUMMARY IN ESTONIAN

### Kasvuhoonegaaside vood hemiboreaalsetes metsaökosüsteemides

Viimase sajandi vältel on meie planeedi kliimamuutused olnud enneolematult kiired. Globaalne soojenemine põhjustab aga kasvuhoonegaaside (KHG) intensiivsemat lendumist ning sisalduse kasvu atmosfääris, mis omakorda kliima soojenemist õhutab. Süsihappegaas ( $\text{CO}_2$ ) on kasvuhoonegaasidest suurima kogusega inimtekkelise päritoluga gaas, mis Maa kliimat enim mõjutab. Ehkki kahe ülejäänud KHG metaani ( $\text{CH}_4$ ) ja dilaammastikoksiidi ehk naerugaasi ( $\text{N}_2\text{O}$ ) heitkogused atmosfääri on  $\text{CO}_2$  kogustest väiksemad, on nende kliimat soojendav kiirguslik toime vastavalt 28 ja 273 korda suurem kui samal kogusel süsihappegaasil.

Metsad etendavad KHG globaalses ringluses olulist rolli, olles üldiselt  $\text{CO}_2$  sidujateks, kuid selle efektiivsus sõltub metsade vanusest, mullastikust, paljudest keskkonnateguritest ning majandamisviisist. Metsamullad üldiselt seovad metaani, kuid mullaniiskuse suurenedes intensiivistub nii metaani kui ka naerugaasi lendumine. Mitmed uuringud on näidanud, et ka puud ise võivad olla KHG allikaks, enamasti juhtides mullas tekkinud gaase atmosfääri, kuid metaani võidakse toota ka tüvede ja võrade sees. Veekoguäärsetes metsades on tänu oma asukohale nii süsiniku (C) kui ka lämmastiku (N) aineringlus intensiivsem kui piirnevates maaismaa- ja veekoguökosüsteemides, mistõttu nad on nii  $\text{CH}_4$  kui ka  $\text{N}_2\text{O}$  kuumadeks täppideks. Halli lepa (*Alnus incana* (L.) Moench) enamusega metsad on tavalised parasvöötme veekoguäärsed kooslused. Tänu leppade sümbioosile õhulämmastikku siduvate mullas elavate Frankia aktinobakteritega on kaldaäärsete lepikevõrgude ringluses osalevad lämmastikukogused suuremad kui muudes ökosüsteemides.

Kõik käesolevas doktoritöös uuritud metsaökosüsteemid asuvad hemiboreaalsetes (boreonemoraalsetes) vööndis, mis paikneb boreaalse (põhjapoolse) ning parasvöötme metsabioomi vahel, kattes suuri alasid Põhja- ja Ida-Euroopas. Tüüpiliselt levivad selles üleminekuvööndis paljude puu- ja põõsaliikidega esindatud segametsad, kus majandamisviisid varieeruvad intensiivsest majandamisest kuni range kaitse-reežiimini. Vaatamata üldiselt heale uuritusele on senised teadmised nende metsade KHG bilansi kohta puudulikud.

2018. aasta kevadel ja suvel tabas Euroopat kuumalaine, mida iseloomutas nii tavapärasest kõrgem õhutemperatuur kui ka sademete vähesus, kuid mille vältel ilmsid kohati ka selged põuatunnused. Kliima soojenemisest tingituna püüavad sagenevad, mistõttu nende mõju uurimine metsade KHG bilansile on väga oluline.

Dokoritöö peamiseks eesmärgiks on selgitada erinevate hemiboreaalsete metsade KHG voogusid ning analüüsida nende voogude seoseid keskkonnamuutustega. Peamine tähelepanu on pööratud hemiboreaalsete metsade süsinikubilansile ning selle muutustele kuumalaine tingimustes, samuti veekoguäärsete hall-lepikevõrgude metaani- ja naerugaasivoogude dünaamikale.

Süsihappegaasi voogude uurimiseks kasutati turbulentsse õhuvoo (eddy covariance) meetodit, mida rakendati aastatel 2017–2018 kuues Lõuna-Eesti

metsaökosüsteemis: okasmetsas Soontagal (CON; harilik mänd/harilik kuusk), veekoguäärses lehtmetsas Agalis (DEC; hall-lepp), segametsas Liispõllul (MIX1; harilik kuusk/arukask), segametsas Apne-Järvseljal (MIX2; harilik mänd,/harilik kuusk/ arukask/ sookask; Eesti SMEAR uurimisala), raiesmikul Kõnnus (CC1, endine männik) ning raiesmikul Tensos (CC2, endine kaasik). Eddy covariance meetodit rakendati aastatel 2017–2019 CH<sub>4</sub> and N<sub>2</sub>O voogude analüüsiks Agali hall-lepikus, mis on esmakordne pikaajaline N<sub>2</sub>O ökosüsteemi tasandi uurimus ja üks esimesi CH<sub>4</sub> bilansi uuringuid.

Uurimistes selgus, et selged süsiniku sidujad olid (kahanevas järjekorras) MIX1, DEC ja CON metsad. Suurem C sidumine MIX1-s oli tingitud väiksemast ökosüsteemi hingamisest (Reco; CO<sub>2</sub> lendumine) kui DEC-s. Põlispuudega okasmetsas (CON) oli C sidumine küll madalam, kuid säilis muutusteta ka põua-tingimustes 2018.a. kuumalaine ajal. Mõlemad raiesmikud (CC1 ja CC2) osutusid süsiniku emiteerijateks (kliima soojendajateks) eeskätt tänu suuremale CO<sub>2</sub> lendumisele mullast. MIX2 segamets oli samal põhjusel kliima soojendaja. Põhjuseks võib siin tuua 130 m kõrguse SMEAR-masti tugitrosside lageraiesihid, kus puudus fotosünteesiline C sidumine puude poolt ja Reco oli kõrge. Ka CO<sub>2</sub> bilansi aastase käigu sarnasus MIX2-s ning raiesmikel viitab sellele põhjusele.

Õhutemperatuur osutus peamiseks keskkonnategurika, mis reguleeris nii ökosüsteemi- kui ka mullahingamist, kuid temperatuurist sõltuvuse dünaamika varieerus nii metsatüüpide, aastate, aastaegade kui ka mullaniiskuse lõikes. Õhutemperatuur on ka oluline fotosünteesi reguleerija. Optimaalse taseme ületavad õhutemperatuurid (nt kuumalaine ajal), mis kombineeruvad õhuniiskuse vajaku ja madala mullaniiskusega, põhjustavad taimede poolt fotosünteesis CO<sub>2</sub> madalamat sidumist ja nn puhta koguproduktiooni (GPP) langust. Ka päikesekiirguse ja GPP vahekorra dünaamika varieerus nii metsatüübiti kui aastaajaliselt.

Uuringutest selgus, et segametsad osutusid kuumalaine ja põua suhtes eeldatust vähem vastupidavaks. Oodatult haavatavamad olid raiesmikud, kus GPP oluline kahanemine viib ka fotosünteesiks vajaliku karbohüdraatide sisalduse vähenemisele järgnevatel aastatel, mis võib pikaajaliselt C sidumist pärssida. Seetõttu on lagereaiete planeerimisel väga oluline arvestada võimalike põua-olukordadega. Kokkuvõttes peaks hemiboreaalsete metsade majandamine tulevikus olema rohkem suunatud stabiilsuse tõstmisele sagenevate ekstreemsete ilmastikunähtuste tingimustes. Veekoguäärne hall-lepik (DEC) osutus selgelt süsinikusidujaks ka põua-tingimustes, kuid selle metsatüübi lühiajalisus ja suhteliselt piiratud levik üldise metsamajanduse lõikes ei taga veel metsade C bilansi stabiilsust. Küll aga võib see osutada tuleviku kiire tsükliliga metsamajandamise tingimustes oluliseks tasakaalustavaks komponendiks. Liivasel mulla kasvav küps okasmets (CON), mis on kohanenud madalale mullaniiskusele, säilitas CO<sub>2</sub> sidumise ka põua ajal. Taoliste vanade metsade säilitamine, mis vaatamata oma vanusele süsinikku seovad, peaks olema tuleviku metsamajanduse praktikas olulisel kohal.

Uuenduslikud pikaajalised ja suure mõõtmissagedusega metaani ja naerugaasi bilansi uuringud veekoguäärses hall-lepikus (DEC) näitasid, et see mets oli aastases tsüklis CH<sub>4</sub> siduja, kuid N<sub>2</sub>O emiteerija. Tänu aga suurele CO<sub>2</sub>

sidumisele oli nii metaani kui ka naerugaasi roll üldises kliimat mõjutavas kiirguslikus toimes suhteliselt madal. Huvitav oli aga CH<sub>4</sub> ja N<sub>2</sub>O aastaajaline dünaamika. Näiteks mõõdeti kõrge mullaniiskusega perioodil 2017.a. sügisel mullas endiselt CH<sub>4</sub> sidumine, kuid puutüvedest kõrge CH<sub>4</sub> lendumine, mis andis ligi 100% kogu ökosüsteemi CH<sub>4</sub> bilansist. See viitab, et antud ökosüsteemis CH<sub>4</sub> ei teki puutüvedes, vaid toodetakse sügavamas mullakihis ja juhitakse puude kaudu atmosfääri. Ülejäänud perioodidel puutüvedest CH<sub>4</sub> emission puudus, kusjuures mullas seoti CH<sub>4</sub> pidevalt. Küll aga lendus põuaperioodil CH<sub>4</sub> võradest, mis viitab selle füüsikaliskemilisele päritolule ja vääriks kindlkasti edasist uurimist.

Naerugaasi aastases dünaamikas ilmnesid väga selgelt suhteliselt lühiajalised kõrged emissioonid, nn kuumad perioodid, mille vältel emiteerus üle poole kogu 2,5 aastase vaatlusperioodi N<sub>2</sub>O mullaemissioonist. Määravaks oli siin mullaniiskuse dünaamika, mis oma kiires muutuses põuaperioodi algul andis kõige suurema N<sub>2</sub>O lendumise. Teiseks oluliseks emissiooni kõrgpunktiks oli talveperioodi lõpp 2019. veebruaris, mil põhjuseks oli ülemise mullakihi külmissulamistsükli kordumine. Selle fenomeni põhjused on veel detailselt selgitamata, kuid võib arvata, et ka sel perioodil mängis olulist rolli ülemise mullakihi veesisalduse pulseerimine. Kõige üllatavam oli aga tulemus, et suured N<sub>2</sub>O mullaemissioonid ei kajastunud eddy covariance meetodil võrade kohal mõõdetud voogudes. Tõenäoliselt pole siin tegu bioloogiliste protsessidega, vaid füüsikaliskemiliste teguritega, mis N<sub>2</sub>O-d voogusid kahandasid, nt võrades oleva õhuniiskuse ja kastepiiskade N<sub>2</sub>O lahustav mõju niiskemal perioodil ning fotokeemilised reaktsioonid intensiivse päikesekiirguse perioodil kevadel ja suve algul. Taolised kompleksed CH<sub>4</sub> ja N<sub>2</sub>O uuringud, mis hõlmavad kõiki ökosüsteemi komponente, on vajalikud ka teistes metsaökosüsteemides.

Lähikümnetel on üldise kliima soojenemise taustal oodata ekstreemsete ilmastikunähtuste sagenemist, mis paratamatult mõjutavad metsaökosüsteeme. Seetõttu on kliimateadlik metsamajandus ülimalt oluline. Eeskätt on muretekitavaks hemiboreaalsete metsade raiemahtude suurenemine, mis võib mõjutada kogu regiooni C bilanssi ning olla kliima soojenemise kiirendajaks.

## ACKNOWLEDGEMENTS

I am grateful to my supervisors Assoc. Prof. Kaido Soosaar, Prof. Ülo Mander, Prof. Steffen M. Noe for their valuable scientific guidance, understanding and support during my studies. I would also like to thank all my co-authors and colleagues from both universities for their help in making all this happen. I would like to express my special gratitude to all the people who maintained the stations and made sure that all equipment worked properly and I've got the best quality data; it would not be possible without their work.

My special gratitude goes to my beloved Dmitrii Krasnov, who was and is the main support and inspiration of my scientific career and life. I would also like to thank our son Adrian who survived all these years with us; my mother for her priceless support, my best friend Irbis who is always there for me and Deimos the cat who spent countless hours with me, while I was writing this thesis

This thesis was supported by the Ministry of Education and Science of Estonia (grants SF0180025s12, SF1090050s07), the Estonian Research Council (IUT2-16, IUT20-52, PRG-352, PRG681, PRG1674), the EU through the European Regional Development Fund (BioAtmos, grant number SLOOM12022T, 3.2.0802.11-004; Centres of Excellence ENVIRON, grant number TK-107; EcolChange, grant number TK-131), the European network for observing our changing planet project (ERA-PLANET, grant agreement no. 689443) under the European Union's Horizon 2020 research and innovation program, Estonian Ministry of Sciences projects (grant numbers P180021, P180274, P200196), and the Estonian Research Infrastructures Roadmap Project Estonian Environmental Observatory (3.2.0304.11-0395), the project of the Estonian Forest Management Centre 1-18/271 "Effect of clearcut and thinning on forest carbon cycling" and the European Social Fund (Doctoral School of Earth Sciences and Ecology, 2014–2020.4.01.16-0027).

## **PUBLICATIONS**

# CURRICULUM VITAE

**Name:** Alisa Krasnova  
**Date of birth:** 10.07.1986  
**E-mail:** alisa.krasnova@ut.ee

## EDUCATION

2018–... PhD student in Landscape Ecology and Environment Protection, University of Tartu, Estonia  
2011–2019 PhD student, Estonian University of Life Sciences, Estonia  
2003–2008 Specialist (equalized to MSc) in biology, Petrozavodsk State University, Russia

## EMPLOYMENT

2011–... Specialist, Institute of Agricultural and Environmental Sciences, Estonian University of Life Sciences.  
2016–2018 Specialist in Physical Geography and Landscape Ecology, Institute of Ecology and Earth Sciences, University of Tartu.

## RESEARCH INTERESTS

Forest greenhouse gas fluxes, forest functioning, landscape ecology, extreme weather events

## SELECTED PUBLICATIONS

- Mander, Ü., **Krasnova, A.**, Schindler, T., Megonigal, J. P., Escuer-Gatius, J., Espenberg, M., Machacova, K., Maddison, M., Pärn, J., Ranniku, R., Pihlatie, M., Kasak, K., Niinemets, Ü., & Soosaar, K. (2022). Long-term dynamics of soil, tree stem and ecosystem methane fluxes in a riparian forest. *Science of the Total Environment*, 809, 151723. <https://doi.org/10.1016/j.scitotenv.2021.151723>
- Mander, Ü., **Krasnova, A.**, Escuer-Gatius, J., Espenberg, M., Schindler, T., Machacova, K., Pärn, J., Maddison, M., Megonigal, J. P., Pihlatie, M., Kasak, K., Niinemets, Ü., Junninen, H., & Soosaar, K. (2021). Forest canopy mitigates soil N<sub>2</sub>O emission during hot moments. *Npj Climate and Atmospheric Science*, 4(1), 1–9. <https://doi.org/10.1038/s41612-021-00194-7>
- Barreira, L.M.F., Ylisirniö, A., Pullinen, I., Buchholz, A., Li, Z., Lipp, H., Junninen, H., Hörrak, U., Noe, S.M., **Krasnova, A.**, Krasnov, D., Kask, K., Talts, E., Niinemets, Ü., Ruiz-Jimenez, J., Schobesberger, S., 2021. The importance of sesquiterpene oxidation products for secondary organic aerosol formation in a springtime hemiboreal forest. *Atmospheric Chemistry and Physics* 21, 11781–11800. <https://doi.org/10.5194/acp-21-11781-2021>
- Lindroth, A., Holst, J., Linderson, M. L., Aurela, M., Biermann, T., Heliasz, M., Chi, J., Ibrom, A., Kolari, P., Klemetsson, L., **Krasnova, A.**, Laurila, T., Lehner, I., Lohila, A., Mammarella, I., Mölder, M., Löfvenius, M. O.,

- Peichl, M., Pilegaard, K., ... Nilsson, M. (2020). Effects of drought and meteorological forcing on carbon and water fluxes in Nordic forests during the dry summer of 2018. *Philosophical Transactions of the Royal Society B: Biological Sciences*, 375(1810). <https://doi.org/10.1098/rstb.2019.0516>
- Krasnova, A.**, Kukumägi, M., Mander, Ü., Torga, R., Krasnov, D., Noe, S. M., Ostonen, I., Püttsepp, Ü., Killian, H., Uri, V., Lõhmus, K., Söber, J., & Soosaar, K. (2019). Carbon exchange in a hemiboreal mixed forest in relation to tree species composition. *Agricultural and Forest Meteorology*, 275(May), 11–23. <https://doi.org/10.1016/j.agrformet.2019.05.007>
- Uri, V., Kukumägi, M., Aosaar, J., Varik, M., Becker, H., Aun, K., **Krasnova, A.**, Morozov, G., Ostonen, I., Mander, Ü., Lõhmus, K., Rosenvald, K., Kriiska, K., & Soosaar, K. (2019). The carbon balance of a six-year-old Scots pine (*Pinus sylvestris* L.) ecosystem estimated by different methods. *Forest Ecology and Management*, 433 (November 2018), 248–262. <https://doi.org/10.1016/j.foreco.2018.11.012>
- Ezhova, E., Ylivinkka, I., Kuusk, J., Komsaare, K., Vana, M., **Krasnova, A.**, Noe, S., Arshinov, M., Belan, B., Park, S.-B., Lavrič, J.V., Heimann, M., Petäjä, T., Vesala, T., Mammarella, I., Kolari, P., Bäck, J., Rannik, Ü., Kerminen, V.-M., Kulmala, M., 2018. Direct effect of aerosols on solar radiation and gross primary production in boreal and hemiboreal forests. *Atmos. Chem. Phys.* 18, 17863–17881. <https://doi.org/10.5194/acp-18-17863-2018>
- Li, X., Xiao, J., He, B., Altaf Arain, M., Beringer, J., Desai, A.R., Emmel, C., Hollinger, D.Y., **Krasnova, A.**, Mammarella, I., Noe, S.M., Ortiz, P.S., Rey-Sanchez, A.C., Rocha, A.V., Varlagin, A., 2018. Solar-induced chlorophyll fluorescence is strongly correlated with terrestrial photosynthesis for a wide variety of biomes: First global analysis based on OCO-2 and flux tower observations. *Global Change Biology* 24, 3990–4008. <https://doi.org/10.1111/gcb.14297>
- Noe, S.M., Krasnov, D., **Krasnova, A.**, Cordey, H.P.E., Niinemets, Ü., 2016. Seasonal variation and characterisation of reactive trace gas mixing ratios over a hemi-boreal mixed forest site in Estonia. *Boreal Environment Research* 21, 332–344.
- Noe, S.M., Niinemets, Ü., **Krasnova, A.**, Krasnov, D., Motallebi, A., Kängsepp, V., Jõgiste, K., Hörrak, U., Komsaare, K., Mirme, S., Vana, M., Tammet, H., Bäck, J., Vesala, T., Kulmala, M., Petäjä, T., Kangur, A., 2015. SMEAR Estonia: Perspectives of a large-scale forest ecosystem – atmosphere research infrastructure. *Forestry Studies* 63, 56–84. <https://doi.org/10.1515/fsmu-2015-0009>

## ELULOOKIRJELDUS

**Nimi:** Alisa Krasnova  
**Sünniaeg:** 10.07.1986  
**E-mail:** alisa.krasnova@ut.ee

### HARIDUS

2018–... doktoriõpe, Tartu Ülikool, Loodus- ja täppisteaduste valdkond, ökoloogia ja maateaduste instituut  
2011–2019 doktoriõpe, Eesti Maaülikool  
2003–2008 Spetsialist (MSc) bioloogias, Petrozavodsk Riigi Ülikool, Venemaa

### TÖÖKOGEVUS

2011–... Eesti Maaülikool, Põllumajandus- ja keskkonnainstituut, spetsialist  
2016–2018 Tartu Ülikool, Loodus- ja täppisteaduste valdkond, ökoloogia ja maateaduste instituut, loodusgeograafia ja maastikuökoloogia spetsialist

### UURIMISVALDKONNAD

Forest greenhouse gas fluxes, forest functioning, landscape ecology, extreme weather events

### PUBLIKATSIOONID

Mander, Ü., **Krasnova, A.**, Schindler, T., Megonigal, J. P., Escuer-Gatius, J., Espenberg, M., Machacova, K., Maddison, M., Pärn, J., Ranniku, R., Pihlatie, M., Kasak, K., Niinemets, Ü., & Soosaar, K. (2022). Long-term dynamics of soil, tree stem and ecosystem methane fluxes in a riparian forest. *Science of the Total Environment*, 809, 151723. <https://doi.org/10.1016/j.scitotenv.2021.151723>

Mander, Ü., **Krasnova, A.**, Escuer-Gatius, J., Espenberg, M., Schindler, T., Machacova, K., Pärn, J., Maddison, M., Megonigal, J. P., Pihlatie, M., Kasak, K., Niinemets, Ü., Junninen, H., & Soosaar, K. (2021). Forest canopy mitigates soil N<sub>2</sub>O emission during hot moments. *Npj Climate and Atmospheric Science*, 4(1), 1–9. <https://doi.org/10.1038/s41612-021-00194-7>

Barreira, L.M.F., Ylisirniö, A., Pullinen, I., Buchholz, A., Li, Z., Lipp, H., Junninen, H., Hörrak, U., Noe, S.M., **Krasnova, A.**, Krasnov, D., Kask, K., Talts, E., Niinemets, Ü., Ruiz-Jimenez, J., Schobesberger, S., 2021. The importance of sesquiterpene oxidation products for secondary organic aerosol formation in a springtime hemiboreal forest. *Atmospheric Chemistry and Physics* 21, 11781–11800. <https://doi.org/10.5194/acp-21-11781-2021>

Lindroth, A., Holst, J., Linderson, M. L., Aurela, M., Biermann, T., Heliasz, M., Chi, J., Ibrom, A., Kolari, P., Klemmedtsson, L., **Krasnova, A.**, Laurila, T., Lehner, I., Lohila, A., Mammarella, I., Mölder, M., Löfvenius, M. O., Pechl, M., Pilegaard, K., ... Nilsson, M. (2020). Effects of drought and

- meteorological forcing on carbon and water fluxes in Nordic forests during the dry summer of 2018. *Philosophical Transactions of the Royal Society B: Biological Sciences*, 375(1810). <https://doi.org/10.1098/rstb.2019.0516>
- Krasnova, A.**, Kukumägi, M., Mander, Ü., Torga, R., Krasnov, D., Noe, S. M., Ostonen, I., Püttsepp, Ü., Killian, H., Uri, V., Lõhmus, K., Sõber, J., & Soosaar, K. (2019). Carbon exchange in a hemiboreal mixed forest in relation to tree species composition. *Agricultural and Forest Meteorology*, 275(May), 11–23. <https://doi.org/10.1016/j.agrformet.2019.05.007>
- Uri, V., Kukumägi, M., Aosaar, J., Varik, M., Becker, H., Aun, K., **Krasnova, A.**, Morozov, G., Ostonen, I., Mander, Ü., Lõhmus, K., Rosenvald, K., Kriiska, K., & Soosaar, K. (2019). The carbon balance of a six-year-old Scots pine (*Pinus sylvestris* L.) ecosystem estimated by different methods. *Forest Ecology and Management*, 433 (November 2018), 248–262. <https://doi.org/10.1016/j.foreco.2018.11.012>
- Ezhova, E., Ylivinkka, I., Kuusk, J., Komsaare, K., Vana, M., **Krasnova, A.**, Noe, S., Arshinov, M., Belan, B., Park, S.-B., Lavrič, J.V., Heimann, M., Petäjä, T., Vesala, T., Mammarella, I., Kolari, P., Bäck, J., Rannik, Ü., Kerminen, V.-M., Kulmala, M., 2018. Direct effect of aerosols on solar radiation and gross primary production in boreal and hemiboreal forests. *Atmos. Chem. Phys.* 18, 17863–17881. <https://doi.org/10.5194/acp-18-17863-2018>
- Li, X., Xiao, J., He, B., Altaf Arain, M., Beringer, J., Desai, A.R., Emmel, C., Hollinger, D.Y., **Krasnova, A.**, Mammarella, I., Noe, S.M., Ortiz, P.S., Reyes-Sanchez, A.C., Rocha, A.V., Varlagin, A., 2018. Solar-induced chlorophyll fluorescence is strongly correlated with terrestrial photosynthesis for a wide variety of biomes: First global analysis based on OCO-2 and flux tower observations. *Global Change Biology* 24, 3990–4008. <https://doi.org/10.1111/gcb.14297>
- Noe, S.M., Krasnov, D., **Krasnova, A.**, Cordey, H.P.E., Niinemets, Ü., 2016. Seasonal variation and characterisation of reactive trace gas mixing ratios over a hemi-boreal mixed forest site in Estonia. *Boreal Environment Research* 21, 332–344.
- Noe, S.M., Niinemets, Ü., **Krasnova, A.**, Krasnov, D., Motallebi, A., Kängsepp, V., Jõgiste, K., Hõrrak, U., Komsaare, K., Mirme, S., Vana, M., Tammet, H., Bäck, J., Vesala, T., Kulmala, M., Petäjä, T., Kangur, A., 2015. SMEAR Estonia: Perspectives of a large-scale forest ecosystem – atmosphere research infrastructure. *Forestry Studies* 63, 56–84. <https://doi.org/10.1515/fsmu-2015-0009>

## DISSERTATIONES GEOGRAPHICAE UNIVERSITATIS TARTUENSIS

1. **Вийви Руссак.** Солнечная радиация в Тыравере. Тарту, 1991.
2. **Urmas Peterson.** Studies on Reflectance Factor Dynamics of Forest Communities in Estonia. Tartu, 1993.
3. **Ülo Suursaar.** Soome lahe avaosa ja Eesti rannikumere vee kvaliteedi analüüs. Tartu, 1993.
4. **Kiira Aaviksoo.** Application of Markov Models in Investigation of Vegetation and Land Use Dynamics in Estonian Mire Landscapes. Tartu, 1993.
5. **Kjell Weppling.** On the assessment of feasible liming strategies for acid sulphate waters in Finland. Tartu, 1997.
6. **Hannes Palang.** Landscape changes in Estonia: the past and the future. Tartu, 1998.
7. **Eiki Berg.** Estonia's northeastern periphery in politics: socio-economic and ethnic dimensions. Tartu, 1999.
8. **Valdo Kuusemets.** Nitrogen and phosphorus transformation in riparian buffer zones of agricultural landscapes in Estonia. Tartu, 1999.
9. **Kalev Sepp.** The methodology and applications of agricultural landscape monitoring in Estonia. Tartu, 1999.
10. **Rein Ahas.** Spatial and temporal variability of phenological phases in Estonia. Tartu, 1999.
11. **Эрки Таммиксаар.** Географические аспекты творчества Карла Бэра в 1830–1840 гг. Тарту, 2000.
12. **Garri Raagmaa.** Regional identity and public leaders in regional economic development. Tartu, 2000.
13. **Tiit Tammaru.** Linnastumine ja linnade kasv Eestis nõukogude aastatel. Tartu, 2001.
14. **Tõnu Mäuring.** Wastewater treatment wetlands in Estonia: efficiency and landscape analysis. Tartu, 2001.
15. **Ain Kull.** Impact of weather and climatic fluctuations on nutrient flows in rural catchments. Tartu, 2001.
16. **Robert Szava-Kovats.** Assessment of stream sediment contamination by median sum of weighted residuals regression. Tartu, 2001.
17. **Heno Sarv.** Indigenous Europeans east of Moscow. Population and Migration Patterns of the Largest Finno-Ugrian Peoples in Russia from the 18<sup>th</sup> to the 20<sup>th</sup> Centuries. Tartu, 2002.
18. **Mart Külvik.** Ecological networks in Estonia — concepts and applications. Tartu, 2002.
19. **Arvo Järvet.** Influence of hydrological factors and human impact on the ecological state of shallow Lake Võrtsjärv in Estonia. Tartu, 2004.
20. **Katrin Pajuste.** Deposition and transformation of air pollutants in coniferous forests. Tartu, 2004.

21. **Helen Sooväli.** *Saaremaa waltz.* Landscape imagery of Saaremaa Island in the 20th century. Tartu, 2004.
22. **Antti Roose.** Optimisation of environmental monitoring network by integrated modelling strategy with geographic information system — an Estonian case. Tartu, 2005.
23. **Anto Aasa.** Changes in phenological time series in Estonia and Central and Eastern Europe 1951–1998. Relationships with air temperature and atmospheric circulation. Tartu, 2005.
24. **Anneli Palo.** Relationships between landscape factors and vegetation site types: case study from Saare county, Estonia. Tartu, 2005.
25. **Mait Sepp.** Influence of atmospheric circulation on environmental variables in Estonia. Tartu, 2005.
26. **Helen Alumäe.** Landscape preferences of local people: considerations for landscape planning in rural areas of Estonia. Tartu, 2006.
27. **Aarne Luud.** Evaluation of moose habitats and forest reclamation in Estonian oil shale mining areas. Tartu, 2006.
28. **Taavi Pae.** Formation of cultural traits in Estonia resulting from historical administrative division. Tartu, 2006.
29. **Anneli Kährrik.** Socio-spatial residential segregation in post-socialist cities: the case of Tallinn, Estonia. Tartu, 2006.
30. **Dago Antov.** Road user perception towards road safety in Estonia. Tartu, 2006.
31. **Üllas Ehrlich.** Ecological economics as a tool for resource based nature conservation management in Estonia. Tartu, 2007.
32. **Evelyn Uuemaa.** Indicatory value of landscape metrics for river water quality and landscape pattern. Tartu, 2007.
33. **Raivo Aunap.** The applicability of gis data in detecting and representing changes in landscape: three case studies in Estonia. Tartu, 2007.
34. **Kai Treier.** Trends of air pollutants in precipitation at Estonian monitoring stations. Tartu, 2008.
35. **Kadri Leetmaa.** Residential suburbanisation in the Tallinn metropolitan area. Tartu, 2008.
36. **Mare Remm.** Geographic aspects of enterobiasis in Estonia. Tartu, 2009.
37. **Alar Teemusk.** Temperature and water regime, and runoff water quality of planted roofs. Tartu, 2009.
38. **Kai Kimmel.** Ecosystem services of Estonian wetlands. Tartu, 2009.
39. **Merje Lesta.** Evaluation of regulation functions of rural landscapes for the optimal siting of treatment wetlands and mitigation of greenhouse gas emissions. Tartu, 2009.
40. **Siiri Silm.** The seasonality of social phenomena in Estonia: the location of the population, alcohol consumption and births. Tartu, 2009.
41. **Ene Indermitte.** Exposure to fluorides in drinking water and dental fluorosis risk among the population of Estonia. Tartu, 2010.
42. **Kaido Soosaar.** Greenhouse gas fluxes in rural landscapes of Estonia. Tartu, 2010.

43. **Jaan Pärn.** Landscape factors in material transport from rural catchments in Estonia. Tartu, 2010.
44. **Triin Saue.** Simulated potato crop yield as an indicator of climate variability in Estonia. Tartu, 2011.
45. **Katrin Rosenvald.** Factors affecting EcM roots and rhizosphere in silver birch stands. Tartu, 2011.
46. **Ülle Marksoo.** Long-term unemployment and its regional disparities in Estonia. Tartu, 2011, 163 p.
47. **Hando Hain.** The role of voluntary certification in promoting sustainable natural resource use in transitional economies. Tartu, 2012, 180 p.
48. **Jüri-Ott Salm.** Emission of greenhouse gases CO<sub>2</sub>, CH<sub>4</sub>, and N<sub>2</sub>O from Estonian transitional fens and ombrotrophic bogs: the impact of different land-use practices. Tartu, 2012, 125 p.
49. **Valentina Sagris.** Land Parcel Identification System conceptual model: development of geoinfo community conceptual model. Tartu, 2013, 161 p.
50. **Kristina Sohar.** Oak dendrochronology and climatic signal in Finland and the Baltic States. Tartu, 2013, 129 p.
51. **Riho Marja.** The relationships between farmland birds, land use and landscape structure in Northern Europe. Tartu, 2013, 134 p.
52. **Olle Järv.** Mobile phone based data in human travel behaviour studies: New insights from a longitudinal perspective. Tartu, 2013, 168 p.
53. **Sven-Erik Enno.** Thunderstorm and lightning climatology in the Baltic countries and in northern Europe. Tartu, 2014, 142 p.
54. **Kaupo Mändla.** Southern cyclones in northern Europe and their influence on climate variability. Tartu, 2014, 142 p.
55. **Riina Vaht.** The impact of oil shale mine water on hydrological pathways and regime in northeast Estonia. Tartu, 2014, 111 p.
56. **Jaanus Veemaa.** Reconsidering geography and power: policy ensembles, spatial knowledge, and the quest for consistent imagination. Tartu, 2014, 163 p.
57. **Kristi Anniste.** East-West migration in Europe: The case of Estonia after regaining independence. Tartu, 2014, 151 p.
58. **Piret Pungas-Kohv.** Between maintaining and sustaining heritage in landscape: The examples of Estonian mires and village swings. Tartu, 2015, 210 p.
59. **Mart Reimann.** Formation and assessment of landscape recreational values. Tartu, 2015, 127 p.
60. **Järvi Järveoja.** Fluxes of the greenhouse gases CO<sub>2</sub>, CH<sub>4</sub> and N<sub>2</sub>O from abandoned peat extraction areas: Impact of bioenergy crop cultivation and peatland restoration. Tartu, 2015, 171 p.
61. **Raili Torga.** The effects of elevated humidity, extreme weather conditions and clear-cut on greenhouse gas emissions in fast growing deciduous forests. Tartu, 2016, 128 p.
62. **Mari Nuga.** Soviet-era summerhouses On homes and planning in post-socialist suburbia. Tartu, 2016, 179 p.

63. **Age Poom.** Spatial aspects of the environmental load of consumption and mobility. Tartu, 2017, 141 p.
64. **Merle Muru.** GIS-based palaeogeographical reconstructions of the Baltic Sea shores in Estonia and adjoining areas during the Stone Age. Tartu, 2017, 132 p.
65. **Ülle Napa.** Heavy metals in Estonian coniferous forests. Tartu, 2017, 129 p.
66. **Liisi Jakobson.** Mutual effects of wind speed, air temperature and sea ice concentration in the Arctic and their teleconnections with climate variability in the eastern Baltic Sea region. Tartu, 2018, 118 p.
67. **Tanel Tamm.** Use of local statistics in remote sensing of grasslands and forests. Tartu, 2018, 106 p.
68. **Enel Pungas.** Differences in Migration Intentions by Ethnicity and Education: The Case of Estonia. Tartu, 2018, 142 p.
69. **Kadi Mägi.** Ethnic residential segregation and integration of the Russian-speaking population in Estonia. Tartu, 2018, 173 p.
70. **Kiira Mõisja.** Thematic accuracy and completeness of topographic maps. Tartu, 2018, 112 p.
71. **Kristiina Kukk.** Understanding the vicious circle of segregation: The role of leisure time activities. Tartu, 2019, 143 p.
72. **Kaie Kriiska.** Variation in annual carbon fluxes affecting the soil organic carbon pool and the dynamics of decomposition in hemiboreal coniferous forests. Tartu, 2019, 146 p.
73. **Pille Metspalu.** The changing role of the planner. Implications of creative pragmatism in Estonian spatial planning. Tartu, 2019, 128 p.
74. **Janika Raun.** Mobile positioning data for tourism destination studies and statistics. Tartu, 2020, 153 p.
75. **Birgit Viru.** Snow cover dynamics and its impact on greenhouse gas fluxes in drained peatlands in Estonia. Tartu, 2020, 123 p.
76. **Iuliia Burdun.** Improving groundwater table monitoring for Northern Hemisphere peatlands using optical and thermal satellite data. Tartu, 2020, 162 p.
77. **Ingmar Pastak.** Gentrification and displacement of long-term residents in post-industrial neighbourhoods of Tallinn. Tartu, 2021, 141 p.
78. **Veronika Mooses.** Towards a more comprehensive understanding of ethnic segregation: activity space and the vicious circle of segregation. Tartu, 2021, 161 p.
79. **Johanna Pirrus.** Contemporary Urban Policies and Planning Measures in Socialist-Era Large Housing Estates. Tartu, 2021, 142 p.
80. **Gert Veber.** Greenhouse gas fluxes in natural and drained peatlands: spatial and temporal dynamics. Tartu, 2021, 210 p.
81. **Anniki Puura.** Relationships between personal social networks and spatial mobility with mobile phone data. Tartu, 2021, 144 p.